IMAGE CLASSIFICATION AND CHANGE ANALYSIS OF CA-MARKOV FOR LAND USE/LAND COVER OF BANG LAMUNG DISTRICT, PATTAYA CITY, CHON BURI PROVINCE, THAILAND

BAWONLUCK WIBOONWATCHARA

A THESIS SUBMITTED IN PARTIAL FULFILLMENT OF
THE REQUIREMENTS FOR MASTER DEGREE OF SCIENCE
IN GEOINFORMATICS
FACULTY OF GEOINFORMATICS
BURAPHA UNIVERSITY
2024

มหาวิทยาลัยบูรพา
BURAPHA UNIVERSITY

-

บวรลักษณ์ วิบูลย์วัชรา

วิทยานิพนธ์นี้เป็นส่วนหนึ่งของการศึกษาตามหลักสูตรวิทยาศาสตรมหาบัณฑิต
สาขาวิชาภูมิสารสนเทศศาสตร์
คณะภูมิสารสนเทศศาสตร์ มหาวิทยาลัยบูรพา
2567

IMAGE CLASSIFICATION AND CHANGE ANALYSIS OF CA-MARKOV FOR LAND USE/LAND COVER OF BANG LAMUNG DISTRICT, PATTAYA CITY, CHON BURI PROVINCE, THAILAND

BAWONLUCK WIBOONWATCHARA

A THESIS SUBMITTED IN PARTIAL FULFILLMENT OF
THE REQUIREMENTS FOR MASTER DEGREE OF SCIENCE
IN GEOINFORMATICS
FACULTY OF GEOINFORMATICS
BURAPHA UNIVERSITY
2024

The Thesis of Bawonluck Wiboonwatchara has been approved by the examining committee to be partial fulfillment of the requirements for the Master Degree of Science in Geoinformatics of Burapha University

Advisory Committee

Principal advisor

.....

(Professor Dr. Hong Shu)

Co-advisor

.....

(Dr. Tanita Suepa)

.....

(Dr. Kitsanai Charoenjit)

Examining Committee

.....

Principal examiner

(Professor Dr. Wolfgang Kainz)

.....

Member

(Professor Dr. Timo Balz)

.....

Member

(Professor Dr. Hong Shu)

.....

Member

(Dr. Kitsanai Charoenjit)

.....

Acting Dean of the Faculty of Geoinformatics

(Associate Professor Dr. Arnon Wongkaew)

.....

This Thesis has been approved by Graduate School Burapha University to be partial fulfillment of the requirements for the Master Degree of Science in Geoinformatics of Burapha University

.....

Dean of Graduate School

(Associate Professor Dr. Witawat Jangiam)

.....

64910086: MAJOR: GEOINFORMATICS; M.Sc. (GEOINFORMATICS)

KEYWORDS: LULC changes; CA-Markov model; Sustainable development; EEC; Pattaya City; Bang Lamung district; Thailand

BAWONLUCK WIBOONWATCHARA : IMAGE CLASSIFICATION AND CHANGE ANALYSIS OF CA-MARKOV FOR LAND USE/LAND COVER OF BANG LAMUNG DISTRICT, PATTAYA CITY, CHON BURI PROVINCE, THAILAND . ADVISORY COMMITTEE: HONG SHU, TANITA SUEPA KITSANAI CHAROENJIT 2024.

The Eastern Economic Corridor (EEC) development lies at the heart of Thailand 4.0 scheme. The EEC is an area-based development initiative, aiming to develop its eastern provinces into a leading ASEAN economic zone. The EEC straddles three eastern provinces of Thailand, namely, Chonburi, Rayong, and Chachoengsao. Pattaya City and Bang Lamung district are located in the southern part of Chonburi province, Thailand.

This study aims to analyze the land use/land cover (LULC) changes in the Bang Lamung district by using a Cellular Automata-Markov (CA-Markov) model. The results show that the first scenario is spontaneous in LULC change, with the highest growth since 2009-2032 in the built-up areas with an average annual change of 94.83%. The agriculture areas have been steadily decreasing with an average annual change of -46.41% and – 25.29% respectively. The second scenario is the green area improvement. The study found that the green area will remain sufficient for the population in 2027 and 2032. However, the annual change rate of green area per population tends to decrease, especially in the area of Pattaya City. From the results, it was found that green areas in urban areas such as Nong Pa Lai Sub-district, Bang Lamung Sub-district and Na Kluea Sub-district which covers the area of Pattaya City and consists mainly of open spaces with a decrease in the average amount of green space per person per year is about -60.74%, -55.63% and -48.31% respectively. The third scenario is the area comprehensive plan. Comparison of the simulation results of the LULC map in 2027 and 2032 with the current Bang Lamung town plan found that the urbanization area has changed expansion according to the overall town plan. The results indicate that the built-up area is expected to increase by an annual

change of 13.10%, while the area used for agriculture is expected to decrease by an annual change of -55.99%. The distribution of controlled and protected areas is inconsistent with the town plan due to the inefficiency of government officials. The results showed that under the controlled area, the share of agriculture is expected to decline on average annually at -8.14% between 2022 and 2032.

These land use changes will be useful in planning the urban administration and management of Bang Lamung City to accommodate the growth of the EEC project.

ACKNOWLEDGEMENTS

The authors would like to thank the Ministry of Higher Education, Science, Research and Innovation that grants a scholarship to support master's degree studies to me, and also to thank the Geo-Informatics and Space Technology Development Agency (Public Organization) (GISDA), The State Key Laboratory of Information Engineering in Surveying, Mapping and Remote Sensing, Wuhan University (LIESMARS) and Burapha University, who supported and educated me on the study life in this program.

I would like to express my sincere gratitude and deep appreciation to my major advisor, Professor Hong Shu for his valuable and kindly providing me with an opportunity and accepting me to joint this master course, and his encouragement and strong motivation during this course. I would also thank you all professors of this master course and the staffs from LIESMARS for their support during the course and activities.

I am thankful to my friends from SCGI batch 4, who offered of help, support, and motivation throughout this dissertation. Sincere thanks go to all of my cutie friends, they always cheer up and are beside me.

Finally, I feel deeply grateful to my family for their sincere love, understanding, and support for me. I never find words to explain how much I appreciate all of you.

Bawonluck Wiboonwatchara

TABLE OF CONTENTS

Page

LIST OF TABLES

Page

LIST OF FIGURES

Page

CHAPTER 1
INTRODUCTION

1.1 Statement and Significance of Problems

In recent years, urbanization and industrialization have become key issues affecting the land use/land cover (LULC) system. LULC has a widespread influence in many fields, not only in urban planning but also in transportation, environment, policy and economy (Wang, Derdouri, & Murayama, 2018). For developed and developing countries, LULC is divided into two categories, i.e. urban redevelopment and urban growth (Barney, 2006). Compared with developing countries, the trend of LULC changes in industrialized countries is more important in creating a green and fertile environment and to enhance comprehensive competitiveness in the world (Pielke et al, 2011).

In Thailand since the adaptation of the fifth national economic and social development plan in 1982, urban areas have significantly expanded. Many cities have surpassed the population growth factor and the industrial factor forces, including policy planning, especially in the eastern coastal area. Consequently, these areas have become the target of a mega project called the Eastern Economic Corridor (EEC) from Thai government with 3 model provinces, including Chachoengsao, Chonburi, and Rayong provinces.

EEC is the enhancement of the former Eastern Seaboard (ESB). This massive investment is Thailand's Special Economic Zone (SEZ) and is currently the leading economic zone in ASEAN attracting multinational companies to invest, especially in the automotive, petrochemical and electronics industries. Leading to the establishment of 30 industrial estates and over 5,000 factories. With this highly successful development of the area, exports in the Eastern Seaboard area have increased from 7% to 12% and the industry in the area has grown 12% over the past 20 years (Eastern Economic Corridor Office, 2019).

Bang Lamung is a district which is a coastal area located in Chonburi Province. In the recent decade, we have witnessed the rapid growth of Bang Lamung City and the surrounding region initiated by EEC allocation and development for new

urban planning, industrial parks, tourism and the main logistics connection model in the region. In addition, Pattaya city is one of the potential centers for tourism and services and foreign investment that promotes by the government. Moreover, the government continues to focus on roadmaps for technological transformation into smart cities, creating a hub for the activities of economic, investment and tourism in this area. These are growing urbanization which puts pressure on green spaces due to the demand for green environments and comfort of living (Waddell, 2002). To maintain the balance, the LULC change is therefore an important task for governments and city planners to formulate policies to regulate the land use development.

Among these impacts, LULC change has been recognized as one of the most important indicators for global and regional eco-environmental changes [6]. Remote Sensing and GIS approaches combined with multispectral satellite data have been commonly used for the acquisition of LULC information (Singh, 2016). Using remote sensing and GIS techniques can be utilized for the measurement of LULC change detection (Aburas, 2016). The simulation of LULC has become one significant application in urban studies involving spatial modeling.

The purpose of this research was to analyse the dynamics and trends of LULC, especially in industries and settlements. The situation of LULC in Bang Lamung District can be simulated using the Cellular Automata Markov (CA-Markov) models. The combination of remote sensing data and CA-Markov models can be used to build a model of LULC, which is an important tool for evaluating and managing the land use policies (Yulianto, Suwarsono & Sulma, 2018). The CA-Markov model is combined with the cellular automata model and the Markov model. The Markov model is a statistical model that computes the probability matrix of the transition between two states by using the transition probability matrix. The state of future time periods can be simulated from the state of previous time periods (Arsanjani et al., 2013).

As a result, this study analyzes the spatiotemporal pattern of LULC from 2009 to 2022 in Bang Lamung District. CA-Markov models and satellite images (ALOS (AVNIR-2) and Sentinel2) with a resolution of 10 meters were used to analyze and simulate the dynamics of the LULC in 2027 and 2032. The LULC simulation between

2027 and 2032 considers three scenarios: spontaneous, green area improvement, and area comprehensive plan scenarios. The results of this study can serve as a medium for the municipal office techniques to develop the land use planning and to support sustainable planning and management.

1.2 Research problem

The EEC is an area-based development initiative, aiming to develop its eastern provinces into a leading ASEAN economic zone. Rapid economic development affects LULC changes uncontrollably. Future LULC simulation aids in more efficient LULC planning.

1.3 Research purpose

This research aims to analyze LULC changes in the Bang Lamung district using the CA-Markov model.

1.4 Research Objectives

1) To study spatiotemporal land use/land cover trends over the periods 2009 to 2022 for urban expansion in Pattaya city towards Bang Lamung district, Chon Buri province, Thailand.

2) To simulate and analyze land use/land cover for Pattaya City towards Bang Lamung district, Chon Buri Province, Thailand, under three scenarios - spontaneous, green area improvement, and area comprehensive plan for the years 2027 and 2032.

1.5 Contribution to Knowledge

1) The research result can guide local governors in terms of urban development and land use management for maintaining sustainable development in Bang Lamung district.

2) The study can provide information about land use/land cover change situation in Bang Lamung district.

3 The researcher acquires knowledge that can be used in the field of urban development, and the planner can use this technique as a tool in future city planning.

1.6 Study area

Bang Lamung is a district in Chonburi province which is located in the eastern region of Thailand and approximately 142 kilometers away from Bangkok. Bang Lamung District covers an area of 524.87 sq.km. The coordination of study area is located between 701000 E to 728000 E and 1412000 N to 1447000 N in WGS 84/ UTM zone 47N (Figure 1). The study area has a total population of 328,961 people (2022) and a population density of approximately 626 people/ sq.km, which is classified as a big-sized city (Pattaya City) according to the Criteria and Standards of Town Planning (DPT) 2006 of Thailand. Bang Lamung is divided into eight sub-districts.

Pattaya City is a special municipality in Bang Lamung District that is considered a Special Administrative Region just like Bangkok as an Autonomous Region located in the eastern part of Thailand. Pattaya City is planned to be a growth center for the central area of Bang Lamung District.

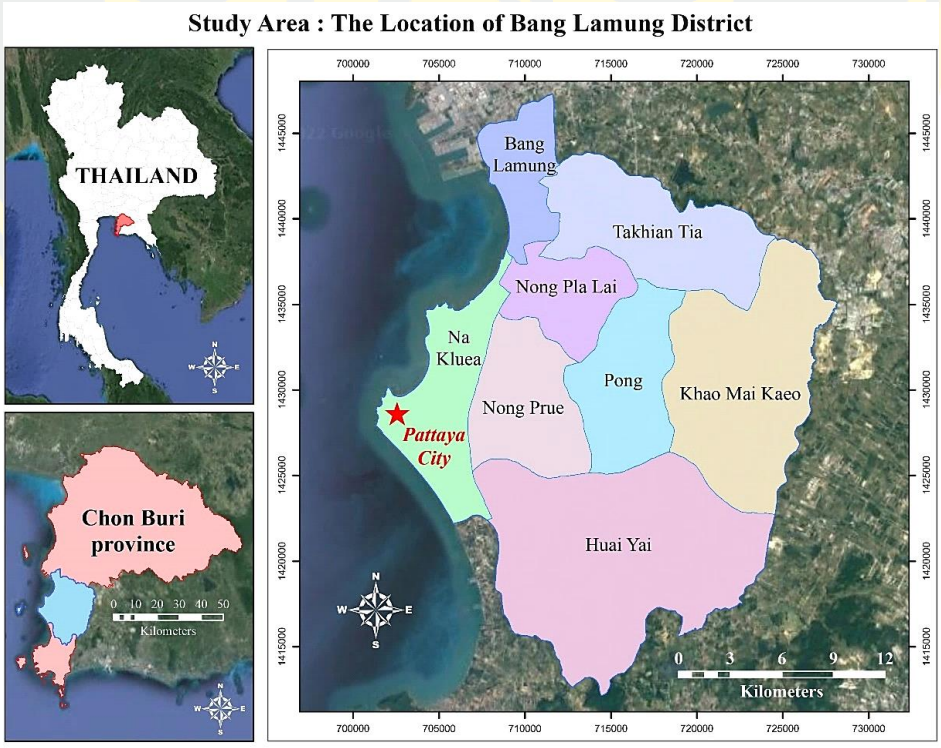

Figure 1: Location map of study area

1.7 Conceptual Framework

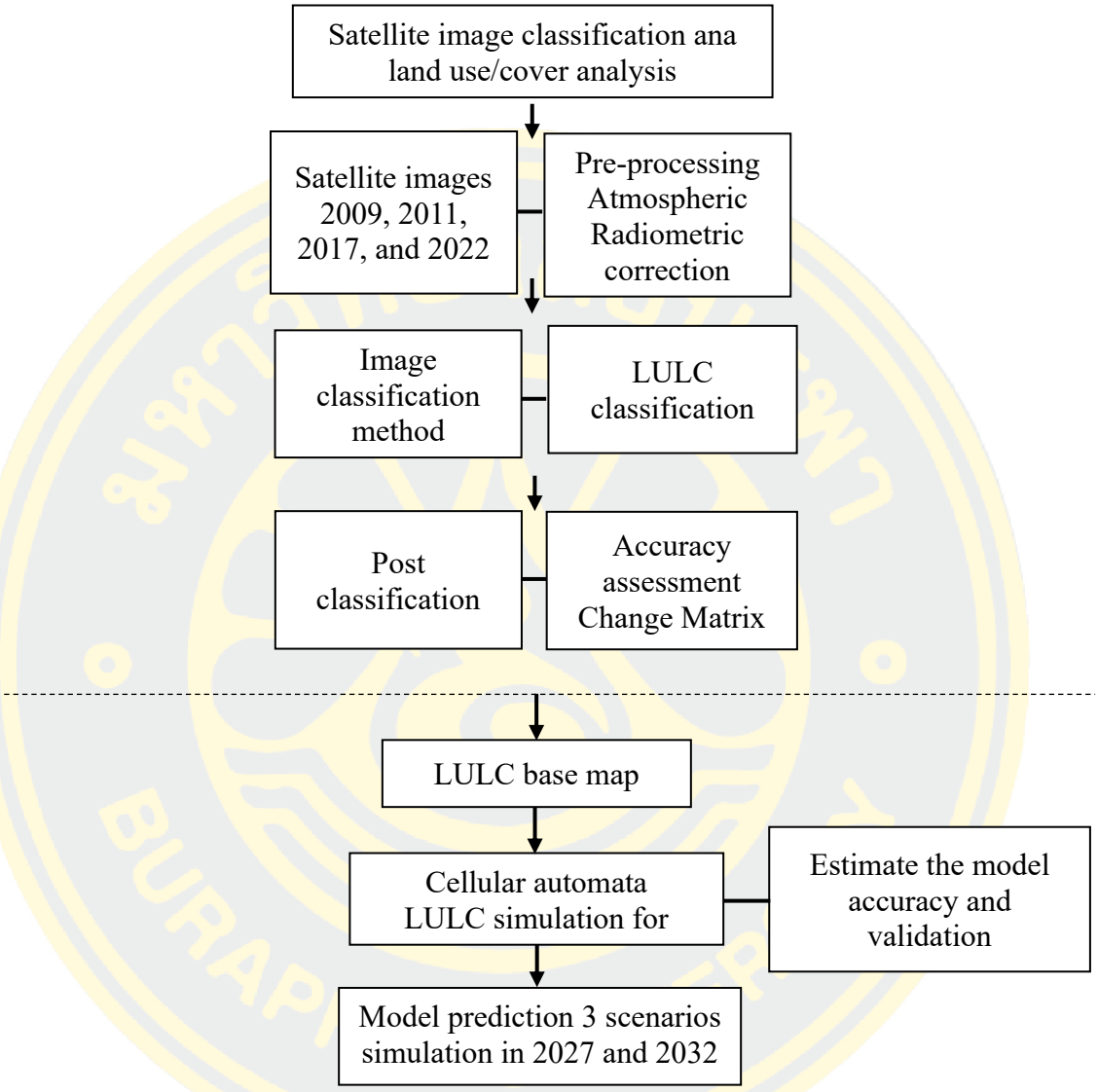

Figure 2: The conceptual framework in this research

CHAPTER 2
LITERATURE REVIEW

This chapter presents the theories, models, and methods used for future land use/land cover (LULC) simulation. Basically, this chapter first introduce the general background of Bang Lamung district and the Eastern Economic Corridor (EEC). Then review basic theories of remote sensing for LULC classification and geographic information system and including LULC dynamics. In addition, review detailed function of the Cellular Automata and Markov Chain model (CA-Markov) LULC simulation model and the research related to this thesis.

2.1 Background of Bang Lamung district

Bang Lamung district is one of the areas for supporting the Eastern Economic Corridor Development (EEC) following the government policy. In terms of economic and urban development, it can be noted that Bang Lamung has been expanding rapidly. However, the expansion also has affected LULC and brought some issues to the area such as land use issues, urban environmental issues, degradation of natural resources, and expansion of community in risk areas.

According to the city plan of Bang Lamung district has an area of approximately 1,326.75 sq.km including the land area of 535.80 sq.km and water area of 790.95 sq.km. It covers the area of seven local governments consisting of Nong Prue town municipality, Bang Lamung sub-district municipality, Huai Yai subdistrict municipality, Pong subdistrict municipality, Ta khian Tia subdistrict municipality, Nong Pla Lai subdistrict municipality, Khao Mai Kaew subdistrict administrative organization, and Pattaya is one special administration area are covered.

Bang Lamung situated on the Eastern Special Economic Zone (EEC) and Pattaya city is the main center for tourism including both natural and cultural attractions that are the potential of Bang Lamung (Figure 3). In addition, the physical is flat, so several open spaces could be used for future land use. Moreover, the region has a widespread of transportation system (DPT, 2019).

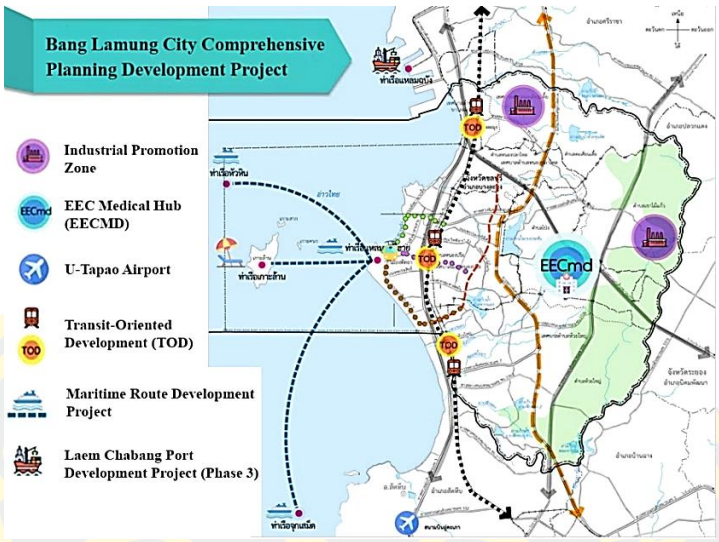

Figure 3: Bang Lamung city planning development project (DPT, 2019)

2.1.1 Topography

Bang Lamung district has an altitude of 0-329 m. above Mean Sea Level (MLS). The highest area is the east side of the district (Figure 4). Furthermore, the terrain features of the area are coastal, hilly, and rolling plains that suite for settlement. Besides, the coast is suited for fishery and tourism activities. The natural resources of Bang Lamung follow as:

- Soil: soil resources in Bang Lamung have good - medium drainage. Soil texture is loamy soils with sandy loam. The suitability for growing plants is relatively low.
- Forest: There are two significant forests in Bang Lamung such as Bang Lamung National Reserved Forest, and Khao Chion Non - Hunting Area.
- Water: water surface in Bang Lamung area consist of fresh water and sea water, while groundwater resource consists of groundwater in loose rocks and groundwater in hard rock.
- Mineral resources: Granite resources for the construction industry are found spread the east in Bang Lamung district to Pluak Daeng district, Rayong Province.

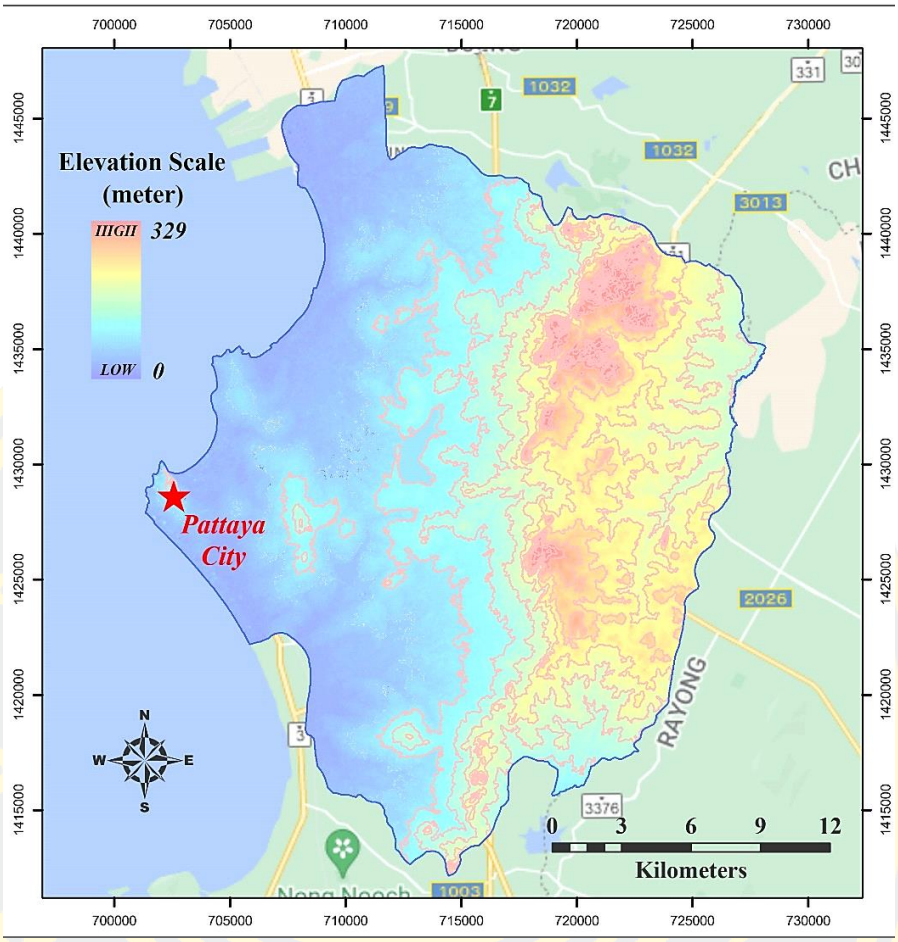

Figure 4: The elevation of Bang Lamung district (ALOS PALSAR, 29 March 2011)

2.1.2 Settlements and urban systems

The settlements and urban system of Bang Lamung district consist of clustered rural settlements (Nong Prue), linear settlements (Huay Yai), coastal settlements (Pattaya city), settlements surrounding the reservoir, and grid settlements (Pong). This can see that the urban system also along with the main road (DPT, 2019).

Each area in Bang Lamung divide following the function of the city such as

- Pattaya city: administrative center
- Nong Prue town municipality: administrative center, economic area, and supporting the expansion from Pattaya city
- Ta Khian Tia sub-district municipality: environment and community tourism development area, supporting resident area
- Nong Pla Lai sub-district municipality: supporting education and public health area

- Huai Yai sub-district municipality: the center of the district in terms of economy, tourism, and supporting the expansion from Pattaya city
- Bang Lamung sub-district municipality: the center of the district in terms of education and government institutions that serve surrounding areas
- Pong sub-district municipality: the center of the district in terms of education and government institutions that serve surrounding areas
- Khao Mai Kaew sub-district administrative organization: watershed forest conservation area

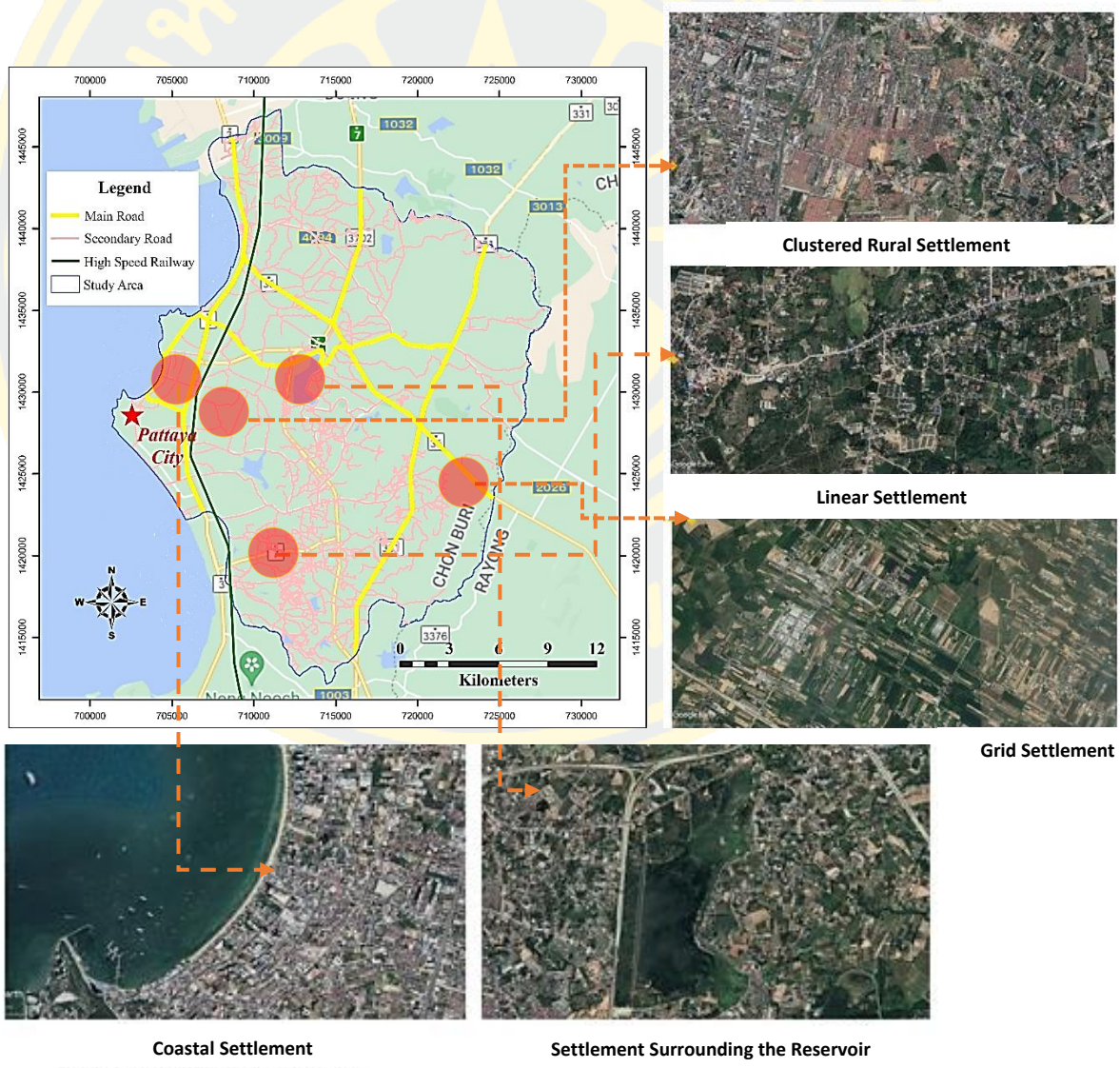

Figure 5: Settlements and urban systems of Bang Lamung district

2.1.3 Land use

According to DPT 2019, agriculture area was the highest at 42.60%, followed by water area at 25.58% and residential area at 9.52%. The impact of residential expansion causes the agriculture area to decrease by 0.13 sq.km per year, resulting in a change in area of 20.84 sq.km (DPT, 2019) (Table 1).

Table 1: Land use of Bang Lamung district

Type of land use	Area (sq.km)	Percent (%)
Residence	125.58	9.52
Commercial	40.89	3.09
Industry and warehouse	5.54	0.41
Agriculture	561.94	42.60
Recreation/ entertainment	27.57	2.09
Forest area	121.75	9.23
Water area	337.43	25.58
Utilities and facilities	56.06	4.24
Others	42.34	3.20
Total	**1,319.10**	**100**

Source: Department of Public works and Town & country planning (DPT), 2019

2.1.4 Population distribution

Based on the information from Department of Provincial Administration (DOPA) in 2022 found that the population of Bang Lamung district is 328,961 and the total number of households is 304,727 which gives an average household size of 1.08 (DOPA, 2022). Most of the population 220,022 people live in municipal areas (66.88%) and 108,939 in non-municipal areas (33.12%). Pattaya city self-administrating municipality is the most population in the district with 116,451 persons (35.40%) and followed by Nong Prue town municipality with 87,985 persons (26.75%) (Table 2).

Table 2: The population census in Bang Lamung district

Administration boundary	Population (person)	Percentage (%)	Number of Household	People/ Household
Pattaya city self-administrating	116,451	35.40	172,313	0.68
Laem Chabang city (Village 4,6,7,8,9)	15,586	4.74	15,390	1.01
Nong Prue town municipality	87,985	26.75	51,625	1.70
Bang Lamung subdistrict municipality	12,751	3.88	9,040	1.41
Huai Yai subdistrict municipality	31,015	9.43	18,120	1.71
Ta khian Tia subdistrict municipality	24,927	7.58	13,005	1.92
Pong subdistrict municipality	10,818	3.29	6,552	1.65
Nong Pla Lai subdistrict municipality	21,649	6.58	14,574	1.49
Khao Mai Kaew subdistrict	7,779	2.63	4,108	1.89
Total	**328,961**	**100.00**	**304,727**	**1.08**
Municipal areas	220,022	66.88	239,328	0.92
Non-municipal areas	108,939	33.12	65,399	1.67

Source: Department of Provincial Administration (DOPA), 2022

The population density of the district is 614 people /sq.km, but the city center of Bang Lamung district (Pattaya) has a relatively high population density of 2,181 people /sq.km. which calculates follow from the administration boundary of Department of Provincial Administration (Table 3). The change rate of population growth from 2011 to 2021 is 2.32 which projected populations in 2042 of the districts expected to increase by 832,400 (Table 4).

Table 3**:** The population density in Bang Lamung district

Administration boundary	Population (person)	Area (sq.km.)	Population density
Pattaya city self-administrating	116,451	53.40	2,180.73
Laem Chabang city (Village 4,6,7,8,9)	15,586	16.03	972.30
Nong Prue town municipality	87,985	45.54	1,932.04
Bang Lamung subdistrict municipality	12,751	6.38	1,998.59
Huai Yai subdistrict municipality	31,015	153.00	202.71
Ta khian Tia subdistrict municipality	24,927	57.85	430.89
Pong subdistrict municipality	10,818	78.60	137.63
Nong Pla Lai subdistrict municipality	21,649	27.00	801.81
Khao Mai Kaew subdistrict	7,779	98.00	79.38
Total	**328,961**	**535.80**	**613.96**
Municipal areas	220,022	114.97	1,913.73
Non-municipal areas	108,939	420.83	258.87

Source: Department of Provincial Administration (DOPA), 2022

Table 4**:** The population projection in 20 years of Bang Lamung district

Year	Total Population
2022	328,961
2027	414,900
2032	523,300
2037	660,000
2042	832,400

Source: Researcher calculated, 2022

Population distribution in Bang Lamung district, it was found that in 202 most of the population was concentrated in Pattaya city with 116,451 people (35.40%), followed by a population between 50,001-100,000 people distributed in

Nong Prue town municipality with 87,985 people. (26.75%). The population distribution can be classified as follows (Table 5).

Table 5**:** Population distribution in Bang Lamung district

Administration boundary	**Population (2021)**	**Number of populations**				
		More than 100,000	50,001-100,000	25,001-50,000	10,001-25,000	Less than 10,000
Pattaya city	116,451	●				
Laem Chabang city	15,586				●	
Nong Prue	87,985		●			
Bang Lamung	12,751				●	
Huai Yai	31,015			●		
Ta khian Tia	24,927				●	
Pong	10,818				●	
Nong Pla Lai	21,649				●	
Khao Mai Kaew	7,779					●
Total	**328,961**	**1**	**1**	**1**	**5**	**1**

2.2 Eastern Economic Corridor (EEC)

According to Thailand 4.0 Economic Policy was the depth-study insight into the Mega Project of Thailand in the Eastern Economic Corridor (ESDZ.Act, 2018).

The Eastern Economic Corridor has been applied since January 2018 and is developed from the former Eastern Seaboard which has been implemented for over thirty years. The Thai government attempts to move the “Detroit of the East” to the manufacturing paradise of Asia, designed to accommodate innovative industries and the Thailand 4.0 era. The EEC consists of the three Eastern provinces: Rayong, Chonburi, and Chachoengsao, aiming to set out infrastructure developments, generous inducements, and investment enablement. The government has set out three pillars including infrastructure developments, super-generous incentives, and investment facilitation in the EEC (Bhrammanachote, 2019).

EEC serves as the best area due to Thailand being the ideal hub that is linked to other economic zones in Asia and is the stronghold of the Asean Economic

Community (AEC) in production, trade, export and import, and logistics. Therefore, Thailand is the best location for an investment in ASEAN where it enables the connection to Asia and rest of the world (Figure 6).

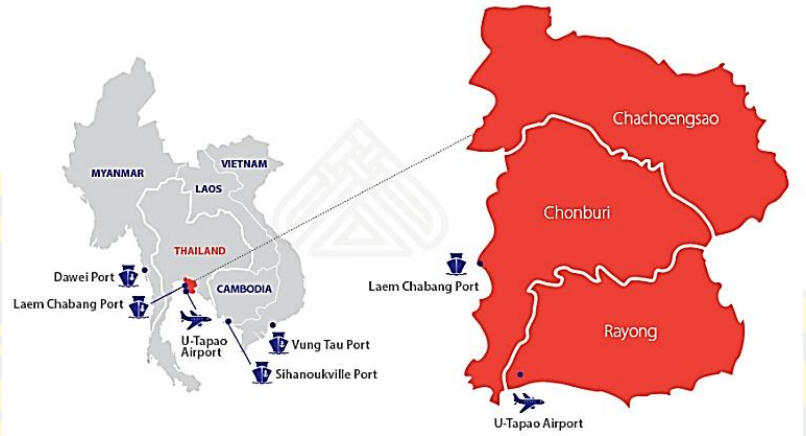

Figure 6: The Eastern Economic Corridor in Thailand
(Aseanbriefing,2022)

The Eastern Economic Corridor (EEC) Office (2018) identified Chonburi province as the "modern factory of the East," with a leading tourist attraction, conference center, international products exhibition, international medical center, and aviation and logistics center.

The main aims of developing the EEC are: (1) to elevate the areas as Asia's leading economy (2) to develop the infrastructure (3) to promote the development of the city and urbanization (4) to facilitate the incentive for investors, and (5) to support high-tech industries and tourism.

2.2.1 Economic development policies and land use changes

For many developing countries, economic development policies have been driven by industrialization, whereby the governments have provided firms with strong financial and non-financial incentives (Stiglitz et al.,1996). Industrialization, however, has been strongly linked to urbanization. Evidence in China, for example, has shown that industrialization has significantly contributed to urban expansions (Deng et al., 2008). Countries relying heavily on natural resource exports are also highly linked to urban expansions. Specifically, countries in Asia with a high percentage share of manufacturing and services in GDP are positively correlated with

the degree of urbanization (Gollin et al., 2016). Industrialization policies certainly have significant ramifications for changes in land use (Kim et al., 2011).

The EEC project in Thailand, being an export-oriented market, has raised expectations of significant changes in the economic landscape. One of the notable changes is the transformation of land uses in the region, brought about by new infrastructure investments and the emergence of new settlements or cities. The government's planning role, as outlined in the EEC Act, pertains to the establishment of infrastructures (as depicted in Figure 7), and it will inevitably impact land use and land cover. Despite these developments, the effects of the EEC project on land use changes remain inadequately understood.

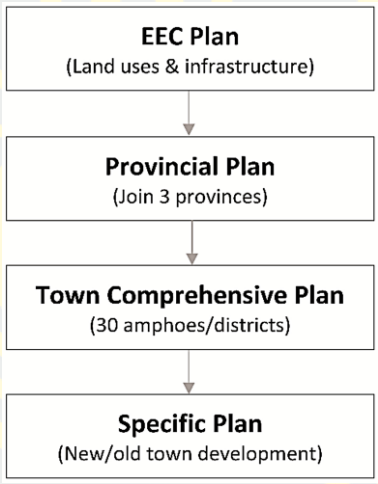

Figure 7: Planning tier of EEC Act.

Nij Tontisirin and Sutee Anantsuksomsri (2021) studied Economic Development Policies and Land Use Changes in Thailand: From the Eastern Seaboard to the Eastern Economic Corridor. Their conclusion emphasizes the importance of prudent planning for future urbanization, fueled by infrastructure investments and industrialization policies such as the ESB and the EEC. They stress the need for thoughtful consideration of urban administration and management, as well as the preservation of agriculture areas (Tontisirin, 2021).

2.3 Remote sensing for LULC classification

2.3.1 Definition of Remote Sensing

Taylor and Francis (2012) identified that remote sensing (RS) is the art, science, and technology of observing an object, scene, or phenomenon by instrument-based techniques. 'Remote' because observation is done at a distance without physical contact with the object of interest. Today most remote sensors are electronic devices. The data recorded by sensors detecting thermal emission (heat), used to be converted to images for visual interpretation.

Aggarwal (2004) discovered that remote sensing uses a part or several parts of the electromagnetic spectrum. It records the electromagnetic energy reflected or emitted by the earth's surface. The amount of radiation from an object is influenced by both properties of the object and the radiation, which hitting the object (Irradiance). The human eyes register the solar light reflected by these objects and our brains interpret the colors, the gray tones, and intensity fluctuations.

2.3.2 Preparation for image classification

The image processing method is a processing for image correction, image enhancement, and image classification method that are as follows:

- Radiometric correction is necessary to eliminate radiometric errors or distortions caused by atmospheric effects when a sensor on an airborne platform observes the emitted or reflected electromagnetic energy. The observed energy differs from the energy emitted or reflected from the same object observed from a close distance. This discrepancy is attributed to various factors such as the sun's azimuth and elevation, atmospheric conditions (e.g., fog or aerosols), and sensor response, which all influence the observed energy. Sensor problems such as noise, banding (striping), line drop, and bit errors are also included. Therefore, to obtain the accurate irradiance or reflectance values of an image, it is essential to eliminate these interferences from the data obtained from satellite imagery using radiometric correction processes (United Nations Educational, Scientific, and Cultural Organization, 1999).

- Geometric correction is applied to rectify geometric distortions in an original image by establishing a relationship between the image coordinate system

and the geographic coordinate system using sensor calibration data, position and attitude measurements, ground control points, and atmospheric conditions. This linking process enables the transformation of the linked image to a geometry-corrected image using three basic models: conformal transform, affine transform (first-order polynomial), and higher-order polynomial transform (Murai, 1993).

- Image enhancement involves modifying the gray scale values or the digital number (DN) intensity of digital image data. Its purpose is to enhance the details in the image to make them simplify/clearer and easier to classify (Polngam, 2003).

- Image transformation generates new images by extracting specific features or properties of interest from multiple bands of data, resulting in better visual representation than the original input images. Common image transformations include the Normalized Difference Vegetation Index (NDVI), which is calculated from reflectance measurements in the red and near-infrared (NIR) parts of the spectrum, and has been widely used to monitor vegetation conditions. NDVI involves a simple algebraic operation to highlight the differences between these two spectral bands (Verhulst, 2010).

$$NDVI=\frac{(NIR-RED)}{(NIR+RED)}$$

Here NIR is spectral reflectance measurements acquired in Near Infrared wavelength. RED is spectral reflectance measurements acquired in RED wavelength. The result showed a Digital Number (DN) value range from -1 to 1. The positive DN values are any portion of vegetation and negative DN values are occupied by water (Geographic Information Technology Training Alliance, 2015).

2.3.3 Image classification

The principle of image classification is that a pixel is assigned to a class based on its feature vector, by comparing it to predefined clusters in the feature space. The definition of the clusters is an interactive process and is carried out during the 'training process. Comparison of the individual pixels with the clusters takes place using “classification algorithms” (Francis, 2012).

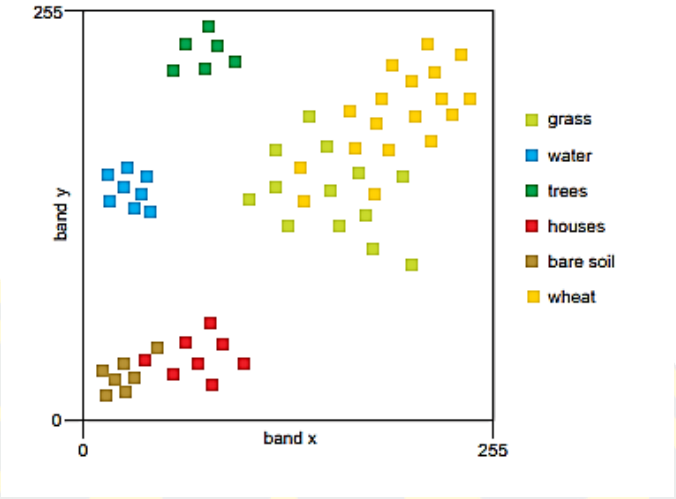

Figure 8: Feature space showing the respective clusters six classes

Figure 8 shows a feature space where feature vectors of six different land cover classes have been plotted for image classification purposes. The figure demonstrates the fundamental principle of image classification, which assumes that a particular region of the feature space corresponds to a specific land cover class. Once the classes have been identified in the feature space, each feature vector of a multi-band image can be plotted and compared against these classes, and assigned to the most appropriate class based on its proximity to the corresponding region of the feature space.

Image classification usually involves five main steps (as shown in Figure 9):

Step 1 Selection and preparation of the remote sensing (RS) images. This step involves selecting the most suitable sensor, acquisition date, and wavelength bands based on the land cover types or the specific classification needs.

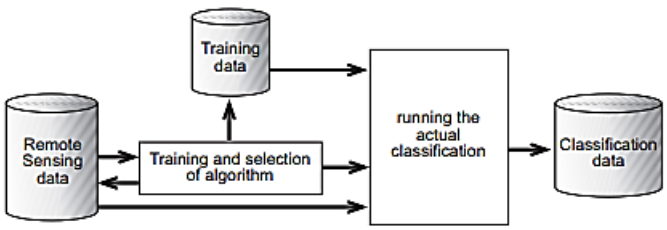

Figure 9: The classification process

Step 2 of image classification involves defining clusters in the feature space, which can be done using either supervised or unsupervised classification

approaches. Unsupervised classification uses a clustering algorithm to identify and define clusters in the feature space, whereas supervised classification relies on the operator manually defining the clusters during the training process.

Step 3 involves selecting a classification algorithm to assign pixels to their respective classes based on their feature vectors.

Step 4 involves running the classification process. After the training data have been established and the classifier algorithm selected, each multi-band pixel in the image is assigned to one of the predefined classes based on its digital numbers (DNs), as shown in Figure 10.

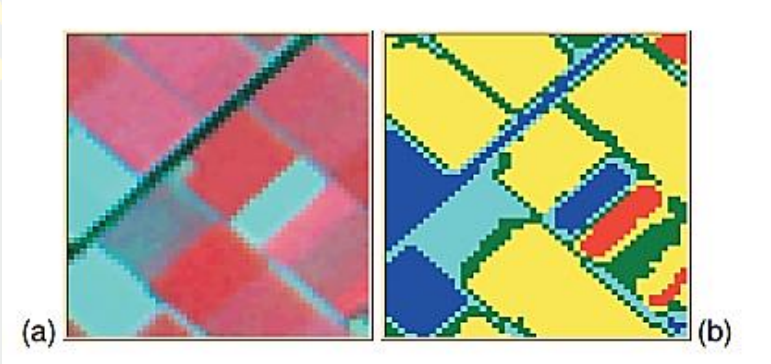

Figure 10: The result of classification of a multiband image
(a) is a raster in which each cell is assigned to some thematic class (b)

Step 5 involves validating the quality of the classified image by comparing it to reference data (ground truth). This validation process involves selecting a sampling technique, generating an error matrix, and calculating error variables.

2.3.4 Type of image classification

- Unsupervised classification is to determine the number of clusters based on the reflectance properties of objects. The image classification software generates clusters for each LULC class using the K-means clustering algorithm. This manually identifies each cluster with a LULC class and merges clusters to create a land cover type (Murai, 1993).
- Supervised classification is representative samples for each LULC class in the digital image process. The image classification software uses these training sites to identify LULC classes in the entire image such as the maximum likelihood classification algorithm (Murai, 1993).

- Visual interpretation is a complex process that involves considering various image elements and the user's experience, including color, shade, tone, shape, size, pattern, texture, and spatial components (Murai, 1993). The researcher identifies LULC by visual interpreting the image with reference to field survey data.

2.3.5 Accuracy assessment

Image classification using each technique shows a different level of accuracy. In order to analyse the final image, accuracy assessment is a vital stage in remote sensing land cover mapping investigations. The purpose of this assessment is to ensure the classification quality and build user confidence in the remote sensing product (Foody, 2002).

Congalton (2019) determined that the accuracy of remote sensing data can be influenced by the selection of sample size and the choice of sampling scheme. It is crucial to carefully consider these factors when evaluating accuracy. If sampling schemes are poorly chosen, they can introduce substantial biases into the error matrix, leading to overestimation or underestimation of true accuracy. The overall accuracy of image classification was calculated using the following formula (1).

$$\text{Overall accuracy } (\%) = \frac{\text{Total number of correct samples} \times 100}{\text{Total number of samples}} \quad (1)$$

Additionally, two other measures of classification accuracy for distinct classes, User accuracy and Producer accuracy were computed in a comparable way. User's accuracy is determined by dividing the number of pixels correctly classified within each category by the total number of pixels classified in that category. Producer's accuracy, on the other hand, is obtained by dividing the number of correctly classified pixels in a specific class by the total number of pixels in that class as identified in the reference data. This metric provides an assessment of how accurately a particular area has been classified.

These two accuracies can also be represented in relation to commission and omission errors. Commission errors refer to the pixels that were assigned to a specific class when they should have been assigned to another class. On the other

hand, omission errors indicate the percentage of pixels that should have been put into a given class following the formula (2) and (3) (Congalton, 1991).

$$\text{Producer's accuracy (\%)} = 100\% - \text{error of omission (\%)} \quad (2)$$

$$\text{User's accuracy (\%)} = 100\% - \text{error of omission (\%)} \quad (3)$$

Moreover, Congalton (1991) determined the type of error utilized to assess the overall accuracy of a classified image, which is commonly referred to as the kappa coefficient. This coefficient is widely recognized as a measure of precision as it represents the level of agreement beyond chance. The kappa statistic is derived from the error matrix and can be computed using the following mathematical formula (4):

$$K = \frac{N \sum_{i=1}^{r} X_{ii} - \sum_{i=1}^{r} (X_{i+} \times X_{j+})}{N^2 - \sum_{i=1}^{r} (X_{i+} \times X_{j+})} \quad (4)$$

Here K for Kappa coefficient
X for Pixel
N for the total number of observed pixels
r for the number of rows,
i for is the number of observations in row
j for column in error matrix
+ for total of rows and column sum

2.3.6 Satellite

1) ALOS (AVNIR-2) is the Advanced Visible and Near Infrared Radiometer type 2, which is a visible and near-infrared radiometer for observing land and coastal areas (Table 6). It provides better spatial land cover maps and land use classification maps for monitoring region environments (JAXA, 2006). According to JAXA EORC, ALOS is one of the largest Earth-observing satellites ever developed. Its objectives are:

- To provide maps for Japan and other countries including those in the Asian-Pacific region (Cartography)
- To perform region observation for "sustainable development", harmonization between Earth environment and development (Regional Observation)
- To conduct disaster monitoring around the world (Disaster Monitoring)
- To survey natural resources (Resources Surveying)
- To develop technology necessary for future Earth observing satellite (Technology Development)

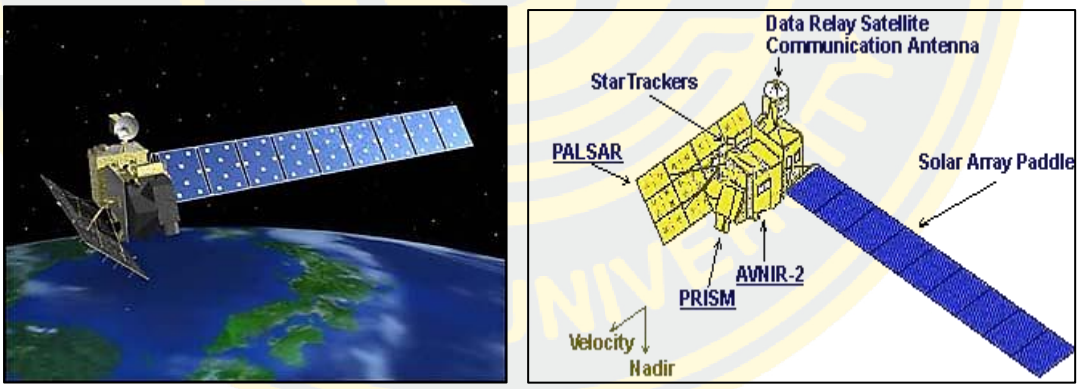

Figure 11: ALOS (AVNIR-2)

2) Sentinel-2 is the mission requirements for a twin-satellite, high revisit frequency, and high-resolution image, which support European Copernicus programs (Table 7). Observation data acquired from the Sentinel-2 mission will be utilized by services such as land monitoring, emergency management, security, and climate change (ESA Standard Document, 2015). Sentinel-2 contributes significantly to land monitoring services by providing the necessary data for mapping changes in land cover.

- Sentinel-2A satellite is the first civil optical Earth observation mission, which provide key information on the vegetation state. Sentinel-2A will be able to see very early changes in plant health due to its high temporal, spatial resolution, and 3 red edge bands. This is particularly useful for the users and policymakers for agriculture applications and to detect early signs of food shortages in developing countries.

Figure 12: Sentinel-2A (10 m) Satellite Sensor
(Satellite Imaging Corporation, 2022)

- Sentinel-2B satellite is the second Sentinel-2 satellite launched as part of the European Space Agency's Copernicus Program and its orbit will be phased 180° against Sentinel-2A. The satellite carries a wide swath of high-resolution multispectral imager with 13 spectral bands. It will provide information for agriculture and forest, among others allowing for simulation of crop yields (ESA, 2022).

Figure 13: Sentinel-2B Satellite Sensor

Main areas of using data obtained from sentinel 2A, 2B satellite:

- monitoring of agriculture areas
- inventory of agriculture areas, creation of land use plans
- monitoring of emergency situations
- inventory and assessment of forest condition
- wide range of tasks in the field of environmental protection

Table 6: The characteristics of ALOS (AVNIR-2)

Instrument	**Advanced Visible and Near Infrared Radiometer type 2 (AVNIR-2)**
Spacecraft	Advance Land Observing Satellite (ALOS)
Launch date	24th January 2006
Design life	3 - 5 years
Orbit	Sun-Synchronous Sub-Recurrent, at an angle of 98.16°, at altitude of 691.65km (at equator).
Spacecraft operations control center	JAXA and JAROS
Channel and wavelength (micrometers)	4 VNIR bands (0.42 - 0.89)
Observation Band (μm)	Band: 1: 0.42-0.50 μm Band 2: 0.52-0.60 μm Band 3: 0.61-0.69 μm Band 4: 0.76-0.89 μm
Signal Noise Rate	> 200
Incidence angle (°)	±44
Swath (km)	70
Spatial resolution (m)	10 at nadir
Temporal resolution	Repeat Cycle: 46 days, Sub Cycle: 2 days

Source: JAXA Earth Observation Research and Application Center, 2006

Table 7: The characteristics of Sentinel 2A and 2B

Instrument	Characteristics
Spacecraft	Sentinel 2A and 2B
Developer	EADS Astrium Satellites (France)
Launch date	June 23rd, 2015 (Sentinel-2A), March 7th, 2017 (Sentinel-2B)
Estimated period of operation (years)	7 years
Orbit: height, km inclination, degree	Solar-synchronous 786 98,5
Geometric revisit time	5 days from two-satellite constellation (at equator)
Spacecraft operations control center	European Space Agency (ESA)
Mass of spacecraft, kg	1200
Channel and wavelength (micrometers)	4 VNIR bands (0.42 - 0.89)
Observation Band (µm)	Band 1 Coastal aerosol: 0.443 µm (60 m) Band 2 Blue: 0.490 µm (10 m) Band 3 Green: 0.560 µm (10 m) Band 4 Red: 0.665 µm (10 m) Band 5 Vegetation Red Edge: 0.705 µm Band 6 Vegetation Red Edge: 0.740 µm Band 7 Vegetation Red Edge: 0.783 µm Band 8 NIR: 0.842 µm Band 8A Vegetation Red Edge: 0.865 µm Band 9 Water vapour: 0.945 µm Band 10 SWIR - Cirrus: 1.375 µm Band 11 SWIR: 1.610 µm Band 12 SWIR: 2.190 µm
Swath (km)	290
Spatial resolution (m)	10 m (four visible and near-infrared bands),

	20 m (six red edge and shortwave infrared bands) 60 m (three atmospheric correction bands).
Radiometric resolution, bits per pixel	12

Source: ESA and AIRBUS Defence & Space, 2022

2.3.7 LULC analysis using satellite remote sensing

The dynamics of land use changes can be monitored using remote sensing data. The accessibility of remote sensing data has made it possible to detect changes to the Earth's surface using a wide range of resolution variations, including spectral, spatial, radiometric, and temporal (Yulianto, Suwarsono & Sulma, 2018).

According to Xiaomei and Rong Qing (1999), it is essential to have knowledge on the current land use/land cover. It's also critical to be able to track changes in land usage due to the needs of an expanding population as well as natural factors that are reshaping the terrain. Due to several natural and artificial processes, the land is constantly undergoing change.

Remote sensing imageries provide an efficient means of obtaining information on temporal trends and spatial distribution of urban areas needed for understanding, modeling and projecting land change (Parveen, 2018).

Thus, remote sensing data have been used widely for land use/land cover identification of various features of the land surface from satellites. Classification in remote sensing involves clustering the pixels of an image to a set of classes, such that pixels in the same class are having similar properties. The detection of the spectral response patterns of land cover classes that can be used for LULC analysis provides the basis for image classification (Eastman, 2003).

2.4 Geographic Information System and spatial analysis

P.L.N. Raju (2006) identified that Geographic Information System (GIS) is used by multi-disciplines as tools for spatial data handling in a geographic environment. The basic elements of GIS consist of hardware, software, data and liveware. GIS is considered one of the important tools for decision making in problem solving environments dealing with geo-information.

In 1980, architect Jack Dangermond founded the company Environmental Systems Research Institute (ESRI) was established and is one of the group's developers of GIS which develop the ability to rewrite structured data as a grid system known as raster analysis. Computer technology has created a GIS system capable of handling large amounts of data. In the recent, GIS is attempted to improve mapping methods to be more accurate coupled with the development of spatial analysis methods which helps greatly in the analytical ability of GIS (Berlin, P., Frunzi, N., Napoleon, E. & Ormsby, T., 1999). Therefore, data analysis is more accurate than before, and GIS has become a tool for urban planning and research.

2.4.1 GIS for land use planning

Irina Strielko and Paulo Pereira (2014) determined that GIS simplifies territorial plan operation by analyzing the spatial relationship that allows for carrying out complex assessments of the situation and creates a basis for scientifically reasonable decisions in the course of land use. GIS allows the integration of diverse spatial data, for example, data about soils, climate, and vegetation, and also to visualize available information in the form of maps, graphs or charts, and 3D models.

Based on the results of the analysis made by GIS, it can provide suitable solutions for land use that provide the optimal minimum impact on the environment, and make decisions of conflict associated with land use. For a variety of land management objectives analysis method is chosen based on the variables of the problem and variables of use.

2.4.2 GIS and RS techniques to detect LULC Change

GIS and RS have the potential to provide accurate information regarding LULC changes. These are useful tools for measuring the change between two or more periods. It can incorporate multi-sources of data into a change detection platform (D. Lu et al., 2004).

For example, the use of multiple layers, such as classified images, topographical maps, soil maps, and hydrological maps provides a greater ability to extract useful information about the changes over a particular area. Moreover, GIS can measure the trends in these changes by modeling the available data and using statistical and analytical functions. The advantage of GIS is that it offers several outputs in various formats (such as maps or tables), allowing users to choose the best output for obtaining the needed information (Abdullah F. Alqurashi & Lalit Kumar, 2013).

Abdullah F. Alqurashi and Lalit Kumar (2013) identified the major techniques that are utilized to detect LULC changes by integrating remotely sensed data with GIS data. They reviewed change detection techniques in many applications, including LULC changes, vegetation and forest changes, urban changes, environmental changes, crop monitoring, forest fires, deforestation, and other applications (Table 8).

Table 8: Examples of the applications using change detection techniques

Application	Most commonly used techniques
Land use/Land cover change	Image differencing, image ratioing, *NDVI, *CVA, *PCA, chi-square, post-classification, hybrid change detection, *ANN, decision tree, GIS
Urban change	Image differencing, post-classification, hybrid change detection, PCA, GIS, chi-square, image fusion
Environmental change	NDVI, ANN, CVA, post-classification, image differencing
Vegetation change	NDVI, CVA, image differencing, post-

	classification
Landscape change	Post-classification, GIS
Deforestation	Post-classification, NDVI, image differencing, PCA
Wetland change	Post-classification, GIS

Noted * NDVI = Normalized Difference Vegetation Index, CVA = Change Vector Analysis
PCA = Principal Component Analysis, ANN = Artificial Neural Networks

They pointed out that all the techniques discussed above are based on pixel-by-pixel change detection analysis of satellite images as well as being based on images only. It is important to use the benefit of collateral information, such as digital elevation models, hydrology, and soil maps which can be provided with the extracted information from RS images into GIS platforms. Thus, the accuracy of the results could be increased by combining RS with GIS data.

2.5 LULC dynamics

Land resources are very important natural resources that serve social, economic, and ecological purposes to ensure the survival of the population (Nunes & Auge, 1999).

The land is described as the area where all human activities take place. People's use of land resources results in "land use" that varies depending on the objectives it serves, including food production, shelter supply, recreation, the extraction and processing of commodities, and the bio-physical properties of the land itself. Consequently, two major sets of forces human demands and environmental characteristics and processes influence how land is used (Turner, 1994).

As Watson et al. (2000), As Watson et al. (2000), land cover is a physical feature of the Earth's surface, but land use is described as how the land is exploited by people and their habitats, typically with a focus on a functional role for land in economic activity (Watson et al., 2000).

Moser (1996) identified the term land cover originally referred to the type of vegetation that covered the land surface, but it has since expanded to apply to other elements of the physical environment, including soils, biodiversity, surfaces, and groundwate.

Meyer and Turner (1996) described there are three ways that land cover might change as a result of land use activity: (1) converting the entire piece of land into a new state; (2) modifying circumstances without a full conversion; and (3) maintaining its condition against natural agents of change. Understanding the importance of the land cover and simulating the effects of land cover change is mainly limited by the lack of accurate land cover data and up-to-date information on land cover and land cover change are required for many applications (Foody, 2002).

According to the “land use” and “land cover” can be determined that LULC dynamics are a well-known, accelerating, and substantial process, mostly driven by human activities, that is contributing significantly to forest fragmentation, land degradation, and biodiversity loss (Maitima et al., 2009). Today, monitoring and mediating the adverse consequences of LULC has become a major priority of researchers and policy makers around the world (Erle, 2007).

2.6 The Cellular Automata and Markov Chain model (CA-Markov)

The CA-Markov model is suitable for detecting land use change and simulation because it considers the spatial and temporal components of land cover dynamics (Hyandye & Martz, 2017).

CA-Markov is a model that combines the Markov Chain and Cellular Automata techniques can be used to simulate land use over the coming year. In addition, the CA-Markov software, which was created by the Clark lab at Clark University, can be used for modeling and land use simulation.

Basically, the CA consists of the following components: The following elements are presented in a cell space or lattice: 1) a finite set of cell states, 2) a definition of a cell's neighborhood, 3) a set of transition rules to calculate a cell's state change, 4) a set of time steps in which all cell states are simultaneously updated (White & Engelen, 2000) (Figure 14). The CA model also requires GIS-based input as image format such as land use maps, road maps, protected areas, etc.

Singh (1989) identified that the CA can perform the spatial dynamics and time explicitly. CA can be combined with the spatial component, and it can deal with dynamism using straightforward rules that improve computing efficiency.

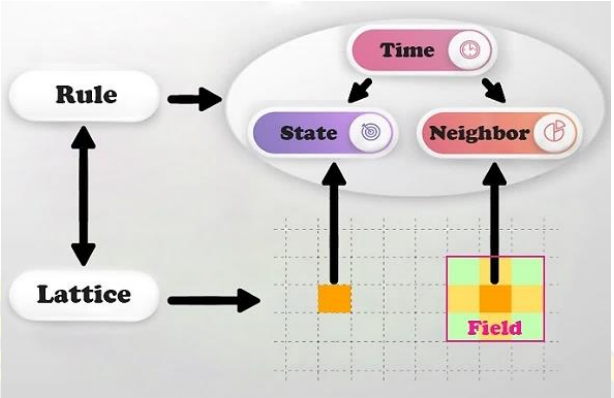

Figure 14: Five components of CA: lattice, cell state, neighbor, transition rule and time (White & Engelen, 2000)

The Markov model is a statistical model to calculate the transition probability matrix between two states. Thomas and Laurence (2006) determined that Markov Chain is a stochastic process model that can describe the change probabilities of one object to another object. The model is one of the recommended methods for land use modeling based on the time evolution trend.

Both the “Cellular Automa” and the “Markov Chain” models are considered to be discrete dynamic models in time and state (Ye & Bai, 2007). A combination of Markov Chain and Cellular Automata used together presents considerable advantages for modeling land use changes (Guan et al., 2011).

Yang, Zheng, and Chen (2014) identified that the steps are be taken to implement the CA-Markov model for simulated land use, namely:

(a) Calculate the transition area matrix using Markov Chain;

(b) Generated transition potential maps;

(c) Simulated LULC map using CA model;

In the first stage, the transition matrix calculations are performed to generate probabilities area the possibility of a change in land uses class becoming more land use class within a certain period, which can be served by formula (5):

$$P_{(N)}=P_{(N-1)}\times P, \tag{5}$$

Here P is the probabilities transition matrix on land use types derived from two different years on land use map. $P_{(N)}$ is a state opportunity during or simulations of the near future (probability of any state times). $P_{(N-1)}$ is the initial state opportunities (preliminary state probability).

In addition, the calculation on that analysis also generates probabilities transition matrix which is the probability of each pixel of the land use class to turn into another land use class. The calculation can be presented in formula (6). The accuracy of the results of the estimation matrix transition area and transition probability matrix is determined based on the value of the error probabilities are 15% (Yang, Zheng, & Chen, 2014).

$$A = \begin{bmatrix} A_{11} & A_{12} & \dots & A_{1n} \\ A_{21} & A_{22} & \dots & A_{2n} \\ . & . & . & . \\ . & . & . & . \\ . & . & . & . \\ A_{n1} & A_{n2} & \dots & A_{nn} \end{bmatrix}, \quad (6)$$

Here A is the transition matrix area. A_{ij} is the total area of land use class i to class j for year simulation from the starting point to the target of the simulation period. n is the number of land use types.

Besides, the second stage, transition potential map simulation based on a CA-Markov model, which is used as a controlling factor for land use spatial distribution. Map of potential transition at earlier stage opportunities created by the transition matrix.

In stage three is simulation land use. The process can be carried out within the framework of the spatial CA-Markov module that can be presented in formula (7) (Thomas & Laurence, 2006). The process takes time iteration, the integration of the transition matrix area, the map of potential transition, and land use to be simulated at the time in the next future (Yang, Zheng, & Chen, 2014).

$$\text{if } S_j = \max (S_1, S_2, \dots, S_n) \text{ and } \text{Area}_{ij} < \frac{A_{ij}}{T} \text{ then } C_i \rightarrow C_j, \quad (7)$$

Here S_j is a class of potential land use that will transit to land use class j. Area ij is the total area of land use from land use class i to class *j* in the iteration process. T is the iteration time. C_i is the i^{th} land use class.

2.7 Relevant research review

Rahel Hamad, Heiko Balzter, and Kamal Kolo (2018) studied simulating land use/land cover changes using a CA-Markov model under two different scenarios. They utilized multi-temporal Landsat imagery from 1993, 1998, 2003, 2008, and 2017 to generate LULC maps, which were subsequently used in the CA-Markov process. The results indicated an accuracy of over 80% in all stages and showed promise for the accuracy and reliability of the CA-Markov modeling approach. The study demonstrated the versatility of remote sensing, GIS, and LULC change models as effective tools for mapping and monitoring changes in land use/land cover. However, traditional methods were found to be lacking in their ability to consider environmental, social, or demographic conditions. To address this limitation, the authors suggested combining CA-Markov with multi-criteria evaluation (MCE) and analytic hierarchy process (AHP) models to better capture dynamic growth in urban areas.

Md Surabuddin Mondal (2019) studied CA-Markov modeling of land use and land cover dynamics and sensitive analysis to identify sensitive parameters. They utilized land use land cover (LULC) maps derived from Landsat MSS image of 1987 and Landsat TM image of 1997 to predict the future land use and land cover of 2007 using a Cellular Automata Markov model. They conducted sensitivity analysis to identify the most influential land use and land cover parameters in the simulated results. The study concluded that the CA Markov land use and land cover simulation and forecast model is a significant approach that combines the CA and Markov chain analysis to account for the complexity of land use and land cover changes through multi-criteria evaluation (MCE) and multi-objective land allocation (MOLA). By incorporating suitable driver variables, the model can produce results that are close to reality. The simulation results provide more than just a probability and offer valuable spatial information to reveal the dynamic of land use and land cover and explore spatiotemporal patterns and distributions of land use and land cover in different scenarios for future forecasting. Their results of sensitivity analysis of all variables indicate that land with or without scrub appeared to be most important sensitive parameter, which has highest influence on predicted results of LULC of 2007 and the agricultural fallow land came out to be the least sensitive parameter, which has least

influence on predicted results of LULC of 2007. The validation of CA Markov land use land cover prediction results shows K standard is 0.7928.

Mas (2017) summarized land use/land cover change detection by combining automatic processing and visual interpretation. They used a classification technique that made it possible to quickly and accurately produce detailed 1:50,000 maps for the years 2004, 2007, and 2014 (one month per date by three GIS/RS technicians). This was made possible by the use of automatic processing for analyzing large amounts of data in a short time and traditional cartographic methods such as visual interpretation, which facilitated the detection of deforestation at a detailed level and enabled supervision of the process. The result land use/land cover change map in previous and later dates was an overall accuracy of 83.3%.

Fajar Yulianto (2018) studied the dynamics of land use change and its simulation based on the integration of remotely sensed data and the CA-Markov model, in the upstream Citarum Watershed, West Java, Indonesia. They conclude that land use change becomes major problem with increasing the disappearance of undeveloped land and catchment area which may result in an increase in surface runoff, and river flow during the rainy season and cause flooding. Based on the input land use pattern and changes over about 20 years, the CA-Markov model was employed as a method for modeling and land use simulation in the next few years. Land use classification outcomes from 2016 served as the foundation for land use reference modeling carried out throughout the CA-Markov model's training phase. The outcomes of this study can then be included in subsequent research that investigates the effects of changing land uses in the study area.

Aqil Tariq (2020) studied seasonal land surface temperature and land use land cover change using optical multi-temporal satellite data of Faisalabad, Pakistan by using CA-Markov Chain analysis. CA-Markov-Chain was developed for simulating long-term landscape changes at 10 years time steps from 2018 to 2048. They conclude that unless control measures are taken, the acceleration of urbanization will increase warming and lead to higher temperatures in the future. are crucial for warning urban planners about the effects of possible temperature changes and urban residents' thermal comfort on future expansion. They recommended that additional research be done to see whether these strategies and methods are practical at both the global and

national levels of geography. The identification of spatial distribution changes was done using the CA model, and the simulation of temporal resolution was done using Markov Chain Analysis. Researchers and decision-makers will utilize this model in the future to develop new regulations to government and control urban expansion.

Carlos Javier Puig (2002) studied digital classification and visual interpretation as methods for analyzing land use and land cover in humid tropical forests of the Peruvian Amazon. The researchers found that both classification methods were comparable in terms of their Kappa statistics, although digital classification provided better spatial detail. However, adapting the classes to a classification scheme proved to be difficult for digital classification, which required more time for editing and processing to reduce errors. Visual interpretation, on the other hand, is preferred for low and medium-resolution satellite images but is limited in its application to high-resolution imagery due to the increased details that need to be recognized. The researchers concluded that visual interpretation was shown to have a similar quality to digital classification for analyzing medium-resolution satellite data. However, the increase in spatial resolution for the new generation of satellites could present a limitation for future studies due to the increased details that need to be identified, requiring more processing time.

Emanuele Loret (2002) studied urban sprawl monitoring over the entire district of Rome through a joint analysis of ALOS AVNIR-2 and Sentinel-2A data. They demonstrated the utility of the application of innovative GIS urban area profile indicators, derived from multi-temporal and multi-source optical remote sensing imagery, for assessing both the spatiotemporal dynamics and the extent of urban sprawl phenomenon over the entire municipality of Rome. Accurate mapping of land cover from high resolution Advanced Visible and Near Infrared Radiometer type 2 (AVNIR-2) sensors from Advanced Land Observing Satellite (ALOS) and Sentinel-2A optical datasets provided essential input to urban expansion analysis. They identified that based on comparisons with their previous work, they found that ALOS AVNIR-2 and Sentinel-2A data provided more accurate land cover/land use classification of the district of Rome. Sentinel-2A mission is routinely providing global high-resolution optical imagery and offering enhanced continuity of SPOT and Landsat-type data.

CHAPTER 3
MATERIALS AND METHODS

This chapter describes the data and methodology used in this study. The remote sensing data and classification identify LULC change. Then, LULC simulated by using CA-Markov model results will be analyzed and discussed. In general, the six major components are used to derive the outcome of the research such as the outcomes of the research, such as data collection and preparation, image classification, accuracy assessment, CA-Markov model implementation, model validation, and LULC simulation outputs analyzed under 3 scenarios.

3.1 Materials

This study requires material and software to reach the purpose including:

- Computer: Intel I7- 5500U Processor, Nvidia Geforce GT940M 2GB DDR3, Memory 12 GB DDRIII, and Hard Disk 1 TB.
- ESRI ArcGIS 10.8 software is used for data preparation and analysis tools.
- TerrSet version 19.0.7 (2020) Geospatial Monitoring and Modeling Software is used for validation results and CA-Markov model implementation to simulate LULC output.
- Satellite imagery from Sentinel 2A, Sentinel 2B, ALOS (AVNIR-2)

3.2 Data collection and preparation

3.2.1 Satellite imagery

In this study, the satellite images of ALOS (AVNIR-2) and Sentinel-2 are obtained from https://scihub.copernicus.eu/dhus and https://search.asf.alaska.edu with a spatial resolution of 10 m. (Tables 9 and 10). For this study, the highest images that can be taken start in 2009.

Table 9: Satellite imagery used in this study

Data Type	Frame	Acquisition date	Season
ALOS (AVNIR-2)	130/3340 (10 m.)	15 January 2009	Winter
ALOS **(**AVNIR-2)	130/3340 (10 m.)	21 January 2011	Winter
Sentinel2A	47PQQ/ (10 m.)	27 January 2017	Winter
Sentinel2B	47PQQ (10 m.)	06 January 2022	Winter

Table 10: ALOS (AVNIR-2) and Sentinel-2 Satellite Sensor Specifications

Character	Specification	
	ALOS (AVNIR-2)	Sentinel-2
Sensor	Panchromatic (PRISM): 2.5 m Multispectral (AVNIR-2): 10 m SAR-L (PALSAR): 10 & 100 m	Multispectral Imager (MSI): 10 m (4 visible and near-infrared bands) 20 m (6 red edge and shortwave infrared) 60 m (3 atmospheric correction bands)
Spectral Range	Pan: 0.52-0.77 µm Band 1 Blue: 0.42-0.50 µm Band 2 Green: 0.52-0.60 µm Band 3 Red: 0.61-0.69 µm Band 4 NIR: 0.76-0.89 µm SAR-L: Frequency 1.3 GHz	Band 1 Coastal aerosol: 0.443 µm Band 2 Blue: 0.490 µm Band 3 Green: 0.560 µm Band 4 Red: 0.665 µm Band 5 Vegetation Red Edge: 0.705 µm Band 6 Vegetation Red Edge: 0.740 µm Band 7 Vegetation Red Edge: 0.783 µm Band 8 NIR: 0.842 µm Band 8A Vegetation Red Edge: 0.865 µm Band 9 Water vapor: 0.945 µm Band 10 SWIR - Cirrus: 1.375 µm Band 11 SWIR: 1.610 µm Band 12 SWIR: 2.190 µm
Swath width	70 km	290 km
Launch date	24 Jan 2006	Sentinel-2A June 2015 Sentinel-2B July 2016
End of life	22 Apr 2011	7 years

3.2.2 Data Specification

Data collected in this study derive from the Department of Public works and Town & country planning (DPT) and the Department of Provincial Administration (DOPA). This study utilized data of GIS digital data for analysis of the study area. The details of the data set detailed input are described in Table 11. For scenario analysis, the draft of the Bang Lamung city plan is brought to categorize into the land use major class such as urbanization area, control area, and protection area (Table 12 and Figure 15).

Table 11: Data availability for the study

Data types	Type	Source
City plan	Spatial data	DPT
Bang Lamung boundary	Spatial data	DPT
DEM	Spatial data	ALOS
Road	Spatial data	DPT
Railway	Spatial data	DPT
Population	Attribute data	DOPA

Table 12: The category of the land use major class in the study

Categories of land use major class	Class description and planning area types
Urbanization area	Resident, commercial area, and involve industry area with covering in city plan and the area that the governor promotes for urbanization
	 Residential land with low population density.
	 Moderately densely populated residential land.
	 Highly densely populated residential land.
	 Land for commercial.
	 Special economic zone for special businesses.
	 Industrial and warehouse land.
	 General industrial land that is not toxic.

Categories of land use major class	Class description and planning area types
	ศึษ. Land for educational institutions.
	ศน. Land for religious purposes.
	ส. Land for government institutions.
Control area	Agriculture involves the environmental preservation area
	ก.1-ก.2 Rural and agricultural land.
	Conservation of rural and agricultural land.
	Land reform for agriculture purposes.
	ล. Recreation and environmental preservation.
Protection area	Areas where urbanization is prohibited such as forest, nation park, and conservation area
	Land preservation for environmental tourism
	Forest conservation land.

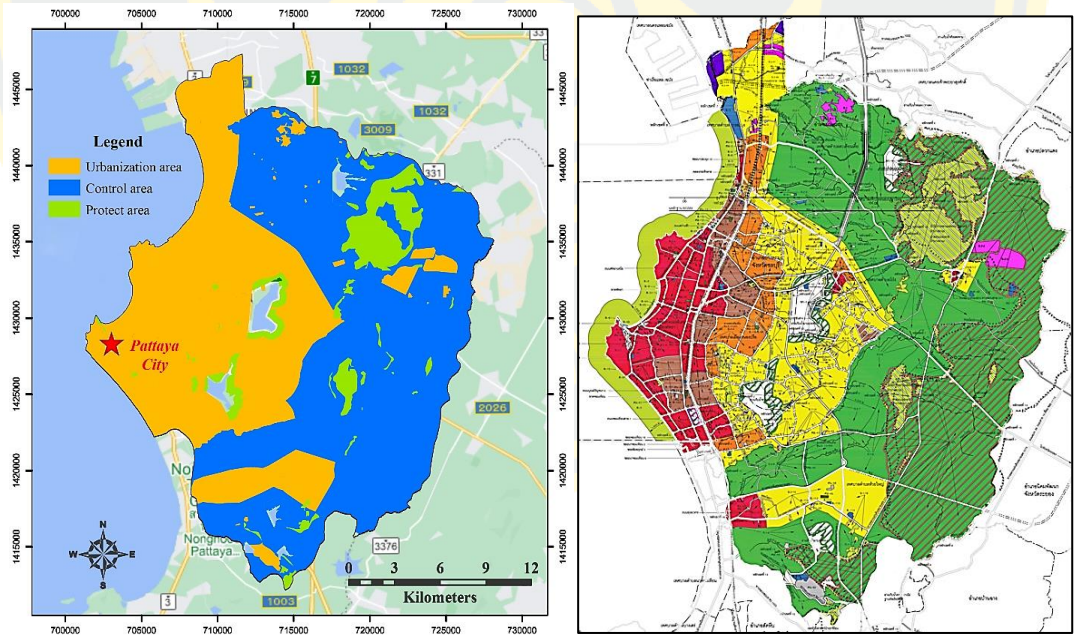

Figure 15: The category of the land use the major class: Urbanization area, Control area, and Protection area and land use type of Bang Lamung city plan

- Population of Bang Lamung district

For the population projection in this research use the amount of population only appears in the civil registration from Bureau of Registration Administration (DOPA), which does not include non-registered population in the study area. The calculation method, the exponential method is used according to the consideration criteria of the Department of Public Works and Town & Country Planning, which is a normal continuous growth rate (Town & Country Planning Standards Development Bureau, 2006). The researcher used the highest population growth rate of 4.64 (Table 13). The formula (8) for calculating the population growth rate is as follows:

$$r = \frac{\log(P_n/P_0)}{n \log_e} \quad (8)$$

Here r for Population growth rate

P_0 for Population (total) at the beginning of the study period

P_n for Population (total) at the end of the study period

n for Number of years between the beginning and the end of the study period

$\log_e$ for Constant value 0.434294

Table 13: Population growth rate in Bang Lamung district

District	Population					
	2011	2017	2022	Rate of Growth		
				2011-2017	2017-2022	2011-2022
Bang Lamung	246,268	260,834	328,961	1.15	4.64	2.89

In addition, population projection is also calculated by using the mathematical calculation formula according to the criteria of the Department of Public Works and Town & Country. The projection is divided into 5 years intervals. Here is the formula (9):

$$P_n = P_0 e^{rn} \quad (9)$$

Here P_n for Population in the target year to be projected

P_0 for Population at base year

r for Population growth rate

n for Number of years between the base year and the target year

e for Constant value 2.718

3.3 Methods

3.3.1 Image-preprocessing

In this study, the remote sensing images of ALOS (AVNIR-2) and Sentinel 2A and 2B are used for creating LULC base maps. In order to assure the accuracy of the extracted LULC maps, all the acquired images are cloud-free (<10%) and are taken in the same seasons in 2009, 2011, 2017, and 2022. In pre-processing stage followed by the atmospheric and radiometric correction are performed. For geometric correction, all data from ALOS (AVNIR-2) and Sentinel -2 have been already geometrically resolved.

3.3.2 Satellite image classification

Due to the different satellite sensors used, the false color composite of RGB band for ALOS (AVNIR-2) is RGB: 421 and Sentinel-2 is RGB: 843. This false color composite images are used to identify of LULC classes by the visualization method (Figure 16-17).

3.3.3 Image classification

Techniques for classifying images come in several forms. In this study, the satellite image is digitized to create LULC maps based on the researcher's knowledge of the study area. To analyze the dynamics of LULC, the classification of LULC is categorized into major classes and sub-classes. The major classes are grouped into 3 types following three major types of Bang Lamung city plan. The sub-classes are grouped into 5 types of land use such as built-up, agriculture, open space, forest, and water bodies. This sub-class is based on the Land Development Department (LDD), Thailand. The details of LULC classes are described in Table 14.

Table 14: Land use land cover class details

Major class	Sub-class name	Class Description
Urbanization area	Built-up	Includes artificial constructions (e.g., concrete, urban areas, industrial areas) including golf course
Control area	Agriculture	Cultivated agriculture including crops, farms, and orchards.
	Open space	Bare soils, bushes, dry land, and meadows including grass along the river and canal

Major class	Sub-class name	Class Description
Protect area	Forest	Forest and nation park
	Water bodies	Includes both natural and artificially created water bodies such as rivers and ponds.

A) 2009 ALOS (AVNIR-2) RGB: 421

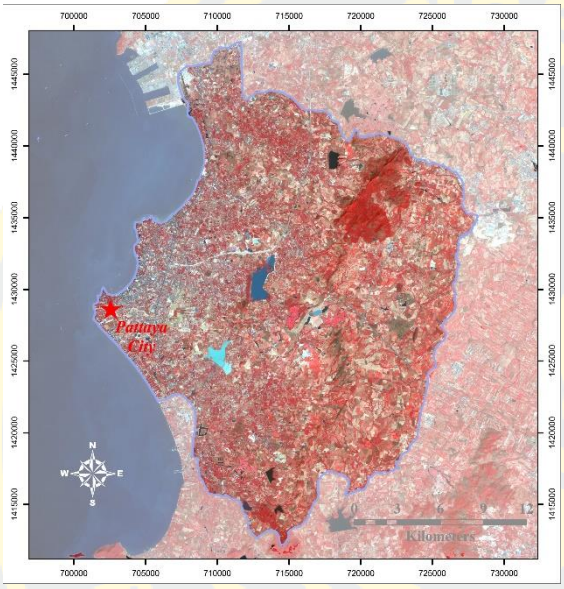

B) 2011 ALOS (AVNIR2) RGB: 421

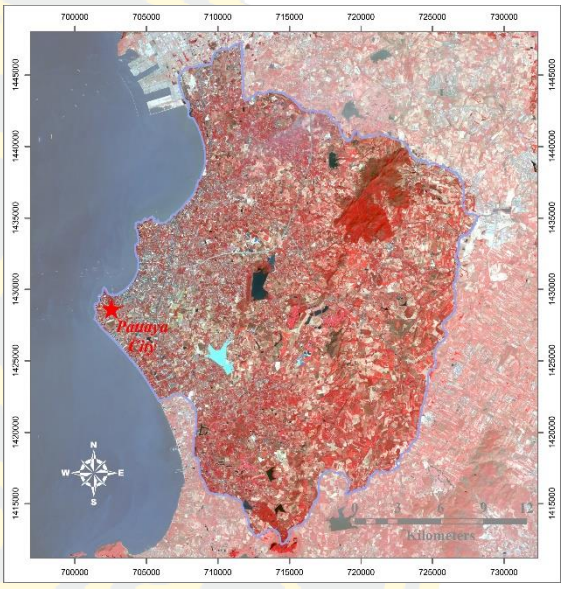

C) 2017 Sentinel 2A RGB:843

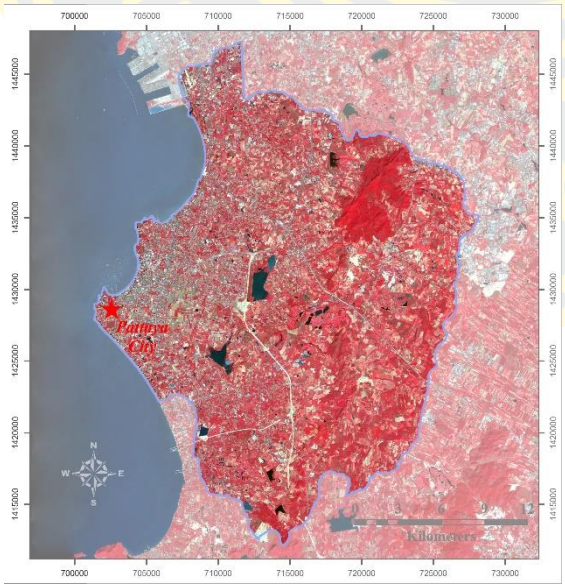

D) 2022 Sentinel 2B RGB:843

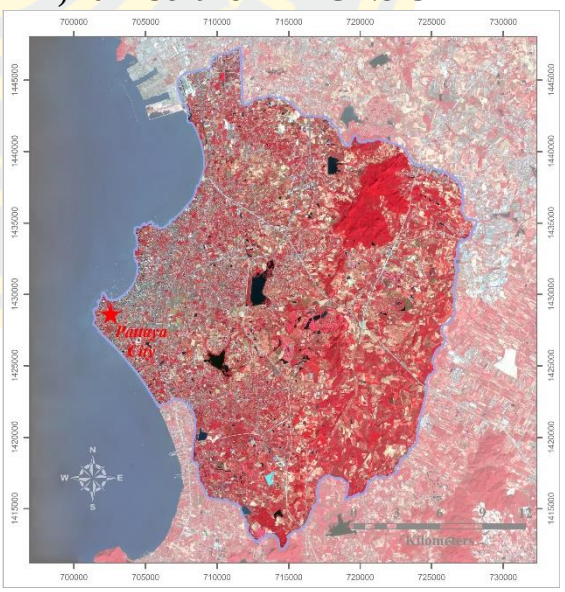

Figure 16: The color composite of RGB band for the image classification of the years 2009 (A), 2011(B), 2017 (C), and 2022 (D)

A) 2009 ALOS (AVNIR-2) RGB: 321

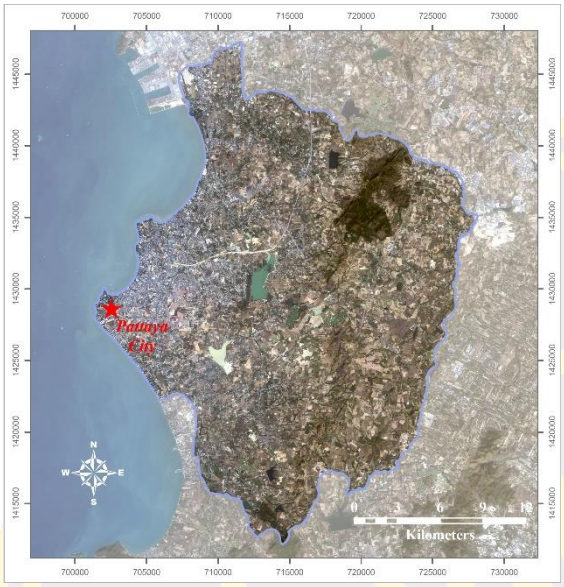

B) 2011 ALOS (AVNIR-2) RGB: 321

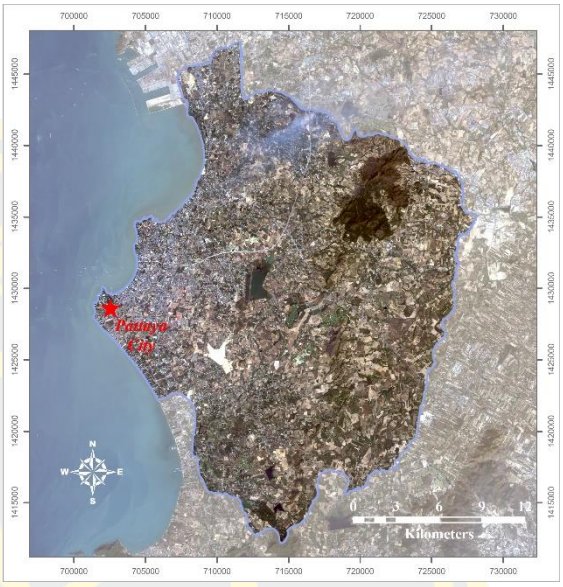

C) 2017 Sentinel 2A RGB:432

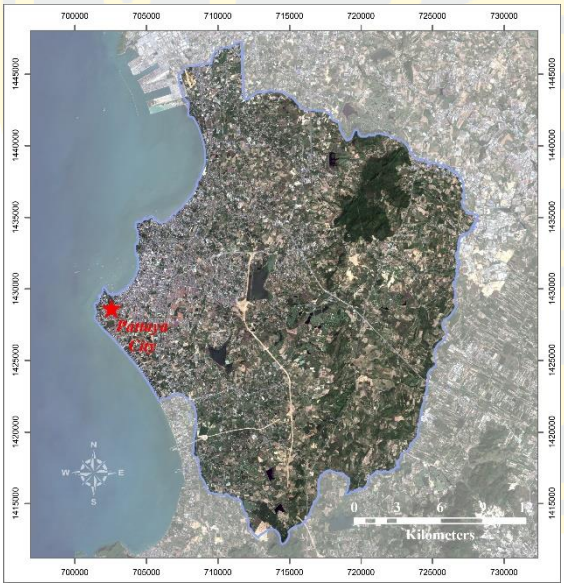

D) 2022 Sentinel 2B RGB:432

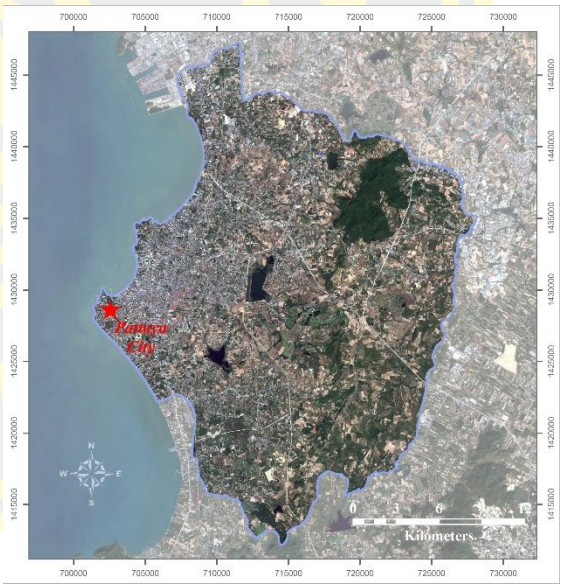

Figure 17: The natural color band combination of the years 2009 (A), 2011(B), 2017 (C), and 2022 (D)

3.3.4 Accuracy assessment of classification

The accuracy assessment process is taken to classify the LULC 2022 map which derive from the satellite image compared to the same area in the field. The sample ground truth is 200 points. In this study, the method of accuracy assessment is based on ground truth in order to derive the accuracy of classification images and calculate the error matrix.

The result of the accuracy assessment provides overall accuracy, user's accuracy, and producer's accuracy of the LULC map. The kappa coefficient formula which calculates the error from classification images described in Chapter 2 (Congalton, 1991).

3.3.5 Cellular Automata-Markov Model

The cellular automata-Markov (CA-Markov) model is composed of the cellular automata model and the Markov model. The Markov model is a statistical model for calculating the transition probability matrix between two states (Jokar Arsanjani, 2013). By combining the cellular automata model and the Markov model, the spatiotemporal distribution of LULC can be simulated (Gong et al., 2013).

The component of a CA-Markov model is a Markov model. A Markov LULC model takes into consideration temporal transitions through a Markovian process. In a Markovian process, the status of a cell in period t + 1 is characterized by its status in the previous period, t. The change from one period to another is defined by the transition probability matrix (Hyandye and Martz, 2017) which can be described in a matrix as follows formula (10).

$$P = P_{ij}, \tag{10}$$

Here P_{ij} denotes the probability of changing from a status i to a status j. The probability has the following formula (11) and (12).

$$\sum_{j=1} P_{ij} = 1, \tag{11}$$

$$0 \leq P_{ij} = 1 \tag{12}$$

Here $P_{(N)}$ denotes a probability in period N, and $P_{(0)}$ denotes a probability from the land use data. With these properties of the probability transition matrix, a Markov model can be used to simulate future land uses from the current ones (Gil et al., 2005).

In this study, the steps of the CA-Markov model have been used TerrSet 19.0.7 software. The simulation process can be shown in Figure 18.

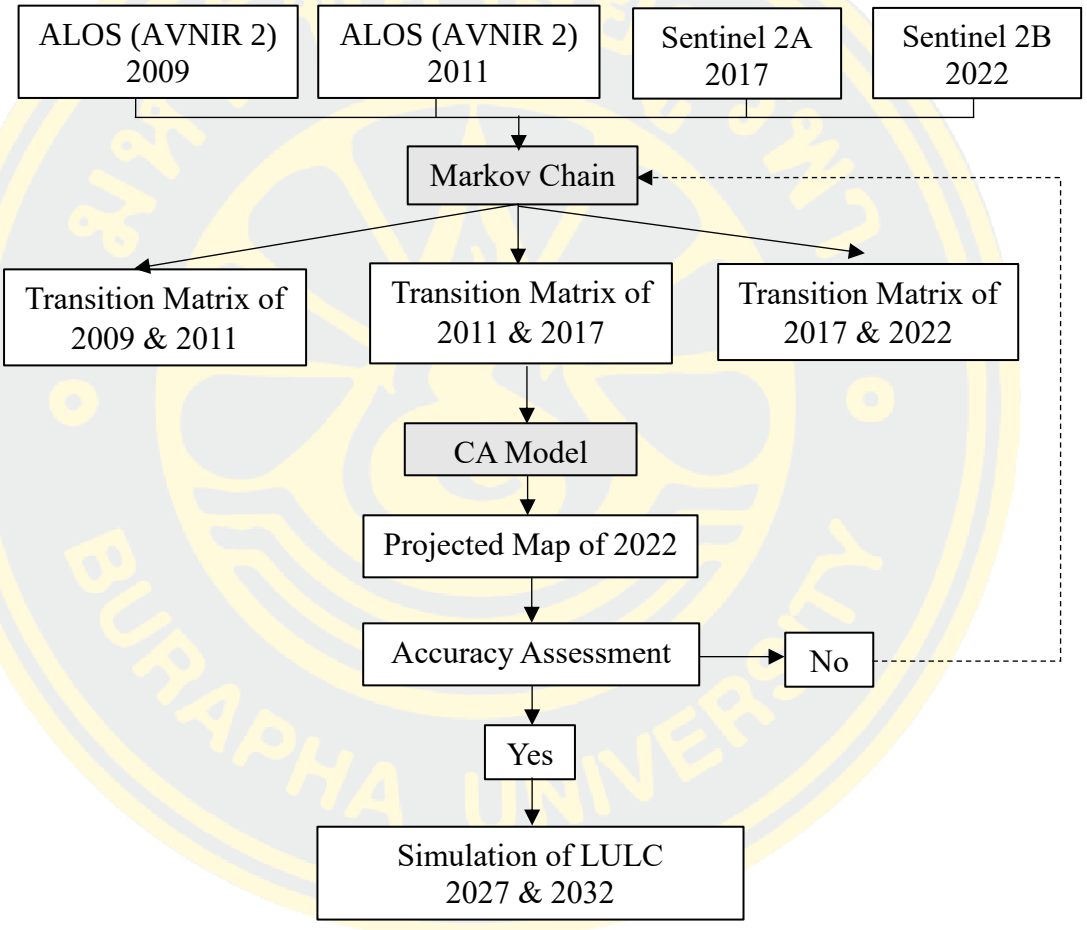

Figure 18: The simulation process in the CA-Markov model

3.3.6 Model validation

For the model validation, the simulated LULC 2022 is compared to the actual LULC 2022 by using the Kappa Indices of Agreement and related statistics (Landis & Koch, 1977) for calibration. After the model is validated, it will be used to simulate LULC for the years 2027 and 2032.

As shown in Figure 19, the LULC of 2022 is simulated by using the 2011 and 2017 LULC maps to measure the agreement between two images: the "comparison" map (simulated LULC 2022 map) and the "reference" map (actual LULC 2022 map). The comparison map is generated by the CA-Markov model, which must be validated against the reference map representing reliability.

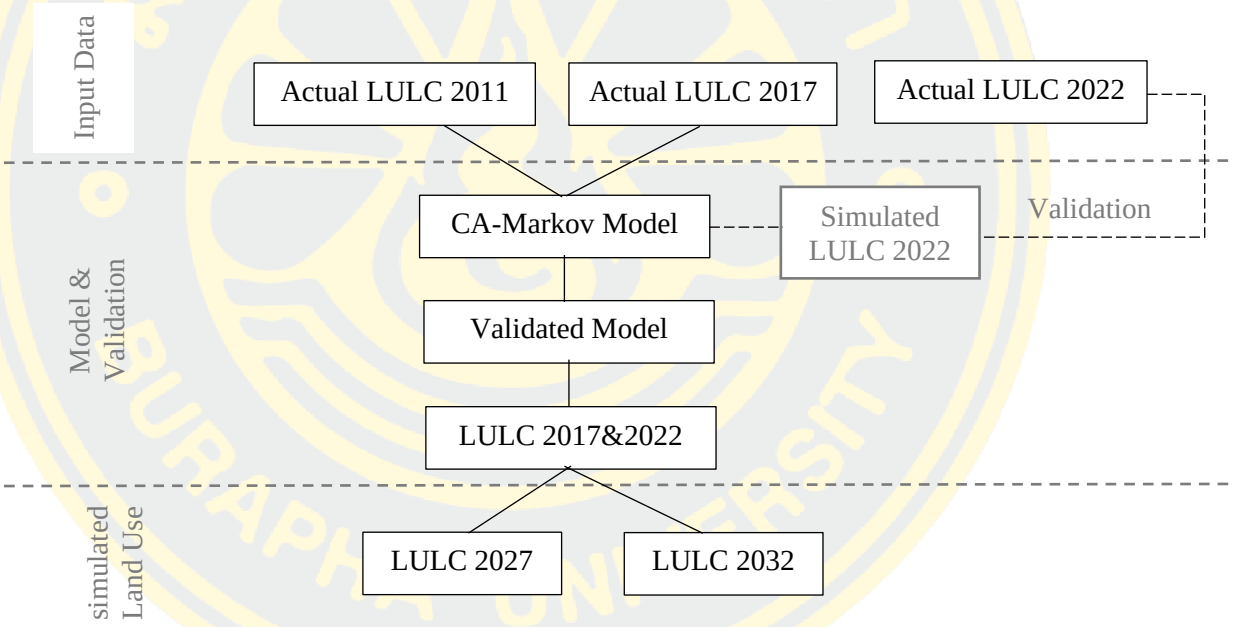

Figure 19: The procedure of validation

3.3.7 Simulation of LULC in 2027 and 2032

The LULC classified maps of 2017 and 2022 are used to generate a transition map, which are then input into the CA-Markov model to simulate LULC in 2027 and 2032. The simulations are conducted for analyzing under 3 scenarios as follows:

- The spontaneous scenario: This scenario analysis the trends of normal LULC changes observed from 2009 to 2022 and will continue until 2027 and 2032.

- The green area improvement scenario: This scenario analysis the trend of green area changes and the sufficient of green area per population in each sub-district.
- The area comprehensive plan scenario: This scenario analysis the LULC change by comparison of LULC map simulation in 2027 and 2032 with the current Bang Lamung city plan.

3.4 Basic Model Overview

In this study, the methodology involves satellite image classification to generate LULC maps for the years 2009, 2011, 2017, and 2022. These maps are utilized to calculate a transition probability matrix which is then incorporated into the CA-Markov model to produce a simulated LULC 2022 map. The result from the simulated LULC 2022 map is compared to the actual classified LULC 2022 map for the validation process. Then, LULC maps between 2017 and 2022 are used to perform LULC map simulation in 2027 and 2032 and analyze under 3 scenarios, as depicted in Figure 20.

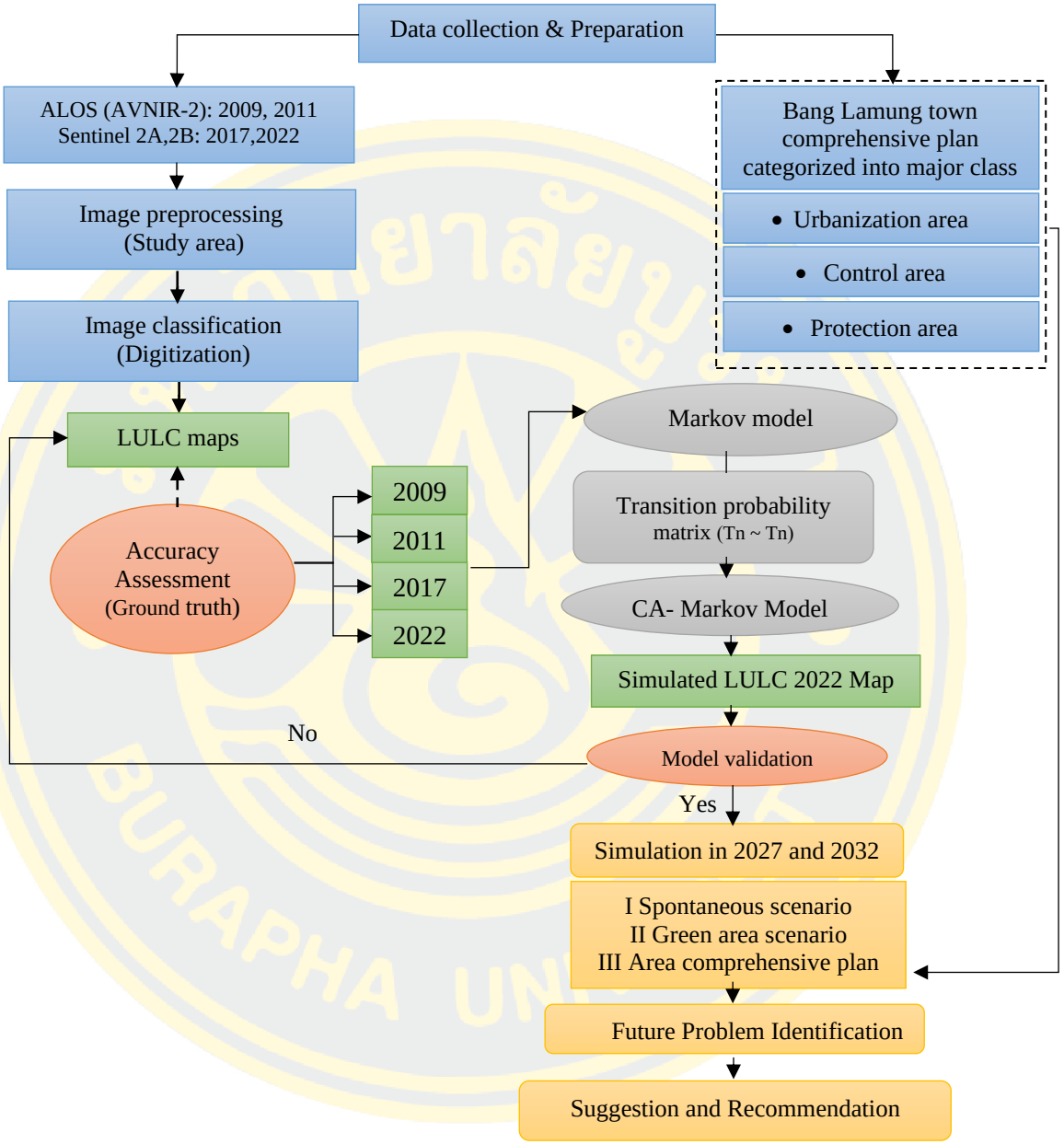

Figure 20: The Methodology for LULC simulation and scenario simulation

CHAPTER 4
RESULTS

In this chapter, the CA-Markov model is introduced as a tool to examine the changes in land use/land cover (LULC) by analyzing historical data in Bang Lamung district. The methods proposed in the previous chapter are applied to assess effectiveness and gain insights into LULC change in the study area. The findings of this analysis are presented and discussed in detail in this chapter.

4.1 LULC mapping

The LULC map outputs from 2009 to 2022 show in Figure 21. The LULC maps from the study are classified into 5 categories: built-up, agriculture, open space, forest, and water bodies. ALOS (AVNIR-2) and Sentinel 2 images are used to extract classified LULC maps from 2009 to 2022.

The result of the LULC map shows the most significant changes being observed in the built-up area. In 2009, the built-up areas are distributed mainly concentrated around Pattaya city which is an existing urban center. However, by 2022, the built-up areas have significantly spread from Pattaya city to surrounding areas, especially agriculture areas and open space areas. Correspondingly, a total of 49.99 sq.km and 32.98 sq.km changed from agriculture areas and open space areas to other LULC areas.

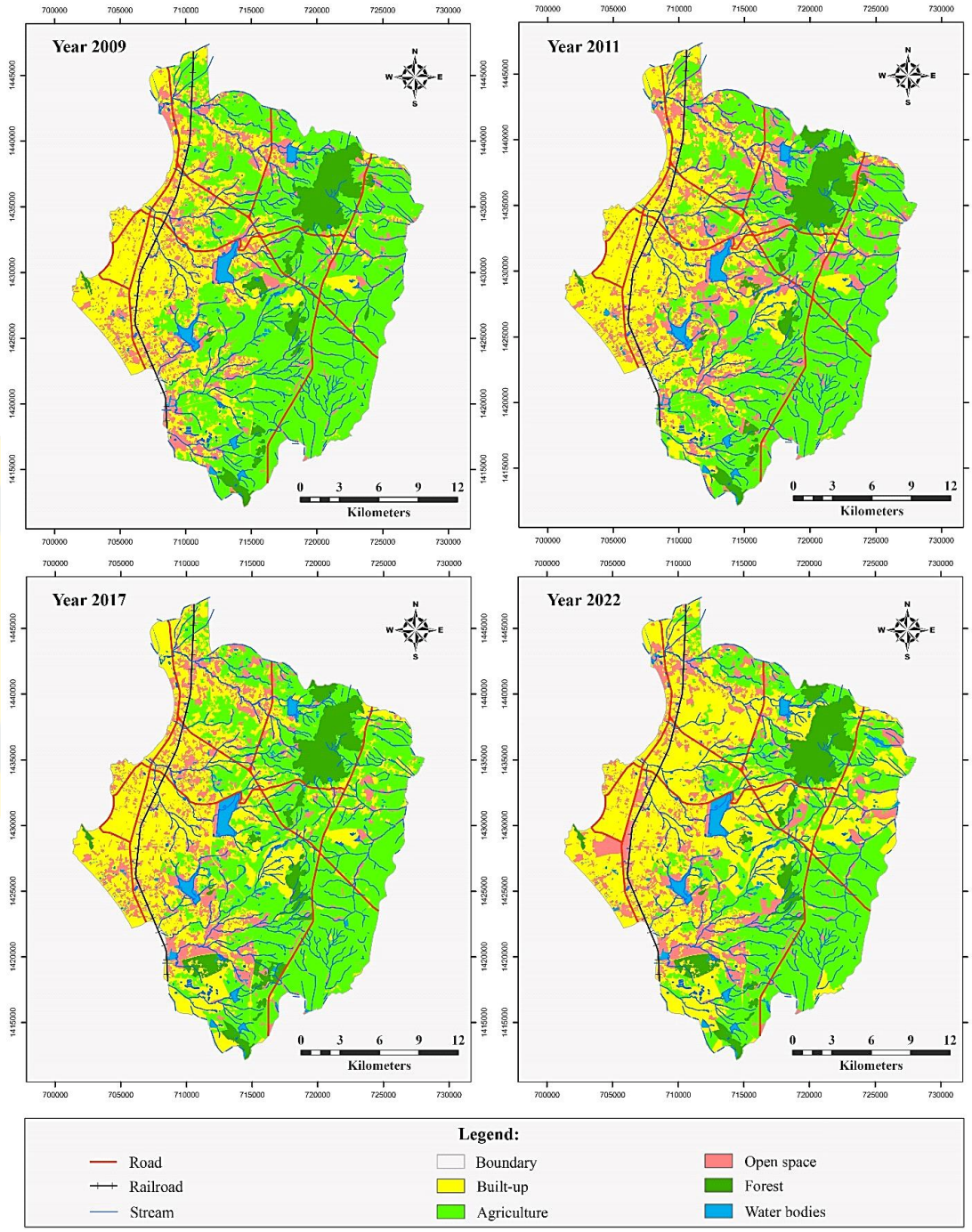

Figure 21: The results of classification LULC mapping in 2009 to 202

(A) 2009, (B) 2011, (C) 2017, (D) 2022

Table 15 displays the percentage of LULC changes from 2009 to 2022, based on the classified LULC maps of 2009, 2011, 2017, and 2022. In 2009, the agriculture area covers the largest area of approximately 221 sq.km (42.10%), followed by built-up areas which occupy around 141 sq.km (26.84%). Open spaces account for approximately 113 sq.km (21.44%). The forest and water bodies cover approximately 32 sq.km (6%) and 17 sq.km (3%) of the land, respectively.

As for 2011, agriculture area still covers the largest area with around 208 sq.km (39.60%), followed by built-up areas which occupy approximately 158 sq.km (30.03%). Open spaces account for around 110 sq.km (21.01%). The remaining classes such as forest and water bodies cover approximately 32 sq.km (6.14%) and 17 sq.km (3.23%) of the land, respectively.

As of the year 2017, the agriculture area covers approximately 198 sq.km or 37.73%, followed by built-up areas at around 179 sq.km (34.08%), while open space accounted for approximately 99 sq.km (18.92%). The remaining land use classes were forests and water bodies, which covered around 32 sq.km (6.18%) and 16 sq.km (3.10%), respectively.

As for 2022, the majority of the area has been developed to built-up area with approximately 222 sq.km or 42.25%, while agriculture accounts for about 175 sq.km or 33.34%. Open spaces occupy approximately 80 sq.km or 15.16%. The remaining land is divided between forests and water bodies, which cover approximately 32 sq.km (6.13%) and 16 sq.km (3.12%), respectively.

The study reveals that the built-up area has been continuously expanding from 2009 to 2022, with an average annual increase of 12.75 sq.km. On the other hand, the agriculture area has been decreasing over the same period, with an average annual decrease of 7.69 sq.km. The open space area has also shown a decreasing trend from 2009 to 2022, with an average annual decrease of 5.07 sq.km. However, forest and water bodies have remained relatively stable in terms of an average area over the same period (as shown in Table 16).

Table 15: The area of LULC changes in 2009 to 2022

Land use class	Year							
	2009		2011		2017		2022	
	Area (sq.km)		Area (sq.km)		Area (sq.km)		Area (sq.km)	
Built-up	140.90	26.84	157.62	30.03(+)	178.87	34.08(+)	221.78	42.25(+)
Agriculture	220.99	42.10	245.84	39.60(-)	198.02	37.73(-)	175.00	33.34(-)
Open space	112.55	21.44	110.25	21.01(-)	99.28	18.92(-)	79.57	15.16(-)
Forest	33.85	6.45	32.23	6.14(+)	32.44	6.18(+)	32.15	6.13(-)
Water bodies	16.58	3.16	16.93	3.23(+)	16.26	3.10(-)	16.37	3.12(+)
Total	524.87	100	524.87	100	524.87	100	524.87	100

Note: Percentage area + = increase and - = decrease

Table 16**:** The estimate of average area LULC changes in 2009 to 2022

Land use class	Change area (sq.km)				Average area (sq km/year)
	2009 to 2011	2011 to 2017	2017 to 2022	2009 to 2022	
Built-up	+16.72	+21.25	+42.91	+82.88	+12.60
Agriculture	-13.15	-9.82	-23.02	-49.99	-7.38
Open space	-2.30	-10.97	-19.71	-32.98	-5.07
Forest	-1.62	+0.21	-0.29	+0.3	-0.11
Water bodies	+0.35	-0.67	+0.11	-0.21	-0.03

Note: + = increase and - = decrease

4.2 LULC classification accuracy assessment

To evaluate the accuracy of the LULC classification is utilized an error matrix, and 200 sampling points are selected from the classification map of 2022 (Figure 22). The LULC (2022) classification map is used in this research for accuracy assessment due to its recentness at the time of the survey, making it the most suitable option. Accuracy of LULC classification in Bang Lamung district in 2022 is verified by ground truth data.

The results showed that the accuracy of the producer's accuracy for built-up and water bodies, agricultural areas, open space, and forest areas are 100%, 97.44%, 88%, and 76%, respectively. While, the user's accuracy for water bodies and forest, built-up, agricultural areas, and open space are 100 %, 94.36%, 93.83%, and 91.67% respectively. The overall accuracy of the classification is 94.50%, with a Kappa coefficient of 0.885, as presented in Table 17, and there are examples of accuracy validation for land use classification in the field, as shown in Table 18.

The overall accuracy is determined by counting the number of pixels that were correctly classified. On the other hand, the Kappa coefficient measures the degree of agreement between observed and expected sets of data. A commonly used scale to interpret the Kappa coefficient is as follows [65]:

- Kappa < 0: No agreement
- Kappa between 0.00 and 0.20: Slight agreement
- Kappa between 0.21 and 0.40: Fair agreement
- Kappa between 0.41 and 0.60: Moderate agreement
- Kappa between 0.61 and 0.80: Substantial agreement
- Kappa between 0.81 and 1.00: Almost perfect agreement

Therefore, the accuracy assessment results of this study are acceptable since the Kappa coefficient of 0.80 suggests an 80% probability of the classification outcomes matching the actual reference data used for validation. Moreover, the producer's accuracy for all classes in the classified map are consistently high, varying from 76% to 100%, indicating that the classification is precise. The built-up and water bodies classes have a 100% correct classification. Additionally, the user's accuracy for all classes varies from 68% to 100%, with a 100% correct classification for the forest and water bodies classes, further confirming the classification's accuracy.

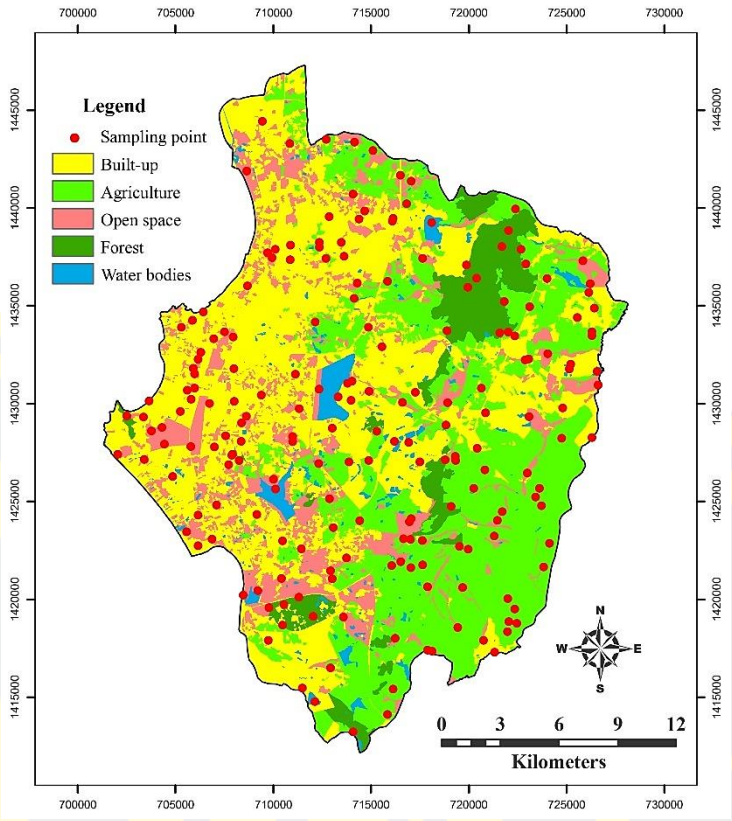

Figure 22: The distribution of sampling points in Bang Lamung district

Table 17**:** Confusion matrix of LULC classification map in 2022

Land use class	Reference data						User's Accuracy (%)
	Built-up	Agriculture	Open space	Forest	Water bodies	Total	
Built-up	**67**		0	2	0	71	94.36
Agriculture	0	**76**	3	2	0	81	93.83
Open space	0	0	**22**	2	0	24	91.67
Forest	0	0	0	**19**	0	19	100
Waterbodies	0	0	0	0	**5**	5	100
Total	67	78	25	25	5	200	Overall Accuracy (94.50%)
Producer's Accuracy (%)	100	97.44	88	76	100		Kappa coefficient 0.885

Note: Number of correctly classified site = 189 points,

Total number of reference sites = 200 pints

Overall Accuracy (%) = 94.50, Overall error (%) = 5.50

Table 18: An example of verifying Ground Truth Data through field observation

1) Built-up area

ID	X	Y	Satellite imagery	Ground Truth
1.1	715300	1428538	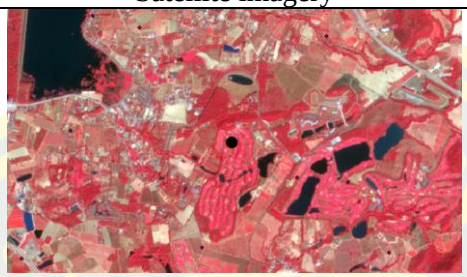	
1.2	704881	1432140	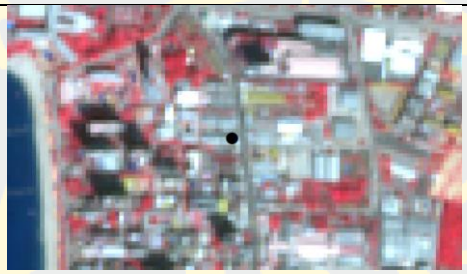	
1.3	704570	1426181		

2) Agriculture area

ID	X	Y	Satellite imagery	Ground Truth
2.1	718009	1417472	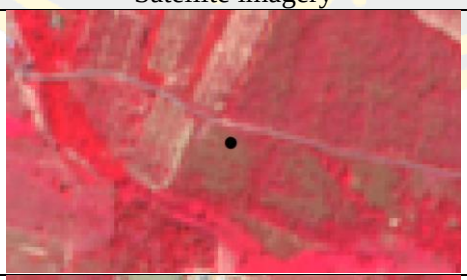	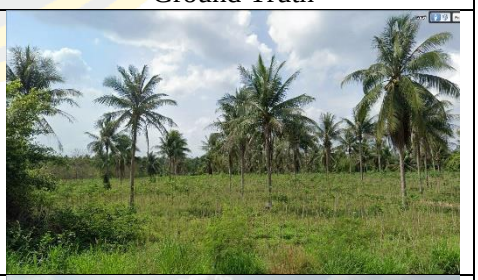
2.2	723734	1424799		

ID	X	Y	Satellite imagery	Ground Truth
2.3	725574	1428706	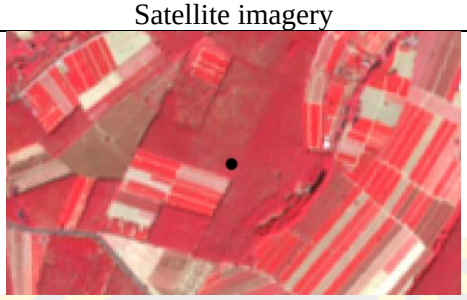	

3) Open space area

ID	X	Y	Satellite imagery	Ground Truth
3.1	709923	1437453		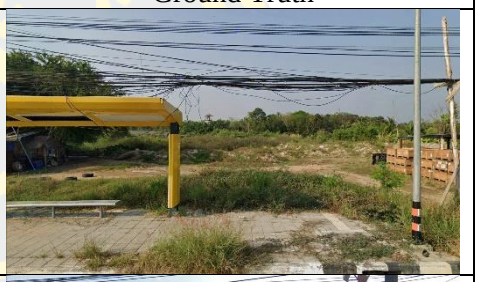
3.2	705773	1427797		
3.3	709738	1417901		

4) Forest area

ID	X	Y	Satellite imagery	Ground Truth
4.1	718950	1433366		

ID	X	Y	Satellite imagery	Ground Truth
4.2	702488	1429456	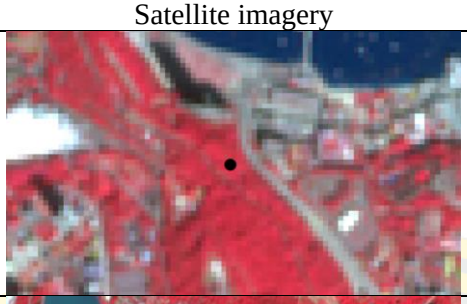	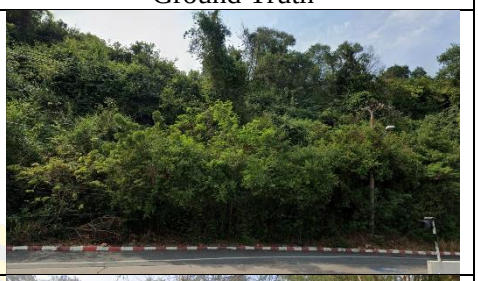
4.3	713032	1414142		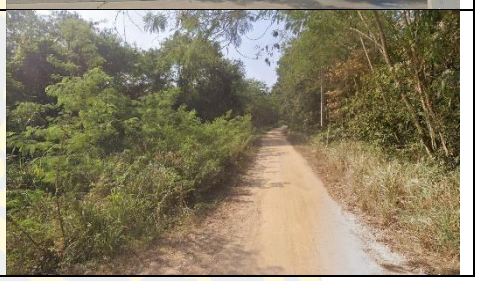

5) Water bodies area

ID	X	Y	Satellite imagery	Ground Truth
5.1	718079	1439007	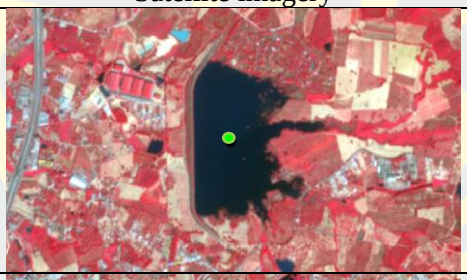	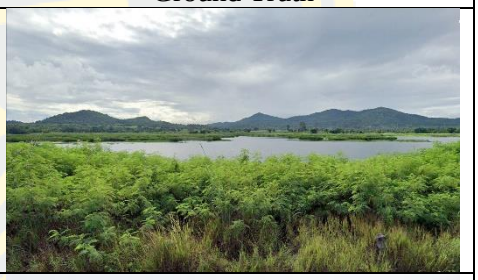
5.2	712882	1430322	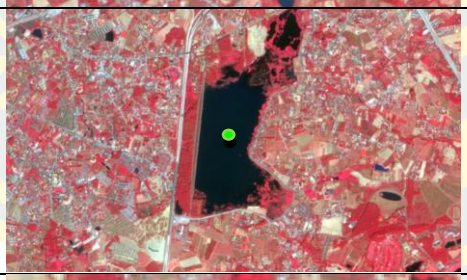	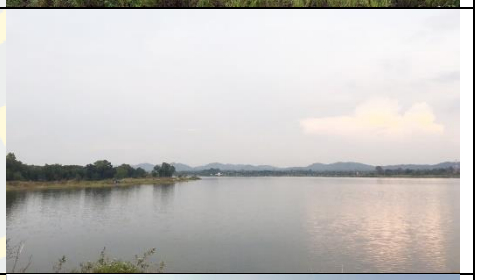
5.3	710866	1426334		

4.3 Transition Probability

The transition probabilities are derived from the land use maps over 3 time periods, from 2009 to 2011, 2011 to 2017, and 2017 to 2022. The results indicate that between 2009 and 2011, the built-up area remain relatively constant, accounting for approximately 90.30%. However, some other LULC classes transitioned into built-up areas, accounting for 21.75% of the total area. For example, the probability of open space changing into built-up area is 15.83%, agriculture into built-up area is 5.46%, water bodies into built-up area are 0.28%, and forest into built-up area is 0.19%. Additionally, there is a 9.70% loss in built-up area to other classes. For instance, the probability of built-up area changing into open space is 4.34%, built-up area into forest is 2.69%, built-up area into agriculture is 2.44%, and built-up area into water bodies is 0.24%.

The calculated percentage for the agriculture area remains unchanged at 81.09%. However, there have been some gains in the agriculture area from other LULC classes, which account for 9.17% of the total changes observed. Specifically, the probability of forest to agriculture area conversion is 3.92%, open space to agriculture area conversion is 2.62%, built-up to agriculture area conversion is 2.44%, and water bodies to agriculture area conversion is 0.19%. Conversely, there has been a loss of agriculture area to other LULC classes, which accounts for 18.91% of the total changes observed. The probability of open space area to agriculture area conversion is 12.78%, built-up to agriculture area conversion is 5.46%, forest to agriculture area conversion is 0.53%, and water bodies to agriculture area conversion is 0.14%.

For the open space area, the result indicates that remain stable at around 77.18%. However, there is a gain of 18.41% in open space area from other LULC classes. For example, there is a change from agriculture area to open space of 12.78%, from built-up area to open space of 4.34%, from forest to open space of 0.87%, and from water bodies to open space area of 0.43%. While, there is a loss of open space area to other LULC classes of 22.82%. For instance, the change from open space to built-up is 15.83%, from open space to agriculture area is 2.62%, from open space to forest is 2.37%, and from open space to water bodies is 2%.

The forest area relatively constant calculate at around 94.62%. However, there is some gain in forest area from other LULC classes, which is computed to be 6.42%. For instance, the probability of change for built-up to forest area is 2.69%, open space to forest area is 2.37%, water bodies to forest area is 0.84%, and agriculture to forest area is 0.53%. On the other hand, some forest area is lost to other classes by 5.38%. For example, the probability of change for forest area to agriculture area is 3.92%, forest area to open space is 0.87%, forest area to water bodies is 0.40%, and forest area to built-up is 0.19%.

The water bodies remain relatively constant, accounting for 98.27%. While, there has some other LULC class gain to water bodies which is computed to 2.78%. Specifically, the probability of open space to water bodies conversion is 2%, forest to water bodies conversion is 0.40%, built-up to water bodies conversion is 0.24%, and agriculture area to water bodies conversion is 0.14%. While, there has been a loss of water bodies to other LULC classes, which accounts for 1.73% of the total changes observed. The probability of water bodies to forest area conversion is 0.84%, water bodies to open space conversion is 0.43%, water bodies to built-up conversion is 0.28%, and water bodies to agriculture area conversion is 0.19% (Figure 23 and Table 19).

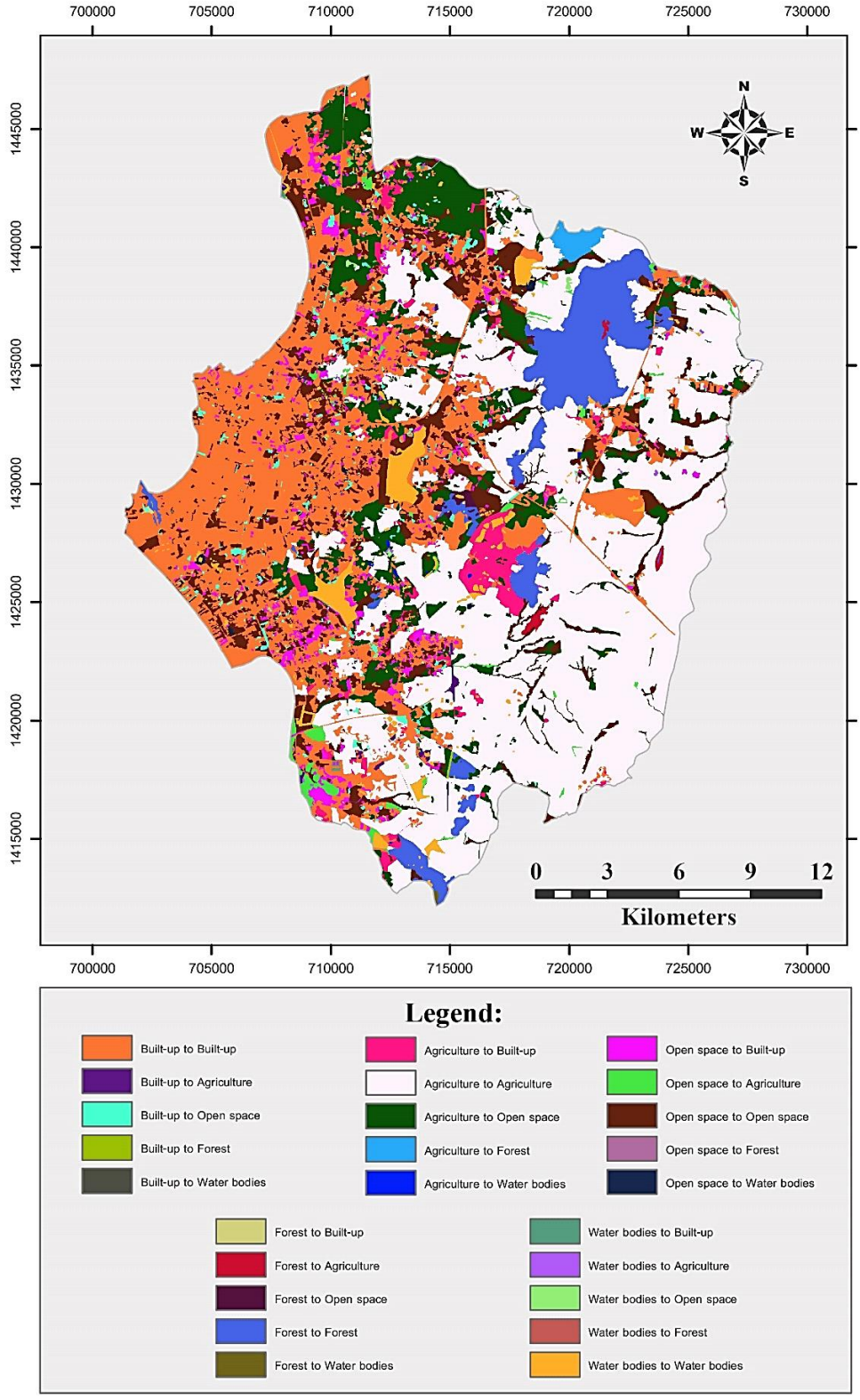

Figure 23**:** LULC change transition between 2009 and 2011

Table 19: Transition percentage matrix derived from the land use maps during 2009 - 2011.

Changing from: 2009	Percentage of Changing by 2011 to:					Subtotals	
	Built-up	Agriculture	Open space	Forest	Water bodies	Total	Loss
Built-up	90.30	2.44	4.34	2.69	0.24	100	9.70
Agriculture	5.46	81.09	12.78	0.53	0.14	100	18.91
Open space	15.83	2.62	77.18	2.37	2.00	100	22.82
Forest	0.19	3.92	0.87	94.62	0.40	100	5.38
Water bodies	0.28	0.19	0.43	0.84	98.27	100	1.73
Gain	21.75	9.17	18.41	6.42	2.78		

During the period between 2011 and 2017, the built-up area remained unchanged, accounting for 86.65% of the total area. However, there have been gains in the built-up area from other LULC classes, which account for 28.31% of the total changes observed. For the probability of open space area to built-up area conversion is 19.31%, agriculture to built-up conversion is 6.31%, water bodies to built-up conversion is 1.85%, and forest to built-up conversion is 0.85%.

The results shows that the agriculture area remained stable at 86.04%. However, have been gains in agriculture area to other LULC classes, which amounts to 9.44%. Specifically, open space area to agriculture change is 6.45%, forest to agriculture change is 1.30%, built-up to agriculture change is 1.13%, and water bodies to agriculture change is 0.55%. While, some agriculture area loss to other LULC classes, total 13.96%. For example, the probability of change for agriculture area to built-up is 6.31%, agriculture area to open space is 6.15%, agriculture area to forest is 1.31%, and agriculture area to water bodies is 0.20%.

For open space area is remained stable at 71.46%. While, there has some other LULC class gain to open space area which is computed to 18.62%. For instance, the probability of change for built-up to open space area is 10.21%, agriculture area to open space is 6.15%, water bodies to open space area is 1.43%, and forest to open space is 0.83%. While, some open space area loss to other class about 28.54%. For instance, the probability of change for open space to built-up is 19.31%, open space to agriculture area is 6.45%, open space to forest is 1.64%, open space to water bodies is 1.13%.

The result of the forest area remained unchanged, accounting for 96.93% of the total area. However, there is a gain of 4.75% from other LULC classes. For example, the probability of change for built-up to forest area is 1.68%, open space to forest area is 1.64%, agriculture to forest area is 1.31%, and water bodies to forest area is 0.12%. On the other hand, there is a loss of 3.07% of the forest area to other LULC classes. For instance, the probability of change for forest area to agriculture area is 1.30%, forest area to built-up is 0.85%, forest area to open space is 0.83%, and forest area to water bodies is 0.09%.

For the water bodies remain relatively stable with 96.05%. While, there has some other LULC class gain to water bodies which is computed to 1.75%. For instance, the probability of change for open space to water bodies is 1.13%, built-up to water bodies is 0.33%, agriculture area to water bodies is 0.20%, and forest to water bodies is 0.09%. While, some water bodies loss to other class about 3.95%. For instance, the probability of change for water bodies to built-up is 1.85%, water bodies to open space is 1.43%, water bodies to agriculture area is 0.55%, and water bodies to forest area is 0.12%. Figure 24 and Table 20 present the results for the period between 2011 and 2017.

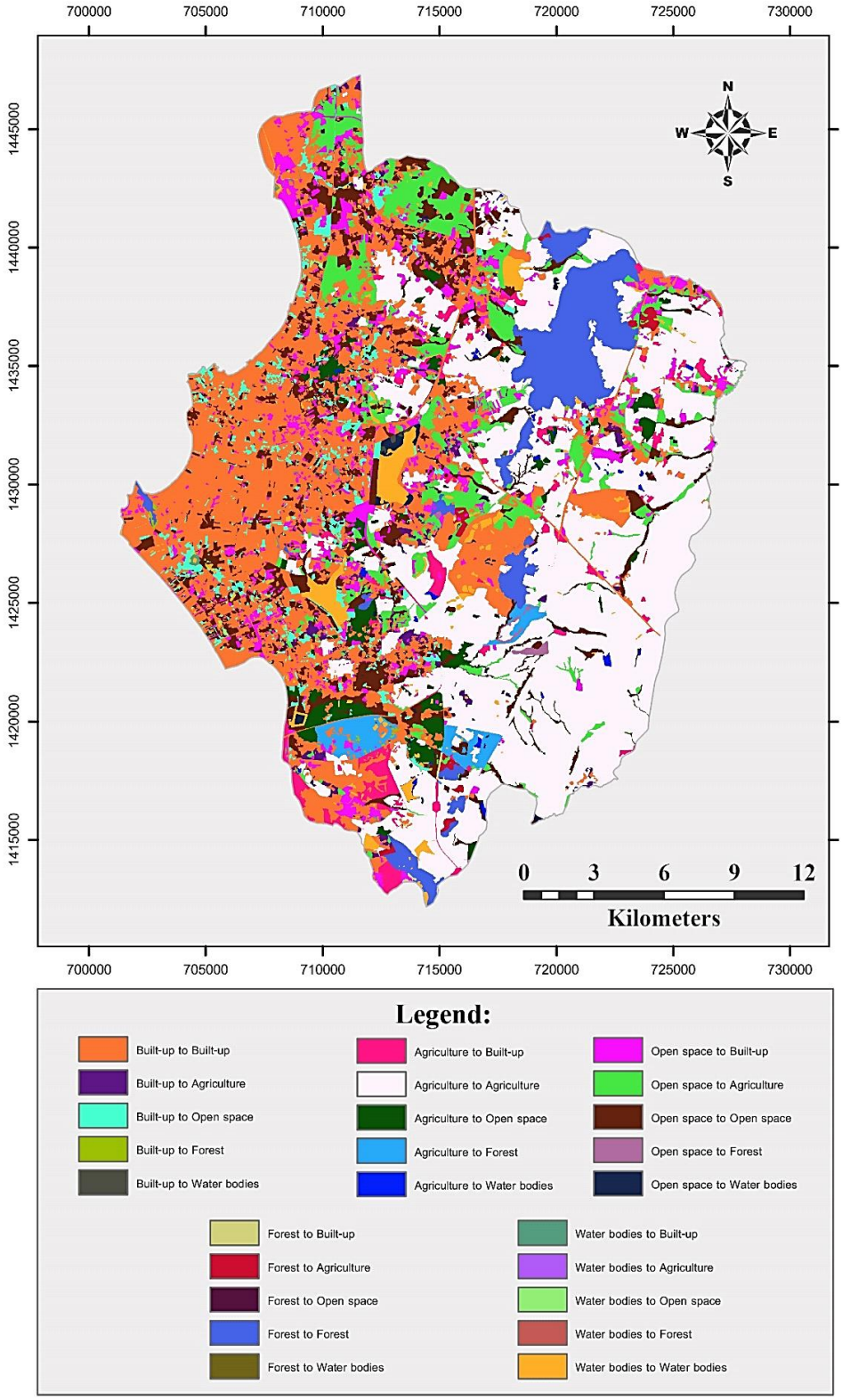

Figure 24: LULC change transition between 2011 and 2017

Table 20: Transition percentage matrix derived from the land use maps during 2011 - 2017

Changing from: 2011	**Percentage of Changing by 2017 to:**					Subtotals	
	Built-up	Agriculture	Open space	Forest	Water bodies	Total	Loss
Built-up	86.65	1.13	10.21	1.68	0.33	100	13.35
Agriculture	6.31	86.04	6.15	1.31	0.20	100	13.96
Open space	19.31	6.45	71.46	1.64	1.13	100	28.54
Forest	0.85	1.30	0.83	96.93	0.09	100	3.07
Water bodies	1.85	0.55	1.43	0.12	96.05	100	3.95
Gain	28.31	9.44	18.62	4.75	1.75		

Between 2017 and 2022, the built-up area remained constant at approximately 80.27%. However, there is an increase in the area of other LULC classes that converted to built-up areas, accounting for 44.29%. For example, the open space area had a 34.59% probability of changing to a built-up area, agriculture had a 7.41% probability, forest had a 1.92% probability, and water bodies had a 0.37% probability. Conversely, some built-up areas converted to other classes, accounting for 19.73%. Specifically, there is a 14.08% probability of built-up areas changing to open space, 3.93% probability to agriculture, 1.07% probability to forest, and 0.65% probability to water bodies.

As agriculture area, this class remain relatively constant at 70.64%. While, there has been an increase in the agricultural area due to a gain from other LULC classes, which amounts to 19.10%. Specifically, the probability of forest changing to agriculture area is 8.81%, open space changing to agriculture area is 6.32%, built-up areas changing to agriculture area is 3.93%, and water bodies changing to agricultural land is 0.04%. On the other hand, there has been a decrease in the agriculture area due to loss to other LULC classes, which amounts to 29.36%. The probability of agricultural land changing to open space is 17.99%, agriculture area changing to built-up areas is 7.41%, agriculture area changing to forest is 2.24%, and agricultural land changing to water bodies is 1.73%.

The open space area remained constant at 48.53%, while there was a 36.39% increase in other LULC classes converting to open space. For example, there is a 17.99% probability of agriculture land changing to open space, 14.08% probability for built-up areas, 3.89% probability for water bodies, and 0.42% probability for forest. However, there is also a loss of open space to other classes, accounting for 51.47%. Specifically, there is a 34.59% probability of open space changing to built-up areas, 10.17% probability to forest, 6.32% probability to agricultural areas, and 0.40% probability to water bodies.

Approximately 86.17% of the forest area remained constant. However, there has some other LULC class gain to forest area which is computed to 13.66%. For instance, the probability of change for open space to forest area is 10.17%, agriculture to forest area is 2.24%, built-up to forest area is 1.07%, and water bodies to forest area is 0.18%. While, some forest area loss to other class about 13.83%. For instance, the probability of change for forest area to agriculture area is 8.81%, forest area to water bodies is 2.67%, forest area to built-up is 1.92%, and forest area to open space is 0.42%.

The water bodies in the study have been observed to remain relatively stable, with no significant change observed, accounting for around 95.52% of the area. However, there has been some gain in the water bodies from other LULC classes, which has been computed to 5.44%. For example, the probability of forest land converting to water bodies is 2.67%, agriculture area to water bodies is 1.73%, built-up to water bodies is 0.65%, and open space to water bodies is 0.40%. At the same time, some water bodies have been lost to other LULC classes, which accounts of 4.48%. For instance, the probability of water bodies to open space is 3.89%, water bodies to built-up is 0.37%, water bodies to forest area is 0.18%, and water bodies to agriculture area is 0.04% (as depicted in Figure 25 and Table 21).

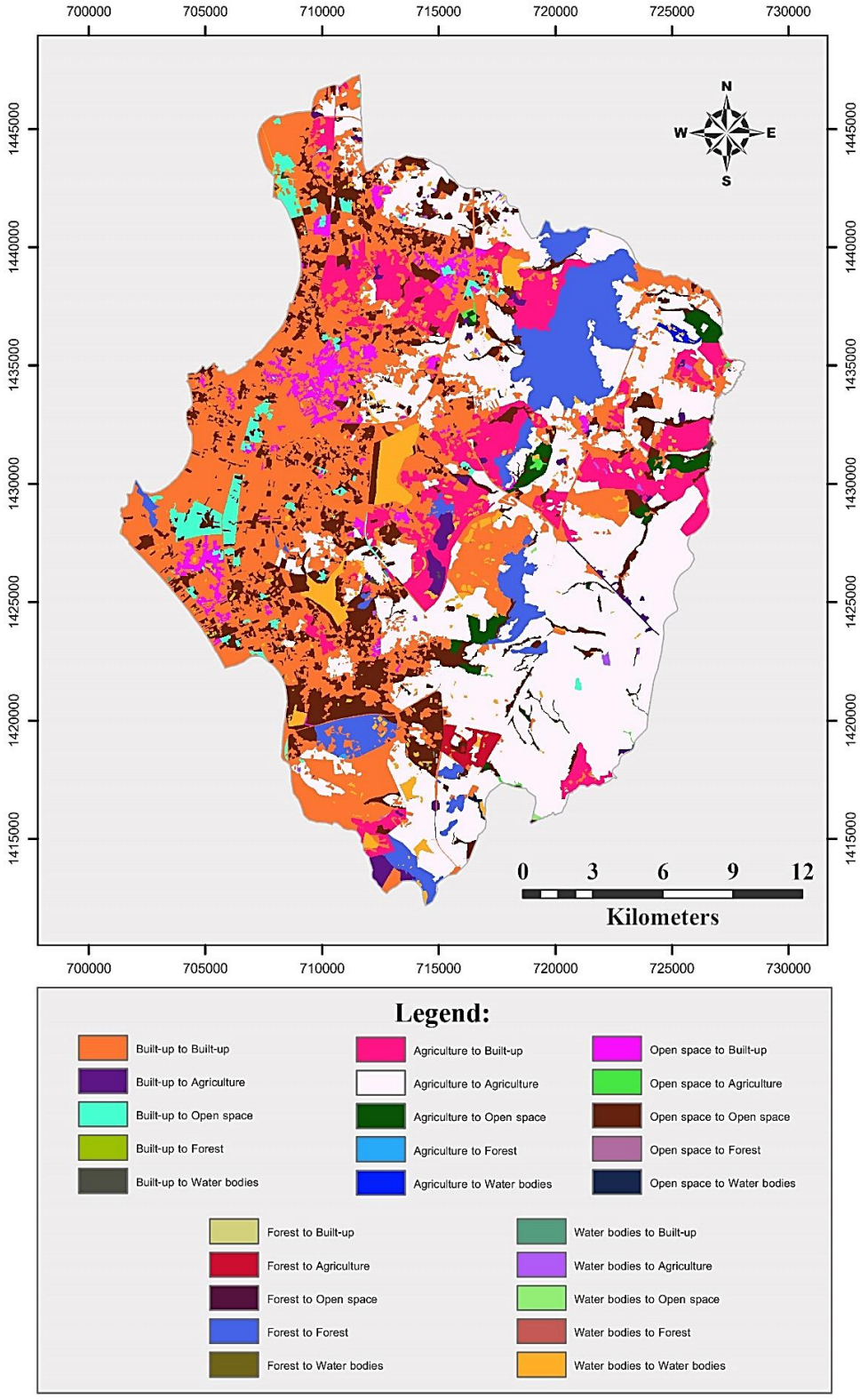

Figure 25: LULC change transition between 2017 and 2022

Table 21: Transition percentage matrix derived from the land use maps during 2017 - 2022

Changing from: 2017	**Percentage of Changing by 2022 to:**					Subtotals	
	Built-up	Agriculture	Open space	Forest	Water bodies	Total	Loss
Built-up	80.27	3.93	14.08	1.07	0.65	100	19.73
Agriculture	7.41	70.64	17.99	2.24	1.73	100	29.36
Open space	34.59	6.32	48.53	10.17	0.40	100	51.47
Forest	1.92	8.81	0.42	86.17	2.67	100	13.83
Water bodies	0.37	0.04	3.89	0.18	95.52	100	4.48
Gain	44.29	19.10	36.39	13.66	5.44		

Thus, the study reveals that agriculture area and open space has the highest percentage of loss both of which are mostly transformed into built-up areas. On the other hand, built-up areas show the highest gain. However, forest and water bodies areas remained largely unchanged. This probability transition matrix serves as an essential indicator of past trends and is integrated into the cellular automata model to simulate the distribution of LULC.

4.4 Markov chain - transition probability matrix

The CA-Markov model for land use produces two main results: (1) a Markov transition probability matrix that shows the probabilities of land use types changing from one time period to the next, and (2) Markovian conditional probability maps. Table 22 and Table 23 display the Markov transition probability matrix for land use change. The values in each row of the matrix add up to one, indicating the likelihood of transitioning from one land use type in the first time period (shown in rows) to other land use types in the second time period (shown in columns). The Markov transition matrix comparison shows shifting patterns of land usage throughout various time periods. Different types of land use patterns can be seen using the Markov transition matrix over different time periods.

In this study, it is found that the likelihood of open space areas being transformed into built-up areas decreased from 25.29% in the period of 2011-2017 to 16.31% in the period of 2017-2022. Conversely, the probability of agriculture areas being converted to built-up areas with 21.17% which is higher than the period of 2011-2017. The expansion of built-up areas was primarily driven by the conversion of open space and agriculture area. Figures 26 and 27 present the Markovian conditional probability maps for transitions in 2011-2017 and 2017-2022, respectively. The maps indicate that areas in the eastern parts of the Bang Lamung district have a high probability of being used for agriculture, while the central and western areas of the region have a higher probability of being designated as open space. Built-up areas are predominantly located along the coast, with an expansion towards the central areas.

Table 22: Markov transition probability matrix 2011 - 2017

Probability of changing to:		**2017**				
		Built-up	Agriculture	Open space	Forest	Water bodies
2011	Built-up	0.8690	0.0354	0.0905	0.0022	0.0029
	Agriculture	0.0590	0.8425	0.0578	0.0343	0.0064
	Open space	0.2529	0.3090	0.4081	0.0074	0.0226
	Forest	0.0069	0.0585	0.0000	0.9335	0.0011
	Water bodies	0.0385	0.0115	0.0298	0.0024	0.9177

Table 23: Markov transition probability matrix 2017 - 2022

Probability of changing to:		**2022**				
		Built-up	Agriculture	Open space	Forest	Water bodies
2017	Built-up	0.9145	0.0301	0.0532	0.0000	0.0022
	Agriculture	0.2117	0.7571	0.0285	0.0002	0.0024
	Open space	0.1631	0.0075	0.8266	0.0000	0.0027
	Forest	0.0000	0.0609	0.0001	0.9390	0.0000
	Water bodies	0.0065	0.0407	0.0152	0.0000	0.9375

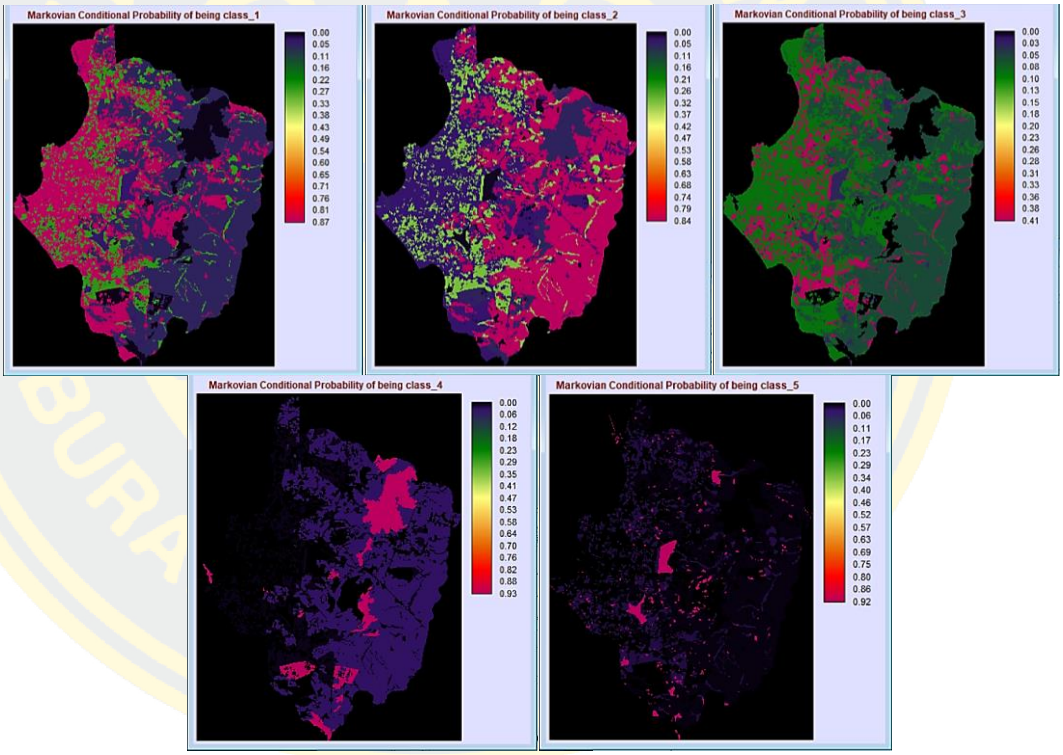

Figure 26: Markovian conditional probability maps 2011 – 2017

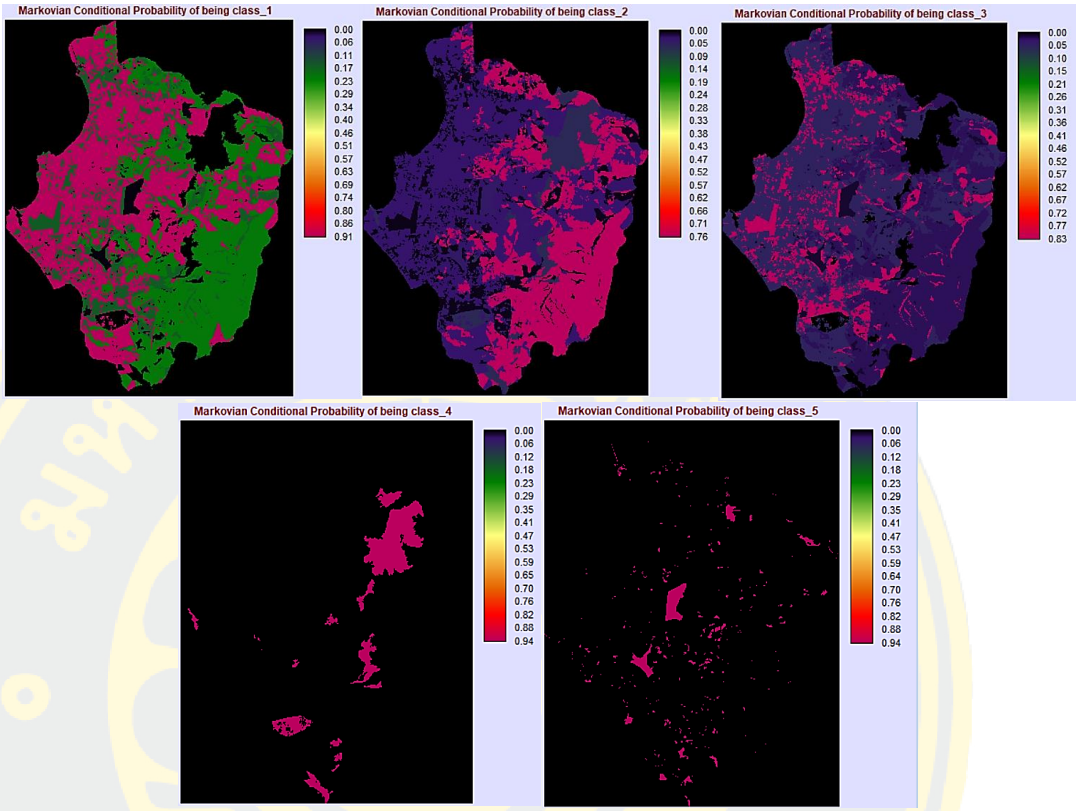

Figure 27: Markovian conditional probability maps 2017 - 2022

4.5 Model Validation

Validation is a crucial process in verifying the efficiency of models for LULC change. In this study, the transition probability matrix is calculated using LULC maps from 2011 and 2017 in the CA-Markov model to generate the 2022 simulation map. The resulting simulation map for 2022 is compared to the classified map for 2022 to assess its accuracy. Table 24 displays the differences of built-up, agriculture and open space areas between the simulated map of 2022 and the reference map of 2022, which are 6.44%, -7.85% and 3.79%, respectively. The difference in water bodies areas between the two maps is slightly different, at approximately -0.18%. Figure 28 illustrates that the simulated map of 2022 indicates an increase in some agriculture and forest areas.

Table 24: Changed areas between the reference LULC map 2022 and the simulated LULC map 2022

Land use class	Reference LULC of 2022		Simulated LULC of 2022		Change detection (%)
	Area(sq.km)	%	Area(sq.km)	%	
1.Built-up	221.78	42.25	187.99	35.82	6.44
2.Agriculture	175.00	33.34	216.18	41.19	-7.85
3.Open space	79.57	15.16	59.63	11.36	3.79
4.Forest	32.15	6.13	43.72	8.33	-2.20
5.Water bodies	16.37	3.12	17.34	3.30	-0.18
Total	524.87	100	524.87	100	

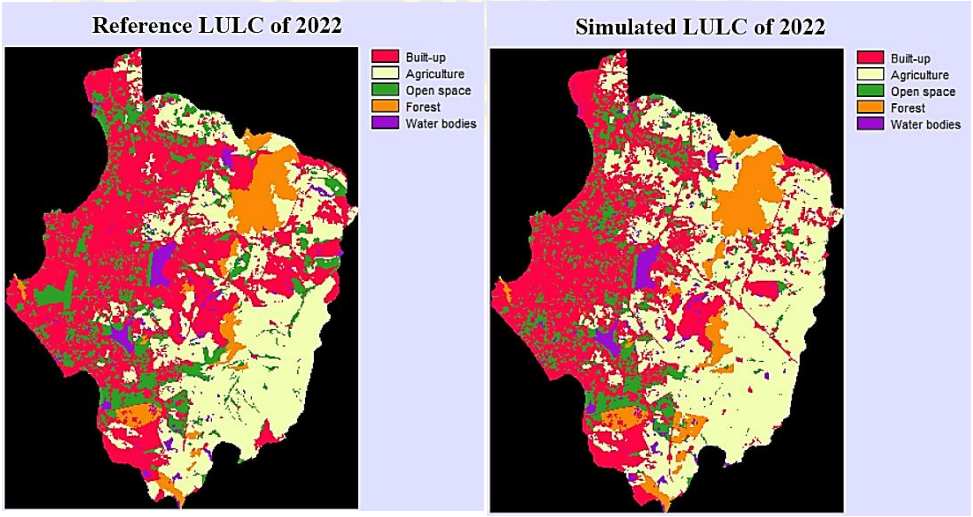

Figure 28: The Reference LULC 2022 and the simulated LULC 2022

To validate the simulated LULC map for 2022, the reference LULC map and the simulated LULC map are compared in Figure 28. The validation process involved the use of the kappa statistic and multiple-resolution analysis. In this study, validation calculates various Kappa indices of agreement and related statistics. The analysis separates agreement and disagreement between the two images into the following components (Pontius et al., 2011):

- agreement due to chance
- agreement due to quantity
- agreement due to location at the stratified level
- agreement due to location at the grid cell level
- disagreement due to location at the grid cell level
- disagreement due to location at the stratified level
- disagreement due to quantity

In addition, validation provides the traditional Kappa Index of Agreement (KIA) and other useful variations of it, such as Kstandard. However, both the percent correct and standard KIA can be misleading as they do not distinguish between disagreement in quantity and disagreement in location. Therefore, besides calculating the standard KIA, validate offers three additional statistics: Kno, Klocation, and KlocationStrata. All of these statistics are linear functions of points in the validate output.

Therefore, validate provides a Kappa statistic for both quantity and location, as shown in Table 25. The location statistics include Kno, which represents the Kappa score for no information and has a value of 0.8691, Klocation with a value of 0.9155, indicating how well the grid cells are located on the landscape, and Klocation Strata also with a value of 0.9155, indicating how well the grid cells are located within the strata. The standard Kappa Index of Agreement, denoted as Kstandard, has a value of 0.8458 (as shown in Table 26). These results suggest that the CA-Markov model can accurately specify the grid cell level location of future changes, with the Klocation value of 0.9155, indicating near-perfect performance (where a value of 1 represents perfect performance). These results support the validity of the simulation model, and a visual representation of KlocationStrata can be found in Figure 29.

```
Number of total runs       :        1
Multi-resolution VALIDATE  :        Categorical Image Comparison
============================================================
Comparison image file      :        patch1177x
Reference image file       :        lu2017r
Strata/Mask image file     :        N/A

Number of valid strata:    1;  Number of valid categories:    6

//Beginning of run:                1
Resolution scale:    1 x 1

                    Classification agreement/disagreement
          According to ability to specify accurately quantity and allocation

                                                  Information of Quantity
  Information of Allocation          No[n]              Medium[m]          Perfect[p]
  Perfect[P(x)]                P(n) =  0.6371    P(m) =  0.9461    P(p) =  1.0000
  PerfectStratum[K(x)]         K(n) =  0.6371    K(m) =  0.9461    K(p) =  1.0000
  MediumGrid[M(x)]             M(n) =  0.5602    M(m) =  0.8909    M(p) =  0.8666
  MediumStratum[H(x)]          H(n) =  0.1667    H(m) =  0.2926    H(p) =  0.2939
  No[N(x)]                     N(n) =  0.1667    N(m) =  0.2926    N(p) =  0.2939


    AgreementChance =  0.1667
  AgreementQuantity =  0.1260
    AgreementStrata =  0.0000
  AgreementGridcell =  0.5983
   DisagreeGridcell =  0.0552
     DisagreeStrata =  0.0000
   DisagreeQuantity =  0.0539

                Kno =  0.8691
          Klocation =  0.9155
    KlocationStrata =  0.9155
          Kstandard =  0.8458
//Ending of run:                1
```

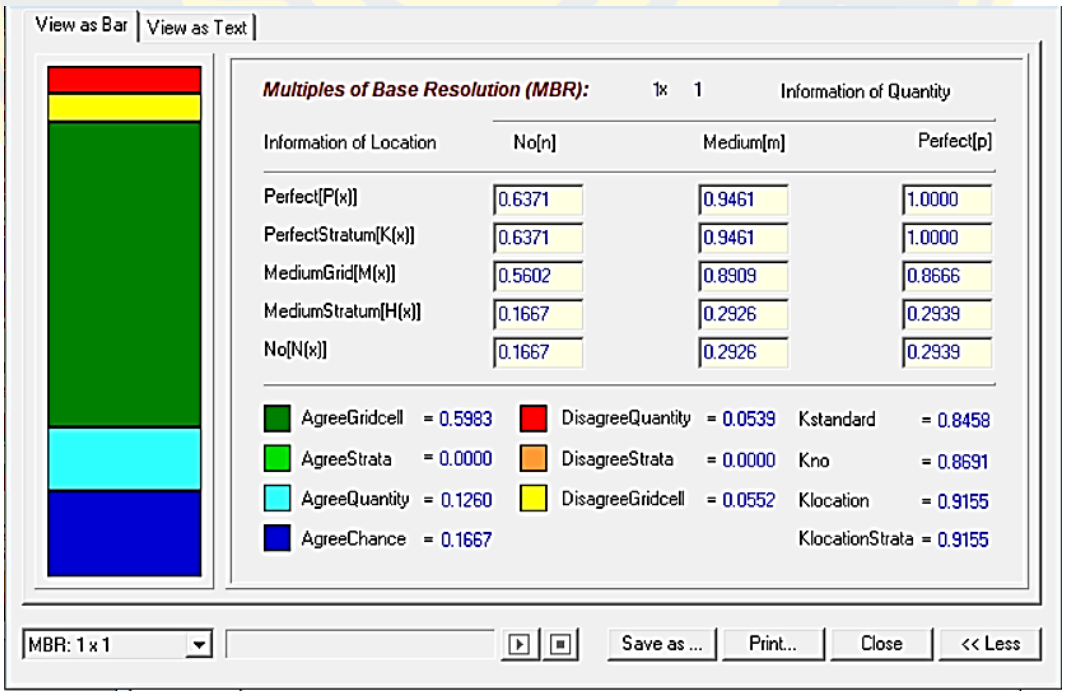

Figure 29: Agreement/disagreement to ability to specify accurately quantity and location result

Table 25: Agreement/disagreement according to ability to specify accurately quantity and location to simulate LULC 2022

Information of location	**Information of quality**		
	No [n]	Medium [m]	Perfect [p]
Perfect [P(x)]	P(n) = 0.6371	P(m) = 0.9461	P(p) = 1.0000
Perfect Stratum [K(x)]	K(n) = 0.6371	K(m) = 0.9461	K(p) = 1.0000
Medium Grid [M(x)]	M(n) = 0.5602	M(m) = 0.8909	M(p) = 0.8666
Medium Stratum [H(x)]	H(n) = 0.1667	H(m) = 0.2926	H(p) = 0.2939
No [N(x)]	N(n) = 0.1667	N(m) = 0.2926	N(p) = 0.2939
Agreement chance	= 0.1667		
Agreement quantity	= 0.1260		
Agreement strata	= 0.0000		
Agreement grid cell	= 0.5983		
Disagree grid cell	= 0.0552		
Disagree strata	= 0.0000		
Disagree quantity	= 0.0539		

Table 26: Kappa Index of Agreement to ability to specify accurately quantity and location to simulate LULC 2022

Statistics	**Index**
Kno	0.8691
Klocation	0.9155
Klocation Strata	0.9155
Kstandard	0.8458

4.6 Simulation Scenarios

To simulate LULC, a modeling approach that integrates the Cellular Automata and Markov Chain models is employed. The simulation utilizes the transition probability between 2017 and 2022. The study conducted LULC change simulations for the years 2027 and 2032. The researcher has analyzed to 3 scenarios: the spontaneous scenario, the green area improvement scenario, and the area comprehensive plan.

4.6.1 Spontaneous scenario

The Spontaneous scenario describes a historical situation where the LULC trends observed between 2017 and 2022 remain constant until 2027 and 2032. The simulation results presented in Figure 30 illustrate that the coastal areas consist mainly of built-up area, with some urban development visible in the west inland areas by 2027 and 2032.

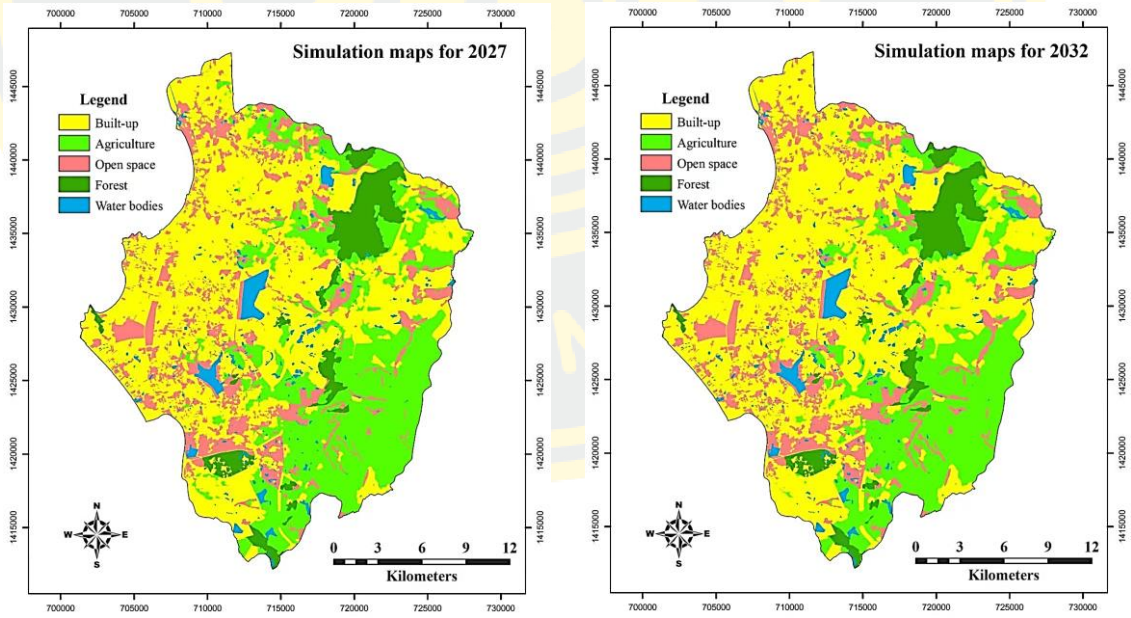

Figure 30: The simulation LULC map of 2027 and 2032 in Bang Lamung district

The result shown in Table 27 presents the results of the LULC map simulations for 2027 and 2032. As of 2022, the built-up area accounted for 42.25% (221.78 sq km) of the district area, and increased by 48.13% (252.63 sq km) and 52.30% (274.51 sq km) in 2027 and 2032, respectively. In contrast, the proportion of agriculture area is expected to decrease by 27.04% (141.95 sq km) and 22.56% (118.42 sq km) in 2027 and 2032, respectively. These simulation results show that with normal LULC change, agriculture area can be replaced by built-up areas.

Table 28 highlights the highest projected growth from 2009 to 2032 in the built-up areas with an average annual change of 94.83%. However, agriculture area and open spaces are expected to decline at an average annual change of -46.41% and -25.29%, respectively. In addition, forest area and water bodies are also projected to experience slight decreases at an annual average change of -5.41% and -4.52%, respectively.

Table 27: The simulated LULC areas for 2027 and 2032 under the spontaneous scenario

Land use Class	**2022**		**2027**		**2032**	
	Area (sq.km)	%	Area (sq.km)	%	Area (sq.km)	%
Built-up	221.78	42.25	252.63	48.13	274.51	52.30
Agriculture	175	33.34	141.95	-27.04	118.42	-22.56
Open space	79.57	15.16	80.36	-15.31	84.09	16.02
Forest	32.15	6.13	33.98	6.47	32.02	-6.10
Water bodies	16.37	3.12	15.94	-3.04	15.83	-3.02
Total	524.87	100	524.87	100	524.87	100

Table 28: The distribution of LULC in square kilometers in 2009 -2032

Land use class	**2009**	**2011**	**2017**	**2022**	**2027p**	**2032p**	**Annual % change**
Built-up	140.9	157.62	178.87	221.78	252.63	274.51	94.83
Agriculture	220.99	207.84	198.02	175.00	141.95	118.42	-46.41
Open space	112.55	110.25	99.28	79.57	80.36	84.09	-25.29
Forest	33.85	32.23	32.44	32.15	33.98	32.02	-5.41
Water bodies	16.58	16.93	16.26	16.37	15.94	15.83	-4.52

4.6.2 Green area improvement scenario

This scenario analysis involves open spaces, agricultural areas, and forests as green areas. Green area in the city is primarily related to the population size. The standardization for the ratio of green area to population size as a benchmark is an important tool to help prevent the reduction of green area (Guidelines for Green Area Management and Green Area Ratio Standards for Urban Communities in Thailand, 2017). As calculated, it is found that the population will increase in 2027 and 2032, which will affect the future demand for green area. In this study, the number of people in each sub-district was used to analyze the ratio of green area to population size (Table 29).

Table 29**:** The population projection in 10 years in each sub-district

Sub-district	**Population (people)**		
	2022	**2027**	**2032**
Na Kluea	128,774	162,400	204,800
Nong Prue	87,985	111,000	140,000
Huai Yai	31,150	39,300	49,600
Ta Khian Tia	24,927	31,400	39,600
Nong Pla Lai	24,777	31,200	39,300
Bang Lamung	12,751	16,100	20,300
Pong	10,818	13,600	17,200
Khao Mai Kaew	7,779	9,800	12,400
Total	**328,961**	**414,800**	**523,200**

Note: The calculation does not include non-registered population

This study examines all green areas in the Bang Lamung district using a simulated map and also utilizes the criteria for green areas specified in the urban planning standards and regulations of the Department of Public Works and Town & Country Planning.

The analysis of green areas is divided into 8 sub-districts, namely Na Kluea (covering Pattaya city), Nong Prue, Huai Yai, Ta Khian Tia, Nong Pla Lai, Bang Lamung, Pong, and Khao Mai Kaew, as shown in Figure 31. The study found that green space decreased in 2027 and 2032. Most of the open space is found in

downtown Pattaya and the central area with bare soil, bushes, dry land and grassy meadows along the canal. Most of the agricultural areas are concentrated in the Khao Mai Kaew and Huai Yai sub-districts, while forest areas are found in Takhian Tia, Khao Mai Kaew, and Huai Yai sub-districts.

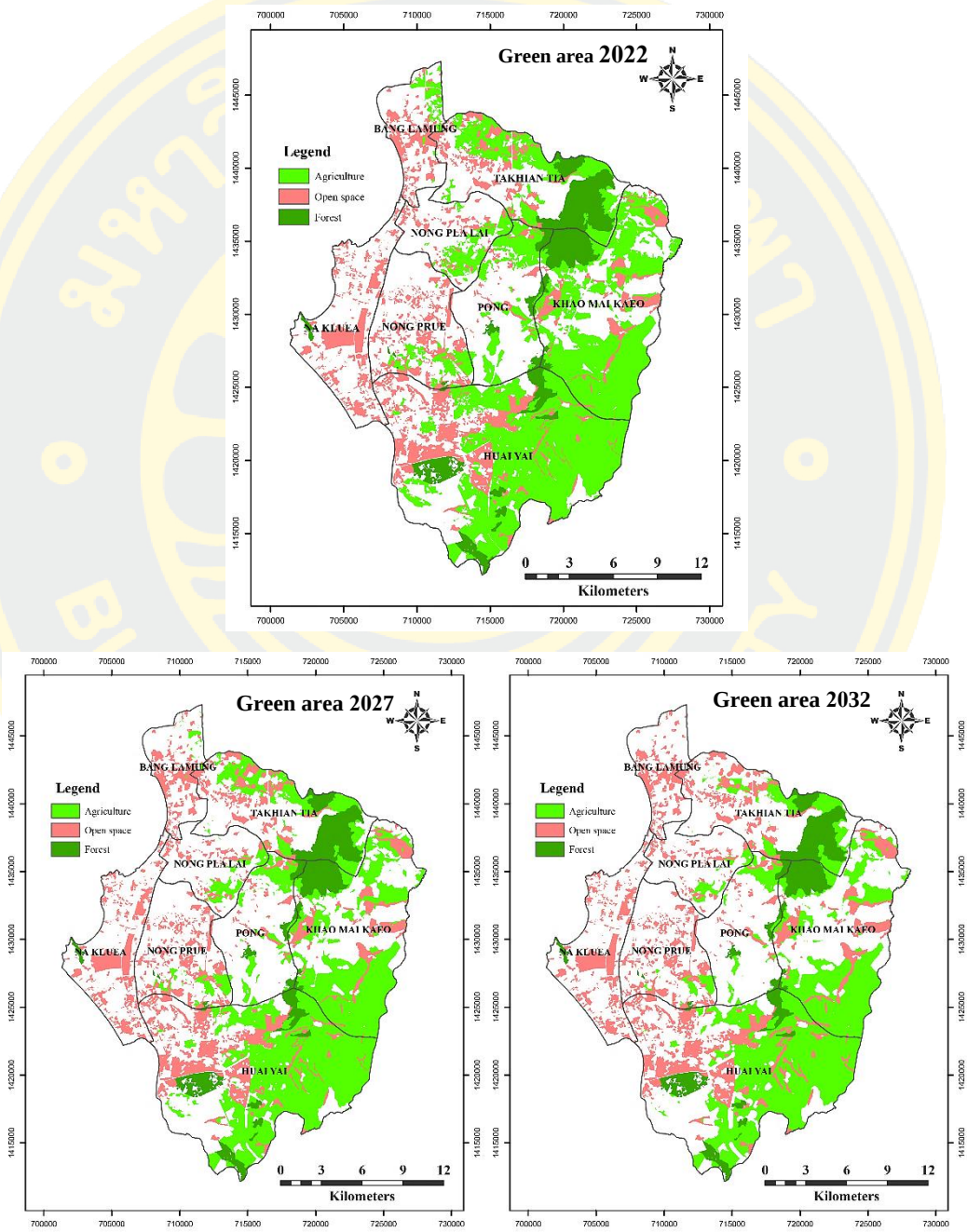

Figure 31: Simulated map of green area in each sub-district of Bang Lamung in 2027 and 2032

Based on the study results, the total green area in the study areas is 54.63% (23.93 sq km) in 2022. However, it is expected to decline to 48.83% (256.29 sq km) and 44.68% (234.53 sq km) by 2027 and 2037, respectively (Table 30).

The sub-district with the highest proportion of green area is Huai Yai, which has 73.09% (109.05 sq km) in 2022, and is expected to decrease to 68.60% (102.35 sq km) and 65.53% (97.17 sq km) in 2027 and 2037, respectively. The second highest green area is in Khao Mai Kaeo sub-district, with 70.77% (71.33 sq km) in 2022, expected to decrease to 61.79% (62.29 sq km) and 55.89% (56.34 sq km) in 2027 and 2037, respectively. The third highest green area is located in Takhian Tia Subdistrict, with 62.07% (41.53 sq km) in 2022, expected to decrease to 55.98% (37.45 sq km) and 47.48% (31.77 sq km) in 2027 and 2037, respectively. The majority of the green areas are forests and agricultural land, while the sub-district with the lowest proportion of green area is Na Kluea, which includes Pattaya City, with 26.37% (13.05 sq km) in 2022, and is expected to decrease to 26.17% (12.95 sq km) and 26.13% (12.93 sq km) in 2027 and 2037, respectively, with most of the area being vacant land.

Table 31 shows the distribution of green area in the study area. Overall, the green area of Bang Lamung district is expected to decrease annually, with the sub-district of Nong Pla Lai having the highest decline at an annual average of -37.73%. Follow closely is Pong sub-district, with an annual average decline of -36.28%. Beside, Bang Lamung and Ta Khian Tia sub-districts are also a significant decline, with annual averages of -29.36% and -23.51%, respectively. Huai Yai sub-district is expected to have a dramatic decline as well, with an annual average of -10.90%. Nong Prue sub-district and Na Kluea sub-district, which covers Pattaya City, are also expected to decline with an annual average of -17.76% and -0.91%, respectively.

Table 30**:** The green areas in each sub-district in 2027 and 2032

Sub-district	Sub-district area (sq.km)	Green area (sq.km)			Green area (sq.km.)/ Sub-district area (%)		
		2022	2027p	2032p	2022	2027p	2032p
Na Kluea (cover Pattaya)	49.49	13.05	12.95	12.93	26.37	-26.17	-26.13
Nong Prue	48.38	15.19	13.35	12.49	31.40	-27.60	-25.82
Huai Yai	149.19	109.05	102.35	97.17	73.09	-68.60	-65.13
Ta Khian Tia	66.90	41.53	37.45	31.77	62.07	-55.98	-47.48
Nong Pla Lai	33.00	9.87	7.36	6.15	29.91	-22.30	-18.62
Bang Lamung	27.84	9.76	7.55	6.90	35.06	-27.13	-24.77
Pong	49.26	16.94	12.99	10.79	34.39	-26.37	-21.91
Khao Mai Kaew	100.80	71.33	62.29	56.34	70.77	-61.79	-55.89
Total	**524.87**	**286.72**	**256.29**	**234.53**	**54.63**	**-48.83**	**-44.68**

Table 31**:** The distribution of green area in each sub-district in 2027 and 2032

Sub-district	Green area (sq.km)			Annual % change
	2022	2027	2032	
Na Kluea (cover Pattaya)	13.05	12.95	12.93	-0.91
Nong Prue	15.19	13.35	12.49	-17.76
Huai Yai	109.05	102.35	97.17	-10.90
Ta Khian Tia	41.53	37.45	31.77	-23.51
Nong Pla Lai	9.87	7.36	6.15	-37.73
Bang Lamung	9.76	7.55	6.90	-29.36
Pong	16.94	12.99	10.79	-36.28
Khao Mai Kaew	71.33	62.29	56.34	-21.02

Table 32: The simulated green area per person in 2027 and 2032

Sub-district	*Population			**Green area (sq.m)/person			Annual % change
	2022	2027p	2032p	2022	2027p	2032p	
Na Kluea (cover Pattaya)	128,774	162,400	204,800	101.33	79.75	63.14	-37.69
Nong Prue	87,985	111,000	140,000	172.67	120.29	89.24	-48.31
Huai Yai	31,150	39,300	49,600	3,500.85	2,604.37	1,958.98	-44.04
Ta Khian Tia	24,927	31,400	39,600	1,665.93	1,192.63	802.16	-51.85
Nong Pla Lai	24,777	31,200	39,300	398.34	235.85	156.38	-60.74
Bang Lamung	12,751	16,100	20,300	765.59	469.13	339.72	-55.63
Pong	10,818	13,600	17,200	1,565.70	954.98	627.48	-59.92
Khao Mai Kaew	7,779	9,800	12,400	9,170.06	6,355.62	4,543.56	-50.45
Total	**328,961**	**414,800**	**523,200**	**871.60**	**617.86**	**448.26**	**-48.57**

Note: *Population from DOPA
**Green area in this research covers open space, agriculture, and forest area counted in square meter

The data shown in Table 32 shows the amount of green space per person in each subdistrict. For analysis, the research has taken the urban planning criteria set by the Department of Public Works and Town & Country Planning, which is an area of 8 square meters per person. It's important to note that the Department's definition of green areas only encompasses open spaces designated for for recreational and environmental conservation purposes, except those found in agricultural and forestry areas. (Guidelines for Green Area Management and Green Area Ratio Standards for Urban Communities in Thailand, 2017). In this study, the researcher counted all green areas, including open spaces, agricultural areas, and forest areas, to be as the total green areas due to the current situation of all green areas in Bang Lamung district.

The research result shows that the overview of the green area per person in the study area is expected to decrease by approximately -48%. In 2022, the green area per person is around 871.60 sq.m/ person. By 2027 and 2032, it is expected to further decrease to 617.86 and 448.26 sq.m/ person, respectively.

However, when considering the green area per person in each sub-district area, it is found that the sub-district with the highest green area per person is Khao Mai

Kaew, with approximately 6,355.62 and 4,543.56 sq.m/ person in 2027 and 2032, respectively, followed by Huai Yai sub-district with approximately 2,604.37 and 1,958.98 sq.m/ person in 2027 and 2032, respectively. It can be seen that Khao Mai Kaew and Huai Yai are mostly forest and agriculture areas, while the green area in the Nong Prue sub-district is expected to be approximately 120.29 and 89.24 sq.m/ person in 2027 and 2032, respectively. Lastly, the green space in the Na Kluea sub-district, which covers Pattaya city, is expected to decrease to approximately 79.75 and 63.14 sq.m/ person in 2027 and 2032, respectively.

It has been noted that the green area in city area such as Nong Pa Lai, Bang Lamung and Na Kluea sub-district, which cover Pattaya City and consists mostly of open space, is decreasing at an average annual of green area per person around -60.74%, -55.63%, and -48.31% respectively. Moreover, Pong, Ta khian Tia, and Khao Mai Kaew sub-district which mostly is forest and agriculture areas, are also expected to decrease in average annual of green area per person over than -50%.

4.6.3 The area comprehensive plan scenario

In this study, the current Bang Lamung city plan has been considered. This research has used the city plan as an example of a government policy for future land use, which has been analyzed in terms of physical, social, economic, and environment to understand the changes in land use within the study area. By analyzing the city plan, it is possible to gain insights into preliminary LULC changes and investigate future land use possibilities.

To analyze this scenario, the study has divided land use into 3 major groups based on the Bang Lamung city plan as described in previous chapter. These groups are (1) Urbanization area, which refers to the residential and commercial areas included in the city plan promoted by the government for urbanization. (2) Control area, which refers to the agricultural and open space areas in the city plan. (3) Protect area, which refers to the areas where urbanization is prohibited, such as forest conservation areas and national parks, as compared to the current city plan (Figure 32).

Figure 33-35 show that the built-up area is expanding towards the east. In 2027 and 2032, a significant portion of agriculture areas has been converted into

urban areas. Therefore, it is evident that the expansion of the built-up area is not in accordance with the boundary set by the current Bang Lamung city plan which determines as the urbanization area.

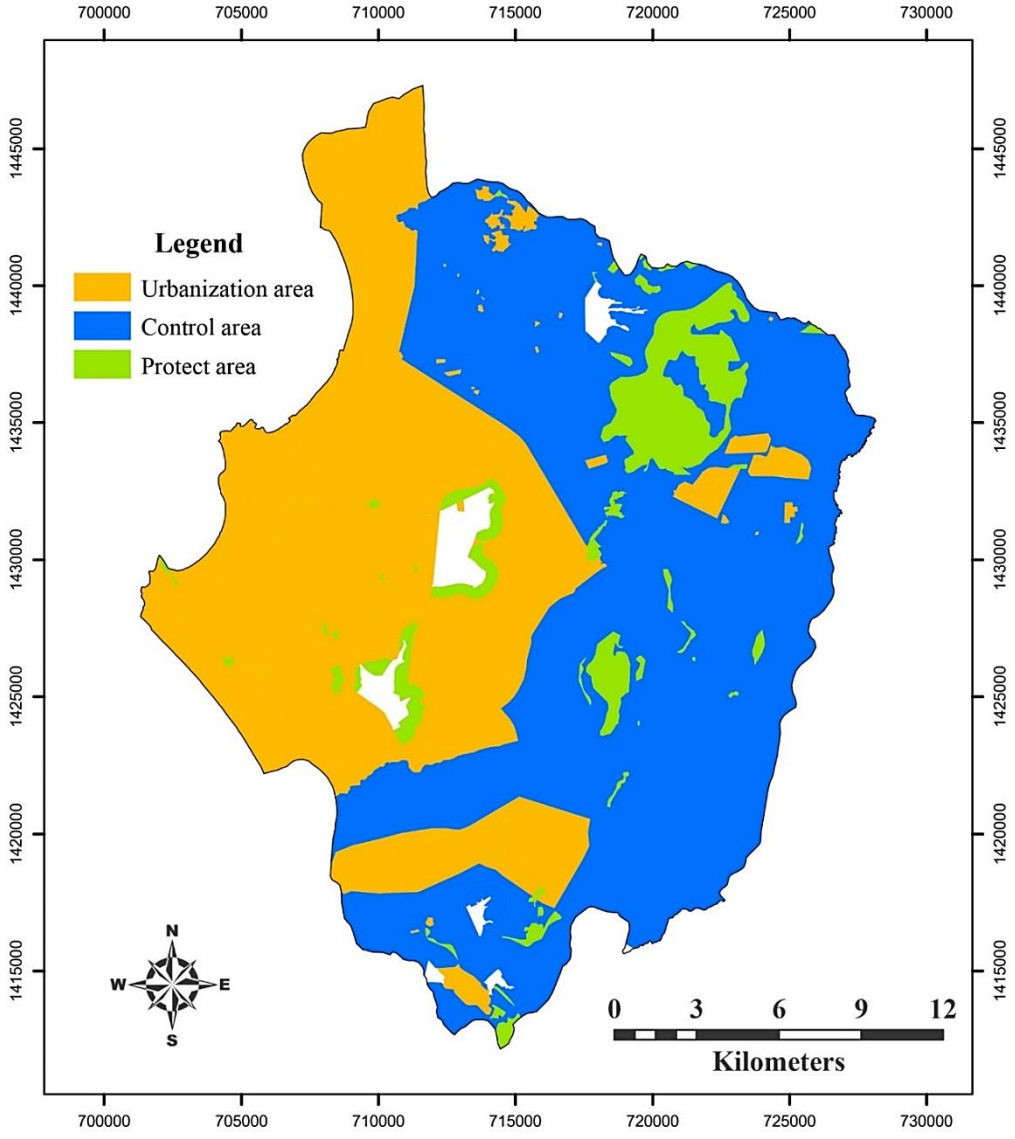

Figure 32: The 3 major groups based on the Bang Lamung city plan

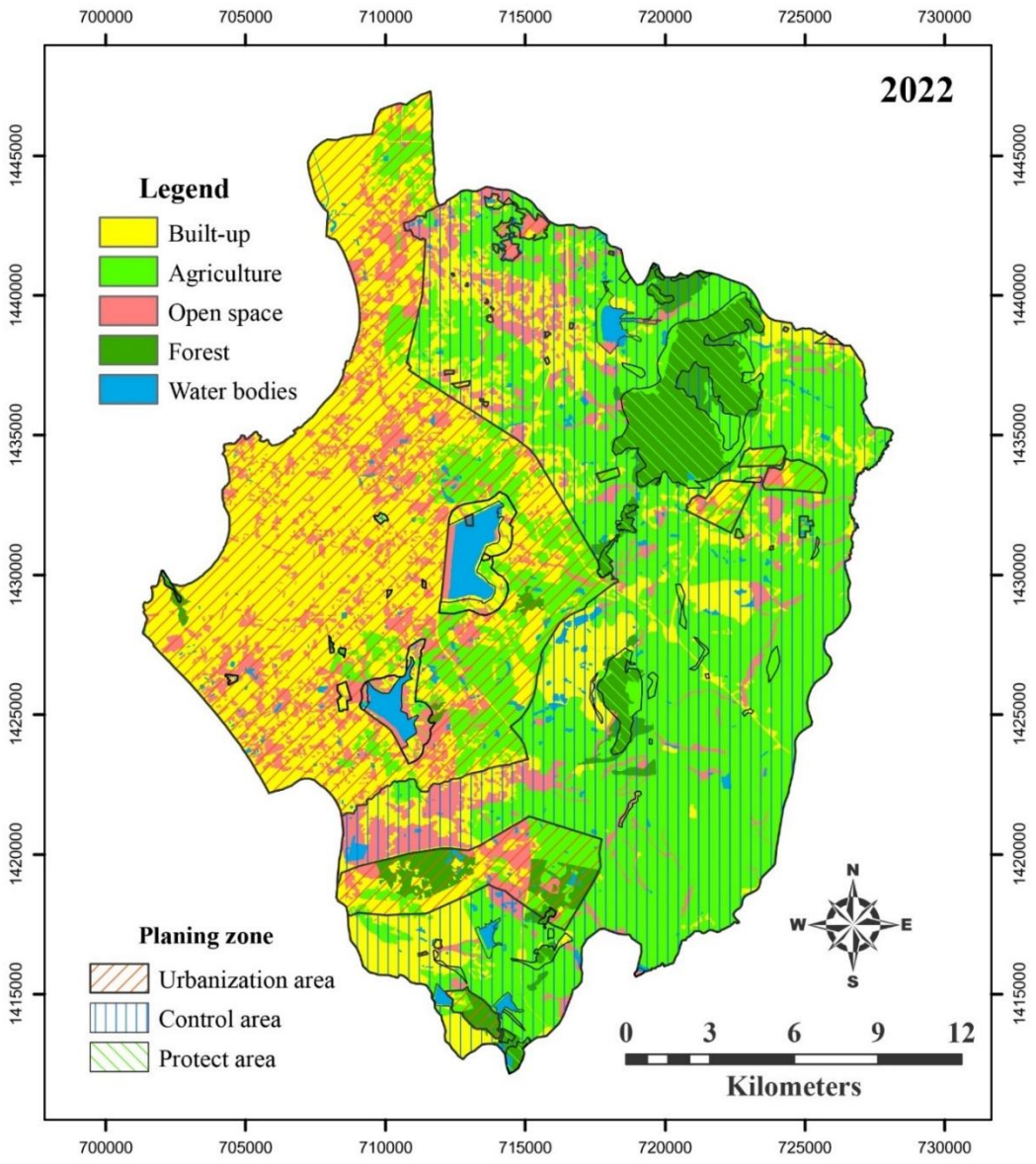

Figure 33**:** Land use of Bang Lamung district in 2022 under the area comprehensive plan

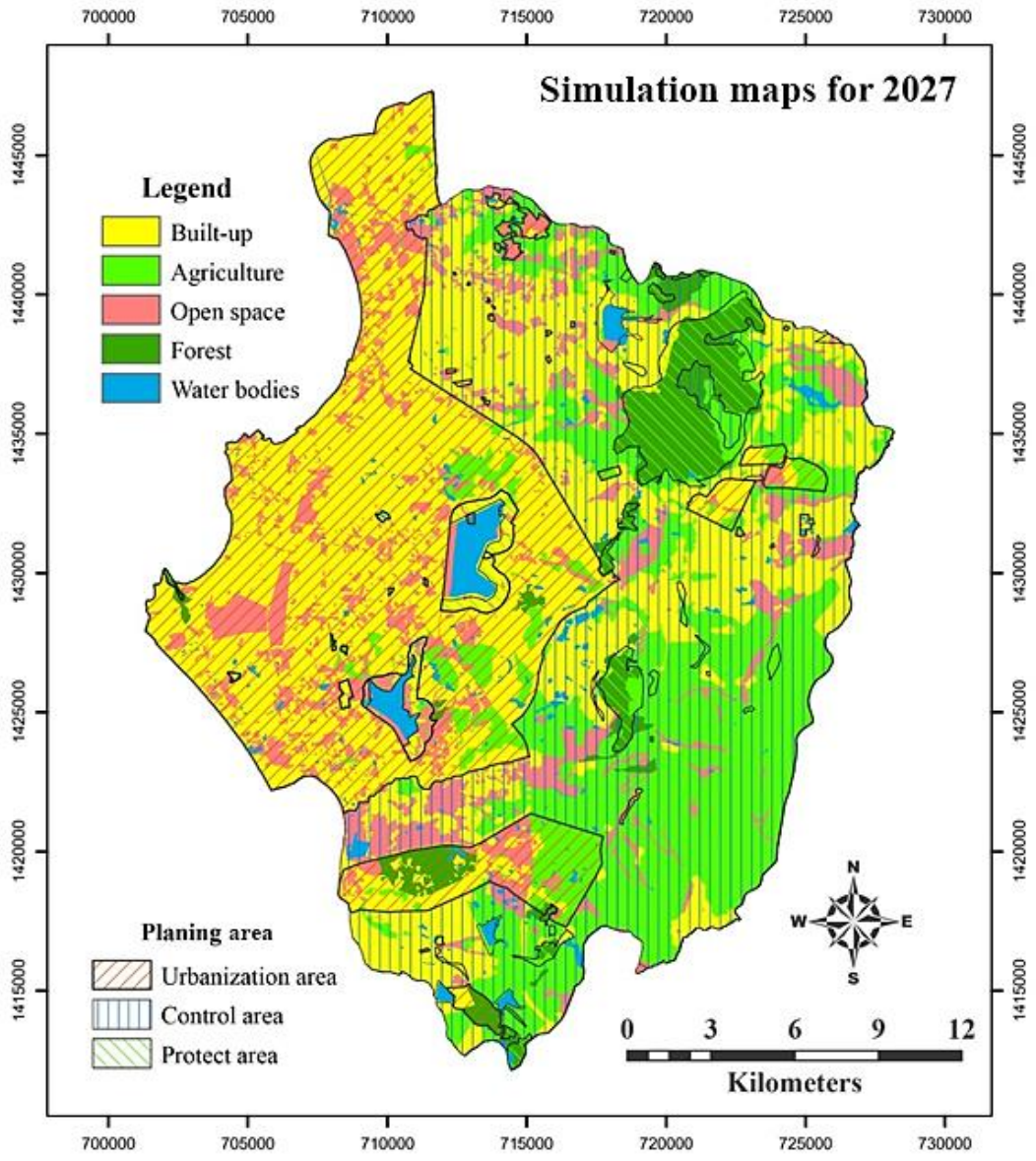

Figure 34: Simulated land use of Bang Lamung district in 2027 under the area comprehensive plan

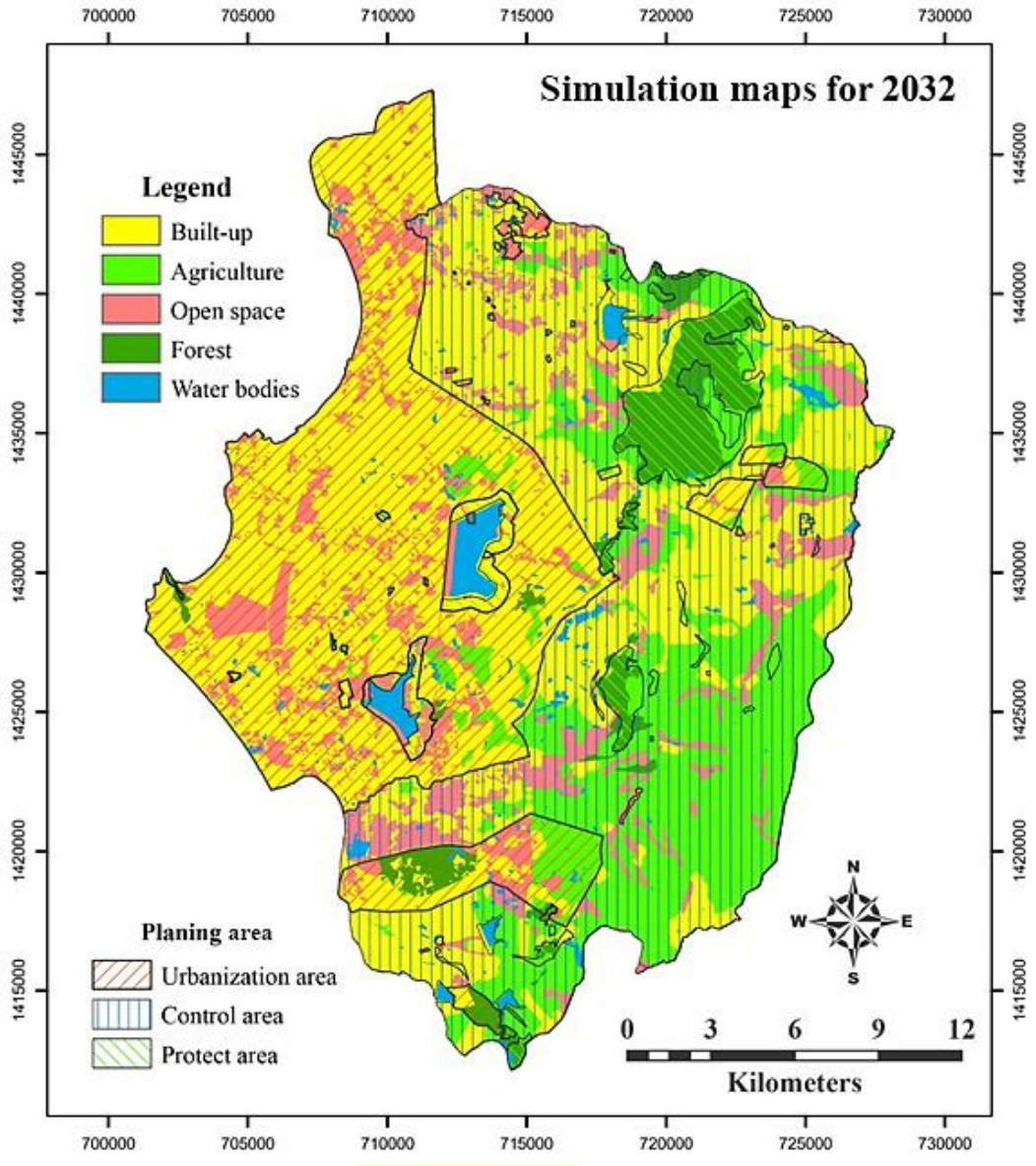

Figure 35**:** Simulated land use of Bang Lamung district in 2032 under area comprehensive plan

Table 33 presents the simulated LULC areas for 2027 and 2032 according to the area comprehensive plan scenario that divides into 3 main areas.

- Urbanization area: The results indicate that in 2022, the built-up area accounts for 25.11% (129.19 sq km) of the urbanization area. By 2027 and 2032, it is expected to increase by 27.27% (140.28 sq km) and 28.40% (146.11 sq km), respectively. Meanwhile, the area used for agriculture is expected to decrease by 3.88% (19.95 sq km) and 2.68% (13.37 sq km) in 2027 and 2032, respectively, as it is converted to built-up areas. Other LULC classes such as open space, forest, and water bodies show minimal changes in their area for both 2027 and 2032. However, the fact that built-up areas are controlled under the city plan (Figure 36).
- Control area: The results show that in 2022, agriculture areas account for 26.86% (138.19 sq km) of the control area. However, under the control area, the proportion of agriculture is projected to decline and be replaced by built-up areas, with an expected decrease of 22.81% (117.36 sq km) and 19.40% (99.82 sq km) in 2027 and 2032, respectively. While, the built-up area is projected to increase by 20.34% (104.62 sq km) and 23.30% (119.86 sq km). The remaining LULC classes, such as open space, forest, and water bodies, are expected to experience slight changes in their areas in 2027 and 2032. It should be noted that the designated areas for agriculture and open space differ from the city plan (Figure 36).
- Protection area: The results show that in 2022, forest areas account for 4.28% (22 sq km) of the protection area. There is a projected slight decrease in the proportion of forest areas within the protected area and be replaced by built-up, agriculture area, and open space, with an expected decrease of 4.13% (21.27 sq km) and 3.93% (20.21 sq km) in 2027 and 2032, respectively. At the same time, built-up, agriculture area, and open space are projected to slightly increase by 1.28% (6.59 sq km), 0.84% (4.35 sq km), and 0.49% (2.51 sq km) in 2027, and by 1.41% (7.25 sq km), 0.91% (4.67 sq km), and 0.50% (2.58 sq km) in 2032. The water bodies class is expected to remain stable in terms of area in 2027 and 2032. However, the fact that forest and water bodies areas do not conform to city plan (Figure 36).

Table 33: The simulated LULC areas for 2027 and 2032 under the area comprehensive plan

Area comprehensive plan	Land use class	2022		2027		2032	
		Area (sq.km)	%	Area (sq.km)	%	Area (sq.km)	%
Urbanization area	Built-up	129.19	25.11	140.28	27.27	146.11	28.40
	Agriculture	31.29	6.08	19.95	-3.88	13.77	-2.68
	Open space	40.12	7.80	40.56	7.89	41.03	7.98
	Forest	6.20	1.21	6.12	-1.19	6.05	-1.18
	Water bodies	3.24	0.63	3.13	0.61	3.09	0.60
	Total	**210.04**	**40.83**	**210.04**	**33.08**	**210.04**	**35.48**
Control area	Built-up	85.42	16.61	104.62	20.34	119.86	23.30
	Agriculture	138.19	26.86	117.36	-22.81	99.82	-19.40
	Open space	32.60	6.34	35.90	6.98	39.10	7.60
	Forest	7.95	1.55	6.60	-1.28	5.75	-1.12
	Water bodies	5.11	0.99	4.81	-0.93	4.74	-0.92
	Total	**269.27**	**52.35**	**269.27**	**52.34**	**269.27**	**52.34**
Protect area	Built-up	6.12	1.19	6.59	1.28	7.25	1.41
	Agriculture	4.10	0.80	4.35	0.84	4.67	0.91
	Open space	2.49	0.48	2.51	0.49	2.58	0.50
	Forest	22.00	4.28	21.27	-4.13	20.21	-3.93
	Water bodies	0.39	0.08	0.38	-0.07	0.38	0.07
	Total	**35.10**	**6.83**	**35.10**	**6.81**	**35.10**	**6.82**
Total		**514.42**	**100**	**514.42**	**100**	**514.42**	**100**

Noted: The reservoir does not count in this scenario

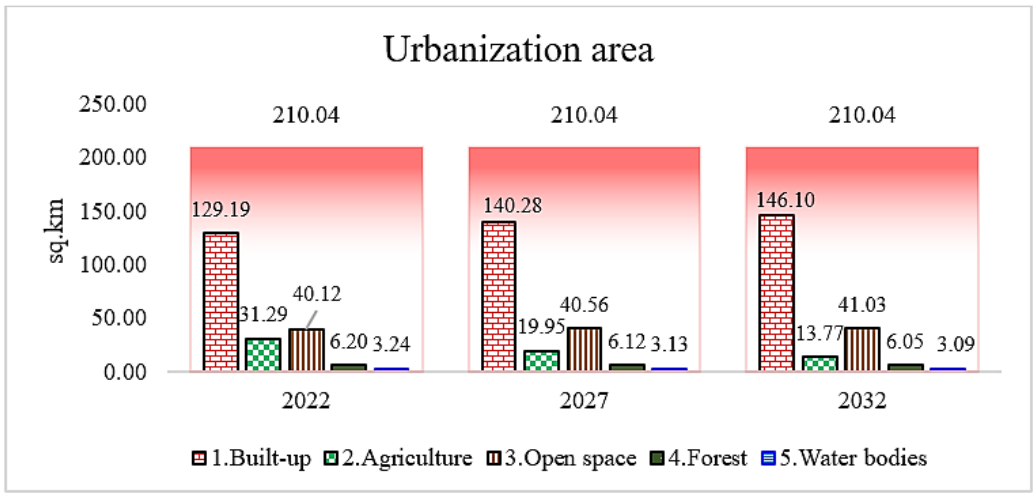

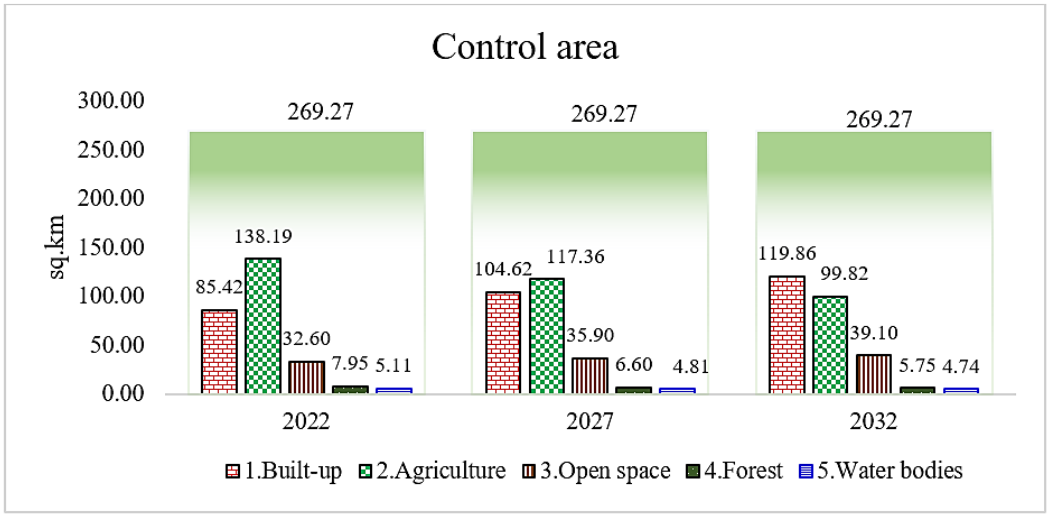

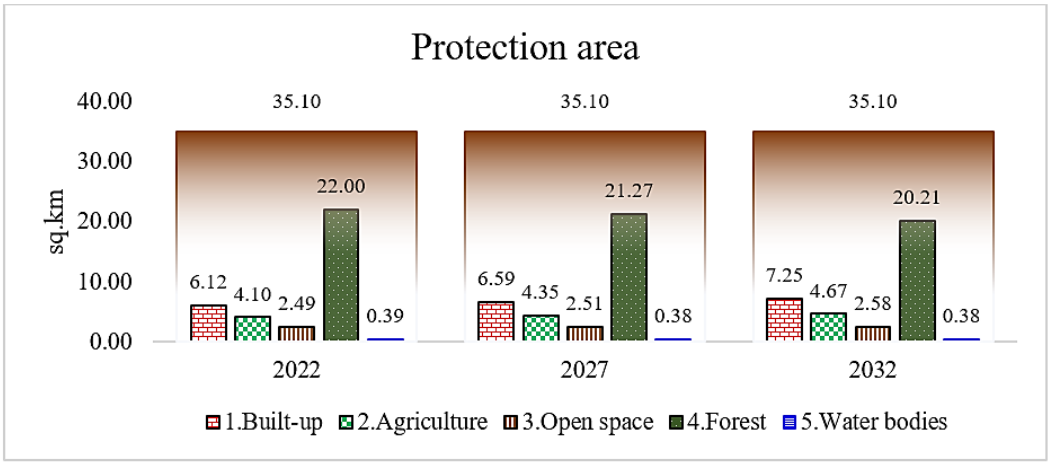

Figure 36: LULC change delineation analysis under 3 major area

Table 34**:** The distribution of simulated LULC in square kilometers in 2027 and 2032 under the area comprehensive plan

Area comprehensive plan	Land use class	2022	2027p	2032p	Annual % change
Urbanization area	Built-up	129.19	140.28	146.11	13.10
	Agriculture	31.29	19.95	13.77	-55.99
	Open space	40.12	40.56	41.03	2.27
	Forest	6.20	6.12	6.05	-2.42
	Water bodies	3.24	3.13	3.09	-4.63
Control area	Built-up	85.42	104.62	119.86	40.32
	Agriculture	138.19	117.36	99.82	-27.77
	Open space	32.60	35.9	39.1	19.94
	Forest	7.95	6.60	5.75	-27.67
	Water bodies	5.11	4.81	4.74	-7.24
Protect area	Built-up	6.12	6.59	7.25	18.46
	Agriculture	4.10	4.35	4.67	13.90
	Open space	2.49	2.51	2.58	3.61
	Forest	22.00	21.27	20.21	-8.14
	Water bodies	0.39	0.38	0.38	-2.56

The results of the annual change in simulated LULC for 2027 and 2032 under the area comprehensive plan scenario are presented in Table 34 as follows.

In the urbanization area, the model simulated growth in built-up areas and open spaces, with an average annual growth of 13.10% and 2.27%, respectively. However, agriculture areas are expected to decline by an average annual of -55.99% in 2027 and 2032, while water bodies and forest areas are also projected to decline slightly with an annual average of -4.63% and -2.42%, respectively.

In the control area, the results show an expected average annual decline of agriculture areas, forest, and water bodies by -27.77%, -27.67%, and -7.24% in 2027 and 2032, respectively. On the other hand, built-up area and open space are expected to increase, with an average annual growth of 40.32% and 19.94%, respectively.

In the protection area, the results show that forest and water bodies are expected to decline by an average annual of -8.14% and -2.56% in 2027 and 2032, respectively. In contrast, built-up areas and agriculture areas are expected to increase with an average annual growth of 18.46% and 13.90%, respectively. Water bodies are projected to decline slightly with an annual average of -2.56%.

CHAPTER 5
DISCUSSION AND CONCLUSION

5.1 Discussion

This study adopts a sustainable development perspective and aims to analysis of LULC changes that have occurred in the past, present, and future. To achieve this, remote sensing is employed as one approach, while the CA-Markov model is utilized for LULC simulation in the future. Both remote sensing and the CA-Markov model are employed to examine and analyze LULC in this study. The CA-Markov model is the most popular method and is often implemented by several studies [9] and provides an answer to the research question of where LULC changes are expected to occur under each scenario (Hamad et al, 2018). The study focuses on the Bang Lamung district, which is part of the Eastern Economic City, and serves as a case study for analysis of the estimation of LULC changes in 2027 and 2032.

5.1.1 LULC classification

This study analyzed LULC in Bang Lamung District by using the satellite image classification (Sentinel 2 and ALOS (AVNIR-2) data). Since spatial resolution is one of the factors affecting the satellite image classification accuracy, therefore, this study used free satellite image data with similar spatial resolution (10 m) and recorded satellite images from the past to the present. In addition, image classification techniques in this study use image interpretation, which is useful for complex areas such as Bang Lamung District. The development of wall-to-wall land cover monitoring system is not a simple task in the cases of large, diverse, and complex countries (Mas et al, 2017). Therefore, the satellite image of Bang Lamung district is digitized to create LULC maps based on the knowledge of the researcher of the study area. This should be able to produce accurate base maps and accurate estimations of LULC changes. This should be able to produce accurate base maps and accurate estimations of the LULC dynamics consistent with Soytong, P., Janchidfa, K. and Chayhard, S. (2019), Chonburi Land Use Classification Report, Year 2017, which can be classified into 9 categories, the highest being agriculture/livestock, which

accounted for 56.67%. Followed by the community and city areas at 16.14 percent; Forest/Wetland Area at 11.14%; and others at 5.40%.

5.1.2 LULC simulation

This study has considered sustainable development and utilized the city plan of Bang Lamung, which serves as a guiding framework for the development of the area. The study has been analyzed into 3 different scenarios.

1) Spontaneous is a consideration of the independent growth of the city. From the simulation results, it can be seen that the built-up areas in the Bang Lamung district will continue to expand until all available space is transformed into built-up areas, especially in the eastern part of the district, which is mostly agriculture area. The annual growth of construction between 2002 and 2032 is estimated to be 94% on average. At the same time, it is evident that the agricultural areas and open spaces have decreased significantly, with an average annual decline rate of -46% and -25%, respectively. According to the research, it is evident that the highest growth rates of construction occurred between 2017 and 2022 (Figure 37).

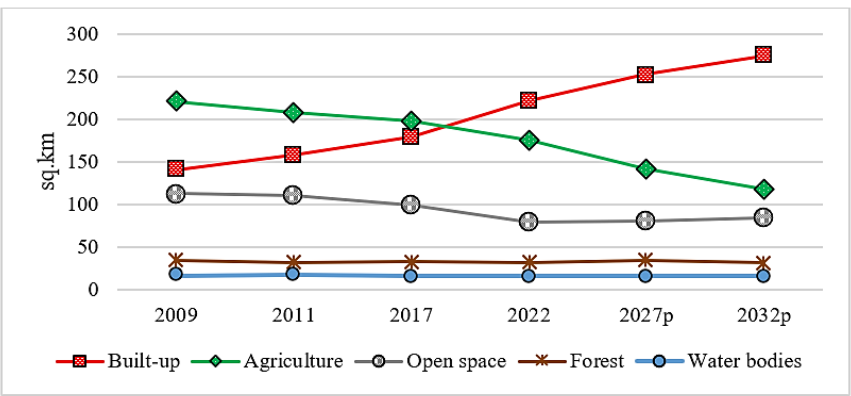

Figure 37: LULC change between 2009 - 2032

2) The green area improvement in Bang Lamung district is analyzed by dividing it into sub-districts to determine the amount of green area per person, using the standard criteria of the Department of Public Works and Town Planning (Guidelines for Green Area Management and Green Area Ratio Standards for Urban Communities in Thailand, 2017). However, this study aimed to provide an overall of green areas in the study area. The green areas include open spaces, which are designated for public use,

such as parks and recreation areas. As for the agriculture, it's a green area for community economy and environmental conservation. Finally, forest are original green areas that are essential to the ecosystem and must be appropriately preserved.

Based on the study, it can be seen that every sub-district has a decrease in green areas per year. When considering the period from 2022 to 2032, the green areas in the Pattaya city (Naklua sub-district) is mostly open space for public use. The study clearly shows that overall green areas in the Pattaya area has decreased by 0.91% per year. The sub-districts of Bang Lamung and Nong Prue, which are connected to Pattaya city and experience expansion of construction, have a significant decrease in green areas, with a decrease of 29% and 17% per year, respectively.

In addition, the research indicates a clear reduction in green areas related to agriculture, particularly in Nong Pla Lai, Pong, and Takhian Tia sub-districts, which are primarily agricultural areas, and the green areas have decreased by -37%, -36%, and -23% per year, respectively. In terms of forested areas, most of the changes occur in Takhian Tia, Nong Mai Kaew, and Huai Yai sub-districts, with yearly reductions of -23%, -21%, and -10%, respectively. Although there is still more green space per person than the city planning standard, open space areas within the Pattaya city and surrounding area should be designated as green zones for public use. This is an issue that relevant organization can manage green area for local.

3) The area comprehensive plan scenario is a consideration of analyzing the future LULC of Bang Lamung district by comparing them with the current city plan of the Bang Lamung (DPT, 2019). The result showed that the built-up area increased in designated urbanization areas, and some built-up areas spread outside the boundaries of urbanization areas, but all built-up areas remain in the Bang Lamung city plan. Agriculture and open space areas are the controlled areas of research. The controlled areas do not match the Bang Lamung city plan boundaries due to the problem of ineffective enforcement of the Comprehensive Plan. The forested areas and water sources do not match the boundary of the Bang Lamung city plan because the satellite images were taken in January, which is a dry winter in Thailand. During this period, the phenomenon of leaves shedding and the amount of water in the water resources decreases. These affect the classification of image classification.

5.2 Conclusion

The CA-Markov model simulates future LULC changes by combining the CA and Markov chain analysis processes. This model is suitable for high spatial simulation accuracy such as quantitative and spatial. The simulation results are not only presented as probabilities, but also provide important insights into the LULC simulation patterns and distribution in the future, which can be analyzed under different scenarios.

This study employs the combination of Markov and Cellular Automata is utilized to simulate LULC change in 2027 and 2032. Although the CA-Markov model has been widely used in developed countries, there have been few investigated on urban planning in developing countries. The study can be analyzed with 3 scenarios in Bang Lamung district.

The first scenario is spontaneous that is a consideration of the LULC change by model. The study found that urban expansion spread along the coastal areas. There has been an increase in built-up areas over the past few decades, but agriculture areas continually reduce annual agriculture areas change.

The second scenario is the green area improvement. According to the analysis, there will still be enough green space for the population between 2027 and 2032. However, there is a decreasing trend in the annual rate of change of green areas per population, particularly in the Pattaya City area and the areas connected to the city. This is the increasing population for green areas. Therefore, it can be seen that there is still a considerable amount of open space in the urban area, and local government organizations can still determine the green zone to support the growing demand. In addition, the agricultural area which serve as green areas for the community's economy, have shown a significant decline in 2027 and 2032. From the local government information, a majority of the population engages in agriculture, particularly in the Pong, Nong Prue, and Nong Pla Lai areas. Therefore, area for agricultural activities should be established in these areas.

The third, the area comprehensive plan scenario, compares the simulated results in 2027 and 2032 with the current Bang Lamung city plan. The study divided the analysis into 3 main areas: the Urbanization area, the Control area, and the Protect area. The urbanization area has undergone changes that comply with the urban plan

and remain within the controllable boundaries of the designated area. However, when considering the results of the simulation, there is a dispersed trend towards the upper part of the plan area, which could lead to uncontrolled dispersion. The control area comprise of agriculture and open spaces do not currently meet the proposed design of planning. Similarly, the protection area compose of forests and water sources do not conform to the city plan.

The LULC map simulation is useful for urban planning in Pattaya City and Bang Lamung District. This study is part of the concept for urban development under the EEC project.

5.3 Recommendation

This study suggests that the use of high spatial resolution satellite images is highly recommended to obtain accurate model simulation results, especially in urban areas like Pattaya. Because urban areas have complex and heterogonous features, the high spatial resolution image provides better information to land use map.

In the future research will bring another LULC model to compare the result because we can see how different the methodology of the model and its accuracy. Increasing the number of survey points in the fieldwork is recommended to improve the reliability of satellite image classification. It will increase more accurate assessment of satellite image classification.

REFERENCES

Aburas, M. M., Ho, Y. M., Ramli, M. F., and Ashaari, Z. H. (2016). The simulation and prediction of spatio-temporal urban growth trends using cellular automata models. *A review. International Journal of Applied Earth Observation and Geoinformation, 52,* 380 - 389.

Aggarwal (2004). *Satellite Remote Sensing and GIS Applications in Agricultural Meteorology*. Retrieved November 15, 2022, from http://www.wamis.org/agm/pubs/agm8/Paper-2.pdf

Alam, N., Saha, S., Gupta, S., and Chakraborty, S. (2021). Prediction modelling of riverine landscape dynamics in the context of sustainable management of floodplain. *a Geospatial approach. Annals of GIS, 27(3),* 299-314.

Alqurashi, A. F. a. L. K. (2013). Investigating the Use of Remote Sensing and GIS Techniques to Detect Land Use and Land Cover Change: A Review. *Advances in Remote Sensing 2(02),* 193.

Arsanjani, J. J., Helbich, M., Kainz, W. and Boloorani, A. D. (2013). Integration of Logistic Regression, Markov Chain and Cellular Automata Models to Simulate Urban Expansion. *International Journal of Applied Earth Observation and Geoinformation, 21,* 265-275.

Aslam, R. W., Shu, H. and Yaseen, A. (2023). Monitoring the population change and urban growth of four major Pakistan cities through spatial analysis of opensource data. *Annals of GIS, 29,* 1-13.

Barney, C. (2006). Urbanization in Developing Countries: Current Trends, Future Projections, and Key Challenges for Sustainability. Technology in Society, *Elsevier, 28(1),* 63-80.

Berlin, P., Frunzi, N., Napoleon, E. and Ormsby, T. (1999). *Getting to Know ArcView GIS (3rd Ed)*. USA: ESRI Press.

Bhrammanachote, W. (2019). The Review of Thailand's Eastern Economic Corridor: Potential and Opportunity. *Local Administration Journal, 12(1),* 73–86.

Congalton, R. G. (1991). A review of assessing the accuracy of classifications of remotely sensed data. *Remote sensing of environment, 46,* 35-46.

Congalton, R. G. and Green, K. (2019). *Assessing the accuracy of remotely sensed data: principles and practices*. CRC press.

Department of Provincial Administration (Dopa) (2022). Official statistics registration

systems. Retrieved December 10, 2022, from https://stat.bora.dopa.go.th/stat/statnew/statMenu/newStat/home.php

Department of Public works and Town & country planning (DPT), (2019). *Banglamung comprehensive plan*. Retrieved November 10, 2022, from https://www.banglamungcomprehensiveplan.com/

Deng, X. H., J., Rozelle, S. and Uchida, E. (2008). Growth, population and industrialization, and urban land expansion of China. *J.Urban Econ, 63*, 96-115.

D. Lu, e. a. (2004). Change Detection Techniques. *International Journal of Remote Sensing, 25(12)*, 2365-2401.

Eastern Economic Corridor (EEC) Office (2019). *The Eastern Economic Corridor Project*. Retrieved November 12, 2022, from http://www1.ldd.go.th/WEB_OLP/report_research_E.html

Eastern Special Development Zone (2018). *ESDZ.Act*. Retrieved December 6, 2022, from https://thelegal.co.th/2018/08/06/2433/

Eastman, J.R. (2003). Guide to GIS and Image Processing 14, 239-247. Clark University Manual, USA.

Erle, E. and Pontius, R. (2007). *Land-Use and Land-Cover Change*. Retrieved November 10, 2022, from http://www.eoearth.org/article/Land-use_and_land-cover_change

ESDZ.Act. (2018). Retrieved from https://thelegal.co.th/2018/08/06/2433/

European Space Agency (ESA). *AVNIR-2 Overview*. Retrieved December 5, 2022, from https://earth.esa.int/eogateway/instruments/avnir-2/description

Foody, G.M. (2002). Status of land cover classification accuracy assessment. *Remote sensing of environment, 80(1)*, 185-201.

Francis, T. (2012). *Remote Sensing of Land Use and Land Cover: Principles and Applications*. Retrieved December 6, 2022,from https://books.google.co.th/books

Geographic Information Technology Training Alliance. (2015). *Essential steps in remote sensing*. Switzerland: University of Zurich.

Gil, R.P. and Jeffrey, M. (2005). Comparison of the structure and accuracy of two land change models. *Int. J. Geogr. Inf. Syst., 19*, 243–265.

Gollin, D. J., R. and Vollrath, D. (2016). Urbanization with and without industrialization. *J. Econ. Growth 21*, 35-70.

Gong, W., Yuan, L., Fan, W. and Stott, P. (2013). Analysis and Simulation of Land Use Spatial Pattern in Harbin Prefecture Based on Trajectories and Cellular Automata - Markov Modeling. *International Journal of Applied Earth Observation and Geoinformation*, *34*, 207-216.

Guan, D., Li, H., Inohae, T., Su, W., Nagaie, T., and Hokao, K. (2011). Modeling urban land use change by the integration of cellular automaton and Markov model. *Ecological Modelling, 222(20)*, 3761-3772.

Guidelines for Green Area Management and Green Area Ratio Standards for Urban Communities in Thailand (2017). *Sustainable Urban and Community Development under ASEAN Working Group on Environmentally Sustainable Cities (AWGESC)*. Retrieved April 6, 2023, from www.onep.go.th

Hamad, R., Balzter, H., and Kolo, K. (2018). Predicting Land Use/Land Cover Changes Using a CA-Markov Model under Two Different Scenarios. *Sustainability, 10*(10), 3421.

Hyandye, C. B. and Martz, L. W. (2017). A Markovian and Cellular Automata Land-use Change Predictive Model of the Usangu Catchment. *International Journal of Remote Sensing, 38*, 64-81.

JAXA EORC (2006). *AVNIR-2 Advanced Visible and Near Infrared Radiometer type 2*. Retrieved December 15, 2022, from https://www.eorc.jaxa.jp/en/news/list.php?year=2006

Kim, J. H. (2011). Linking land use planning and regulation to economic development: A literature review. *J. Plan. Lit., 26*, 35-47.

Landis, J. R. and Koch, G. G. (1977). The Measurement of Observer Agreement for Categorical Data. *Biometrics*, *33(1)*, 159-174.

Loret, E., Martino, L., Fea, M. and Sarti, F. (2017) Enhanced Urban Sprawl Monitoring over the Entire District of Rome through Joint Analysis of ALOS AVNIR-2 and SENTINEL 2A Data. *Advances in Remote Sensing, 6*, 76-87.

Maitima, J. M., Mugatha, S. M., Reid, R. S., Gachimbi, L. N., Majule, A., Lyaruu, H. and Mugisha, S. (2009). The linkages between land use change, land degradation and

biodiversity across East Africa. *African Journal of Environmental Science and Technology, 3*(10).

Mas, J. F., Lemoine-Rodríguez, R., González-López, R., López-Sánchez, J., Piña-Garduño, A. and Herrera-Flores, E. (2017). Land Use/land Cover Change Detection Combining Automatic Processing and Visual Interpretation. *European Journal of Remote Sensing, 50(1),* 626-635.

Meyer, W. B. and Turner, B. L. (1996). Land-use/land-cover change: challenges for geographers. *GeoJournal, 39*(3), 237-240.

Mondal, D. M. S., Sharma, N., Kappas, M., and Garg, P. (2019). CA-Markov modeling of land use land cover dynamics and sensitive analysis to identify sensitive parameter(s). *The International Archives of the Photogrammetry, Remote Sensing and Spatial Information Sciences, XLII-2/W13,* 723-729.

Moser, S. C. (1996). A partial instructional module on global and regional land use/cover change: assessing the data and searching for general relationships. *GeoJournal, 39(3),* 241-283.

Murai, S. (1993). *Remote sensing note*. Tokyo: Japan Association on Remote Sensing.

Nunes, C. G. F. and Auge, J. (1999). *Land-Use and Land-Cover Change (LUCC): Implementation Strategy*.

Parveen, S., Basheer, J., and Praveen, B. (2018). A literature review on land use land cover changes. *International Journal of Advanced Research, 6(7)* 1-6.

Pielke Sr, R. A., Pitman, A., Niyogi, D., Mahmood, R., McAlpine, C., Hossain, F., Goldwijk, K. K., Nair, U., Betts, R., Fall, S., Reichstein, M., Kabat, P. and Noblet, N. (2011). Land Use/land Cover Changes and Climate: Modeling Analysis and Observational Evidence. Wiley Interdisciplinary Reviews: *Climate Change, 2(6),* 828-850.

Polngam, S. (2003). *Principle of satellite data Processing by computer*. Bangkok: GISTDA.

Pontius, R. G. and M. Millones (2011). Death to Kappa: birth of quantity disagreement and allocation disagreement for accuracy assessment. *International Journal of Remote Sensing 32(15),* 4407-4429.

Puig, C., Hyman, G., and Bolanos, S. (2002). Digital Classification vs. Visual Interpretation: a case study in humid tropical forests of the Peruvian Amazon. *Int.*

*Cent. Trop. Agric.*1-5.

Raju, P. L. N. (2006). Fundamentals of geographical information system. *Satellite Remote Sensing and GIS Applications in Agricultural Meteorology*, *103*.

Singh, A. (1989). Digital Change Detection Techniques Using Remotely-Sensed Data. *International Journal of Remote Sensing, 10*, 989-1003.

Singh, R. P., Singh, N., Singh, S., and Mukherjee, S. (2016). Normalized difference vegetation index (NDVI) based classification to assess the change in land use/land cover (LULC) in Lower Assam, India. *International Journal of Advanced Remote Sensing and GIS, 5(10)*, 1963-1970.

Soytong, P., Janchidfa, K. and Chayhard, S. (2019). Strategic Environmental Management Plan for Green Growth Development in the Special Economic Eastern Region: Case Study of Chonburi Green Space Network Master Plan Development. *Faculty of Geoinformatics, Burapha University. Chonburi province, Thailand*, 204 p.

Stiglitz, J. E. (1996). *Whither socialism?*. MIT press.

Strielko, I. and Pereira, P. (2014). *Land-use planning of Volyn region (Ukraine) using Geographic Information Systems (GIS) technologies*. Retrieved November 18, 2022, from https://ui.adsabs.harvard.edu/abs/2014EGUGA.16.3084S

Tariq, A., and Shu, H. (2020). CA-Markov Chain Analysis of Seasonal Land Surface Temperature and Land Use Land Cover Change Using Optical Multi-Temporal Satellite Data of Faisalabad, Pakistan. *Remote Sensing, 12*(20), 3402.

Thomas, H. and H. M. Laurence. (2006). Modeling and Projecting Land-use and Land-Cover Changes with a Cellular Automaton in Considering Landscape Trajectories: An Improvement for Simulation of Plausible Future States. *EARSeLeProc, 5*, 63-76.

Tontisirin, N. A., S. (2021). Economic Development Policies and Land Use Changes in Thailand: From the Eastern Seaboard to the Eastern Economic Corridor. *Sustainability, 13(11)*: 6153.

Town & Country Planning Standards Development Bureau (2006). *Handbook of data analysis for comprehensive urban planning*. Department of Public works and Town & country planning (DPT), 58-59.

Turner, B. L., Meyer, W. B. and Skole, D. L. . (1994). Global land-use/land-cover change: towards an integrated study. *Ambio. Stockholm, 23(1)*, 91-95.

United Nations Educational, Scientific and Cultural Organizatio (1999). *Application of Satellite and Airborne Image Date to Coastal Management*. Paris: UNESCO.

Verhulst, N., and Govaerts, B. (2010). The normalized difference vegetation index (NDVI) GreenSeeker handheld sensor: *Toward the integrated evaluation of crop management*. Retrieved December 15, 2022, from http://hdl.handle.net/10883/550

Waddell, P. (2002). A Behavioral Simulation Model for Metropolitan Policy Analysis and Planning: Residential Location and Housing Market Components of UrbanSim. *Environment and Planning B: Planning and Design, 27(2)*, 247-263.

Wang, R., Derdouri, A. and Murayama, Y. (2018). Spatiotemporal Simulation of Future Land Use/Cover Change Scenarios in the Tokyo Metropolitan Area. *Sustainability, 10(6)*, 2056.

Watson, R. T., Noble, I. R., Bolin, B., Ravindranath, N., Verardo, D. J. and Dokken, D. J. (2000). *IPCC: Land Use, Land-Use Change and Forestry*: Cambridge University Press.

White, R. and Engelen, G. (2000). High resolution integrated modeling of the spatial dynamics of urban and regional systems. *Computers, Environment and Urban Systems, 24*, 383-400.

Xiaomei, Y. and RongQing, L. Q. Y. (1999). Change Detection Based on Remote Sensing Information Model and its Application on Coastal Line of Yellow River Delta. *Earth Observation Center*, NASDA, China.

Yang, X., X. C. Zheng, and R. Chen. (2014). A Land use Change Model: Integrating Landscape Pattern Indexes and Markov-CA. *Ecological Modelling 283*, 1-7.

Ye, B. and Bai, Z. (2007). Simulating Land Use/Cover Changes of Nenjiang County Based on CA-Markov Model. *Comput. Comput. Technol. Agric., 1*, 321-329.

มหาวิทยาลัยบูรพา
BURAPHA UNIVERSITY

BIOGRAPHY

NAME	Bawonluck Wiboonwatchara
DATE OF BIRTH	8 September 1988
PLACE OF BIRTH	Mueang District, Phetchaburi Province
PRESENT ADDRESS	25 Prokarong Road, Tharap Sub-district Mueang District, Phetchaburi Province, Thailand 76000
POSITION HELD	2012-2015: Policy and plan Analyst at Department of Public Works and Town & Country Planning 2016-present: Urban planning Analyst at Department of Public Works and Town & Country Planning
EDUCATION	2006 – 2011: Bachelor of Arts (Geography), Silpakorn University, Nakhon Pathom, Thailand 2013 – 2015: Master of Public Administration, Ramkhumhaeng University, Bangkok, Thailand
AWARDS OR GRANTS	The Ministry of Higher Education, Science, Research and Innovation by the Geo-Informatics and Space Technology Development Agency (Public Organization) (GISDA) and Burapha University.